A Postsynaptic Mechanism of Zinc Transport Driving Inhibition of NMDA Receptors

by

Rebecca Frances Krall

B.S, University of Pittsburgh, 2015

Submitted to the Graduate Faculty of the

School of Medicine in partial fulfillment

of the requirements for the degree of

Doctor of Philosophy

University of Pittsburgh

2020

UNIVERSITY OF PITTSBURGH

SCHOOL OF MEDICINE

This dissertation was presented

by

Rebecca Frances Krall

It was defended on

October 22, 2020

and approved by

Dr. Anne-Marie Oswald, Associate Professor, Neurobiology, University of Chicago

Dr. Jon Johnson, Professor, Neuroscience and Psychiatry

Dr. Amantha Thathiah, Assistant Professor, Neurobiology

Dr. Richard Dyck, Professor, Psychology, University of Calgary

Dissertation Directors: Dr. Thanos Tzounopoulos, Endowed Professor and Vice Chair of Research, Otolaryngology

Dr. Elias Aizenman, Professor, Neurobiology

A Postsynaptic Mechanism of Zinc Transport Driving Inhibition of NMDA Receptors

Rebecca Frances Krall, PhD

University of Pittsburgh, 2020

Zinc is an essential element with diverse signaling functions in the central nervous system. Extracellular zinc acts on a variety of receptors to modulate neurotransmission. Notably, zinc binds and inhibits the GluN2A subunit of NMDA receptors (NMDARs) with high affinity. Inside the cell, zinc also triggers diverse signaling cascades, ranging from zinc-induced gene expression to cell death triggered by high concentrations of zinc. To maintain sufficient signaling without tipping the scales towards cell death, a complex system of transporters, metalloproteins, and ion channels regulate the localization and concentration of zinc. The zinc transporter, ZnT3, concentrates the majority of loosely bound 'labile' zinc into synaptic vesicles from where it then is released into the cleft in an activity-dependent manner. Current modeling of vesicular zinc assumes that ZnT3-dependent zinc is released and subsequently diffuses across the cleft and this is sufficient to account for its actions on postsynaptic targets, including NMDARs. Interestingly, the transporter ZnT1 is located in the postsynaptic density and binds directly to the GluN2A subunit of NMDARs, suggesting that ZnT1's transport of zinc out of the cytoplasm into the extracellular space may contribute to NMDAR inhibition. This suggests that ZnT1 and intracellular zinc may critically regulate zinc inhibition of NMDARs through ZnT1's interaction with GluN2A. To explore this question, we developed a novel peptide that specifically disrupts the interaction between GluN2A and ZnT1. We found that either disrupting ZnT1's association with GluN2A or chelating intracellular zinc is sufficient to block endogenous inhibition of NMDARs, even in the presence of presynaptic zinc release. ZnT1, in addition to transporting cytosolic zinc, is also upregulated by

intracellular zinc through the metal regulatory transcription factor 1. We found that increasing intracellular zinc is sufficient to drive upregulation of ZnT1-GluN2A interactions and subsequent inhibition of NMDARs. Together these data reveal a novel mechanism in which presynaptic release, intracellular zinc, and ZnT1 cooperatively drive inhibition of NMDARs. These findings add complexity to our current understanding of zinc dynamics at the synapses and provide a novel mechanism for modulating zinc and NMDAR signaling.

Table of Contents

List of Tables

List of Figures

Preface

I would like to thank all the people who provided support and guidance throughout my graduate career. First, I would like to thank my mentors, Drs. Elias Aizenman and Thanos Tzounopoulos for their continued guidance and encouragement. I'm grateful for their investment in my development as a scientist. I would like to thank my whole committee, Drs. Anne-Marie Oswald, Jon Johnson, and Amantha Thathiah for their advice and feedback as well as Dr. Richard Dyck for his time and effort as serving as my outside examiner. I would also like to thank all the members of both the Aizenman and Tzounopoulos labs for their feedback, friendship, and assistance over the years in lab. In particular I'd like to thank Karen Hartnett and Charlie Anderson for their training and assistance. I would also like to thank our collaborators, Michal Hershfinkel, Hila Asraf, Rajesh Khanna, Aubin Moutal, Jon Johnson, and Matt Phillips.

The work in this dissertation would not have been possible without the support from my family and friends. I want to thank all my lab mates, particularly Nate Vogler, Amanda Henton, Yang Yeh, and Tony Schulien. I'd also like to thank my all friends in the CNUP especially, Jake Wright, Jill Weeks, Jake Mann, Emily Parker, Jane Huang, Meghan Bucher, Brooke Bender, Dana Smith, and Karen Clark. Finally, I would like to thank my family for their lifelong support of me and my goals.

1.0 Introduction

1.1 Zinc Biology in the Central Nervous System

Zinc is essential for survival. Zinc deficiency is linked to a variety of adverse conditions including growth retardation, impaired immune function, improper skin and bone formation and repair, as well as cognitive disfunction (Prasad, 2003). Indeed, mutations in the principal zinc importer in the gut, ZIP4, lead to *acrodermatitis enteropathica*, a zinc-deficiency disease characterized by failure to thrive, severe dermatitis, hair loss, and diarrhea, which can be lethal if left untreated (Dufner-Beattie *et al.*, 2007). These severe zinc deficiency outcomes are largely due to the impact of the essential structural and enzymatic functions of the metal. An estimated 10% of the human genome encodes zinc-binding proteins, which serve a diverse and rich array of roles in the cell (Andreini *et al.*, 2006). Zinc catalyzes reactions of all the major classes of enzymes (Laitaoja *et al.*, 2013) and stabilizes zinc-finger proteins, whose functions include transcriptional activation, protein folding, and RNA regulation (Laity *et al.*, 2001). In the brain, labeling zinc with autometallography, more commonly referred to as Timm staining, reveals that a high concentration of zinc exists in a separate reserve pool of loosely bound, chelatable or "labile" zinc that is contained within synaptic vesicles (Timm, 1958; Haug, 1967). This points to additional, unique signaling roles for zinc within the central nervous system.

Initial evidence for the potential role for zinc as a synaptic signaling molecule came when multiple groups observed that exogenous zinc application inhibited NMDA and $GABA_A$ receptors (Smart & Constanti, 1982; Peters *et al.*, 1987; Westbrook & Mayer, 1987). Within this same time

period, evidence for vesicular release of zinc was observed following chemical stimulation as well as electrical stimulation of the mossy fiber pathway in hippocampal slices (Assaf & Chung, 1984; Howell *et al.*, 1984). This activity-dependent increase in extracellular zinc suggested that the ion is released from presynaptic vesicles as a neuromodulator. In agreement with this, it was observed that zinc labeled with Timm-staining accumulated in the synaptic cleft over time (Pérez-Clausell & Danscher, 1985; 1986). Critically for the development of this field, ZnT3 (Slc30a3) was identified as the transporter responsible for sequestering zinc into synaptic vesicles (Palmiter *et al.*, 1996; Wenzel *et al.*, 1997). ZnT3 knockout (KO) mice showed a striking near absence of Timm staining in the brain, thereby demonstrating that most of labile zinc in the brain is contained within synaptic vesicles (Cole *et al.*, 1999).

These studies provided compelling evidence that vesicular zinc is released into the cleft similar to traditional neurotransmitters, however the absence of a high-affinity rapid extracellular zinc chelator initially made disrupting synaptic zinc signals challenging. Anderson and colleagues demonstrated that tricine, previously considered a preferred chelator for studying the role of synaptic zinc, is unable to efficiently prevent zinc from binding low-nanomolar zinc-binding sites due to its micromolar dissociation constant (Anderson *et al.*, 2015). In contrast, the chelator ZX1 has a 1 nM zinc dissociation constant and second-order rate constant for binding zinc (Anderson *et al.*, 2015). As such, ZX1 is the most appropriate chelator for investigating the effects of fast, transient elevations of zinc on synaptic targets with nanomolar affinity, such as GluN2A-containing NMDARs. It has been used in conjunction with ZnT3 KO mice to better understand zinc's contribution to synaptic transmission (Pan *et al.*, 2011; Kalappa *et al.*, 2015).

1.2 Postsynaptic Targets of Zinc

Zinc regulates glutamatergic transmission through its action on all three ionotropic glutamate receptors. The best characterized modulatory action of zinc is its inhibition of NMDA receptors (NMDAR), which will be discussed in detail below (Section 1.3). AMPA receptors (AMPAR) are biphasically modulated by exogenous zinc application. Lower concentrations of zinc potentiate AMPAR responses whereas higher concentrations inhibit the receptor (Figure 1A,B) (Rassendren *et al.*, 1990; Bresink *et al.*, 1996). Interestingly, chelation of zinc in acute brain slices reveals that zinc endogenously inhibits AMPAR EPSCs in the zinc-rich dorsal cochlear nucleus as well as the hippocampus. Furthermore, this effect is lost in ZnT3 knockout animals, showing that vesicular zinc mediates endogenous inhibition of AMPARs (Kalappa *et al.*, 2015). Kainate receptors are also inhibited by zinc, with their affinity dependent on subunit composition (Figure 1A) (Mott *et al.*, 2008). Isolated kainate EPSCs in CA3 neurons evoked by mossy fiber stimulation are potentiated when zinc is chelated. Furthermore, this effect is lost in mocha mutant mice, which lack zinc in the mossy fiber pathway, strongly suggesting that the action of chelators occurs through removal of synaptic zinc inhibition of kainate receptors (Mott *et al.*, 2008). Therefore, there is significant evidence that vesicular zinc can regulate glutamatergic transmission through its modulation of AMPA and kainate receptors.

Zinc's modulatory actions at synapses extend beyond glutamatergic transmission. P2X purinergic receptors (P2XRs) are ionotropic receptors activated by extracellular ATP. Zinc differentially modulates P2XRs depending on which of the P2X subunits are expressed. P2X1Rs and P2X7Rs are inhibited by μM concentrations of extracellular zinc, whereas P2X2-4Rs exhibit potentiation at μM concentrations and inhibition at higher concentrations (Figure 1A,B)

(Nakazawa *et al.*, 1997; Wildman *et al.*, 1998; 1999a; b). Zinc also alters inhibitory transmission through its actions on $GABA_A$ and glycine receptors. $GABA_A$ receptors are allosterically inhibited by exogenous application of micromolar concentrations of zinc (Figure 1) (Smart & Constanti, 1982; Westbrook & Mayer, 1987; Celentano *et al.*, 1991; Barberis *et al.*, 2000). However, recent work has suggested that endogenous zinc potentiates $GABA_A$Rs, as chelation reduced $GABA_A$R-mediated IPSCs at cortical synapses (Kouvaros *et al.*, 2020). Glycine receptors (GlyR), similar to AMPARs, are bidirectionally modulated by zinc; exhibiting potentiation at submicromolar zinc concentrations (20 nM – 1 µM) and inhibition at micromolar concentrations (20 – 50 µM) (Figure 1A,B) (Bloomenthal *et al.*, 1994).

In addition to its modulatory actions on other receptors, zinc acts as a ligand for its own metabotropic receptor (Figure 1C). The first evidence suggesting the existence of a metabotropic zinc receptor (mZnR) was obtained by Michal Hershfinkel and colleagues, demonstrating that the application of zinc led to IP_3-dependent increases in intracellular calcium and consequent upregulation of the Na^+/H^+ exchanger in the colonocytic cell line HT29 (Hershfinkel *et al.*, 2001). Multiple studies on the orphan receptor, GPR39, showed that zinc, but not its putative ligand, the peptide hormone obestatin, activated GPR39 (Zhang *et al.*, 2005; Lauwers *et al.*, 2006; Holst *et al.*, 2007). Further studies revealed that siRNA against GPR39 as well as genetic knockdown of GPR39 prevented the intracellular calcium increase triggered by synaptic zinc release in the CA3 region of the hippocampus (Chorin *et al.*, 2011), demonstrating that GPR39 was conclusively mZnR.

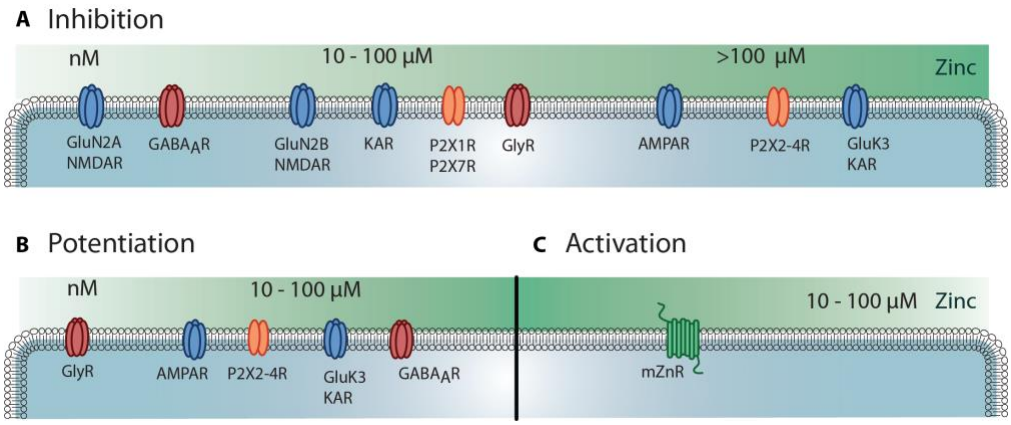

Figure 1 Postsynaptic Targets of Zinc

Legend for Figure 1: The green gradient represents the approximate concentration of zinc necessary for modulation each receptor. (**A**) Zinc-dependent inhibition has been observed for receptors with affinities ranging from nanomolar to high micromolar. (**B**) Multiple receptors that are inhibited by zinc are also potentiated by the ion at lower (GlyR, AMPAR, GluK3 KAR, and P2X2-4R) or higher ($GABA_AR$) concentrations. (**C**) mZnR/GPR39 is directly activated by zinc

1.3 Zinc Inhibition of NMDA Receptors

The best characterized modulatory action of zinc is its inhibition of NMDARs. Initial studies using exogenous application of zinc found that micromolar concentrations of zinc inhibited NMDAR currents. These studies suggested that this inhibition had two components; a voltage-independent block at lower µM concentrations and a voltage-dependent block at higher concentrations (>10 µM) (Christine & Choi, 1990; Legendre & Westbrook, 1990). Further investigations found that buffering with tricine removed low levels of zinc contamination in standard solutions that could occupy high-affinity zinc binding sites. These studies revealed low nanomolar concentrations of zinc inhibit GluN2A-containing NMDARs (Paoletti *et al.*, 1997).

This high affinity inhibition of GluN2A-containing NMDARs occurs through zinc binding to the N-terminal domain, which allosterically reduces NMDAR channel open probability via an enhancement of proton inhibition (Low *et al.*, 2000; Paoletti *et al.*, 2000; Erreger & Traynelis, 2008). A comparable, albeit micromolar affinity allosteric binding site also exists on GluN2B's N-terminal domain (Rachline *et al.*, 2005).

Endogenous zinc released from presynaptic terminals has been shown to inhibit postsynaptic NMDARs. Recordings of ZnT3-containing synapses in acute brain slices showed that chelating zinc with ZX1 disinhibits NMDARs, revealing an endogenous zinc inhibition in both the hippocampus and dorsal cochlear nucleus (DCN) (Pan *et al.*, 2011; Anderson *et al.*, 2015). Notably this effect is lost in ZnT3 knockout animals, suggesting vesicular zinc release is necessary for endogenous modulation of NMDAR by zinc (Pan *et al.*, 2011; Anderson *et al.*, 2015). Moreover, a knock-in mutation (H128S) on the N-terminal domain of GluN2A removes high affinity zinc binding from NMDARs and eliminates the potentiating effect of tricine on NMDAR EPSCs in the hippocampus. This result convincingly reveals the physiological relevance of zinc modulation of NMDAR (Vergnano *et al.*, 2014).

Interestingly, an additional ZnT3-independent zinc inhibition of DNC extrasynaptic NMDARs was also observed (Anderson *et al.*, 2015). In this study, multiple frequencies of presynaptic electrical stimulation were used to activate different pools of extrasynaptic NMDARs on DCN cartwheel cells. At lower frequencies, which preferentially activated receptors closest to presynaptic release sites, endogenous zinc inhibition was completely dependent on ZnT3. Higher frequencies of stimulation activated more distal NMDARs and revealed a pool of extrasynaptic

receptors that maintain endogenous zinc inhibition in the absence of presynaptic release. This suggests that an additional mechanism beyond presynaptic vesicular release may regulate extracellular zinc and subsequent zinc signaling.

1.4 Distribution and Function of Zinc in the Central Nervous System

Labile zinc is not uniformly distributed throughout the brain, but instead is localized to specific regions. Histochemical staining of zinc demonstrates that it is highly concentrated in the cerebral cortex, hippocampus, amygdala, and dorsal cochlear nucleus (DCN) (McAllister & Dyck, 2017). Within these regions, ZnT3 and synaptic zinc are further restricted to a subset of glutamatergic neurons. For example, in the DCN, zinc is released from parallel fibers of granule cells, but is absent from auditory nerve terminals (Frederickson *et al.*, 1988). Therefore, zinc in the DCN endogenously inhibits AMPAR EPSCs following parallel fiber, but not auditory nerve stimulation (Kalappa *et al.*, 2015). This allows zinc to modulate neurotransmission in a synapse- and circuit-specific manner.

Zinc modulates synaptic transmission and plasticity at synapses where it is released presynaptically. In the amygdala, synaptic zinc gates long term potentiation of principal neurons through its reduction of feedforward GABAergic inhibition (Kodirov *et al.*, 2006). In the dorsal cochlear nucleus, zinc reduces spontaneous firing by enhancing glycinergic inhibition (Perez-Rosello *et al.*, 2015). Additionally, zinc inhibits presynaptic release by promoting endocannabinoid synthesis through its activation of mZnRs (Perez-Rosello *et al.*, 2013). In the

hippocampus, mZnR activation upregulates K^+/Cl^- cotransporter 2 (KCC2) activity which leads to hyperpolarization of $GABA_AR$ reversal potential (Chorin *et al.*, 2011). Furthermore, zinc was found to regulate synaptic plasticity in the CA1 region of the hippocampus via P2X4Rs. At relatively low concentrations (5-50 µM), application of zinc enhanced LTP evoked by theta burst stimulation of Schaffer collateral fibers. The zinc effect was lost with P2XR antagonists and could be mimicked using a P2X4R positive allosteric modulator, suggesting that zinc facilitates LTP via P2X4Rs (Lorca *et al.*, 2011).

Multiple studies in the hippocampus have shown that zinc modulates long term potentiation (LTP) at the zinc-rich mossy fiber to CA3 synapse in the hippocampus. Zinc is required for the induction of a form of presynaptic LTP, which can be blocked with zinc chelation (Pan *et al.*, 2011). In fact, exogenous zinc is sufficient to potentiate this synapse through its activation of TrkB receptors (Huang *et al.*, 2008). However, slices from ZnT3 knockout animals exhibit postsynaptic LTP that is absent in wildtypes controls, suggesting that vesicular zinc also precludes induction of postsynaptic LTP (Pan *et al.*, 2011). Furthermore, when zinc inhibition is selectively disrupted using a mutant GluN2A knock in model that lacks high affinity zinc inhibition of NMDARs, only the magnitude of potentiation is reduced with no impact on LTP induction (Vergnano *et al.*, 2014). Together these studies demonstrate that zinc drives complex signaling consequences within a single synapse.

Synaptic zinc also regulates sensory processing. A knock-in mutation (H128S) on the N-terminal domain of GluN2A removes high affinity zinc binding and zinc modulation of NMDARs. Mice with this mutation exhibit hypersensitivity to pain stimuli, suggesting endogenous zinc

inhibition may attenuate pain processing (Nozaki *et al.*, 2011). Importantly, synaptic zinc modulates sensory processing in the auditory and somatosensory systems. Chelation of extracellular zinc with ZX1 in the primary auditory cortex (A1) increases the responsiveness (gain) of sound-evoked responses of inhibitory interneurons, and decreases the gain of pyramidal neurons (Anderson *et al.*, 2017). This effect on gain is eliminated in ZnT3 KO mice. Furthermore, synaptic zinc regulates frequency tuning in A1 in a cell specific manner (Kumar *et al.*, 2019). Consistent with these findings, ZnT3 KO mice exhibit reduced frequency discrimination compared to wild-type controls suggesting that zinc modulation of auditory circuits is critical for normal sensory processing (Kumar *et al.*, 2019). Interestingly, ZnT3 KO mice also exhibit deficits in whisker texture discrimination, suggesting a similar requirement of zinc for fine-tuning of somatosensory processing (Patrick Wu & Dyck, 2018).

Sensory regions that express ZnT3 also exhibit experience-dependent changes in zinc content, suggesting zinc signaling may contribute to changes in response to sensory experience. For example whisker plucking or stimulation leads to increase or decrease respectively in synaptic zinc staining (Brown & Dyck, 2002; 2005; Nakashima & Dyck, 2010). Similarly, zinc levels in the DCN decrease following noise exposure (Kalappa *et al.*, 2015; Vogler *et al.*, 2020). In the dorsal cochlear nucleus high frequency stimulation of the ZnT3-containing parallel fibers reduces zinc signaling whereas low frequency stimulation increases zinc signaling. Metabotropic glutamate receptor activation is necessary and sufficient to induce this zinc plasticity. In fact, injection of a mGluR antagonist prevents noise-induced reductions in DCN zinc signaling, suggesting a the same mechanism of plasticity in slice preparations also occurs *in vivo* (Vogler *et al.*, 2020).

1.5 Zinc Toxicity

Zinc signaling can also trigger cell death. These pathological actions of zinc in neurons were first identified following the observation that exposure to extracellular zinc causes widespread neuronal cell death *in vitro* (Yokoyama *et al.*, 1986; Choi *et al.*, 1988). The extent of damage in cultured neurons varied with the concentration and duration of zinc treatment, suggesting a direct relationship between zinc and cell death (Choi *et al.*, 1988). Furthermore, both kainate-induced seizures and ischemia were later noted to trigger zinc translocation from presynaptic bouton to degenerating postsynaptic cell bodies (Frederickson *et al.*, 1989; Koh *et al.*, 1996). Injured animals exhibit reduced vesicular zinc staining and increased somatic staining compared to control animals (Frederickson *et al.*, 1989; Koh *et al.*, 1996; Suh *et al.*, 2000). Furthermore, extracellular chelation *in vivo* attenuates cell death and degeneration induced by ischemia or traumatic brain injury, suggesting that the extracellular movement of the vesicular pool contributes to the zinc toxicity (Koh *et al.*, 1996; Suh *et al.*, 2000).

A common feature of deleterious zinc signaling cascades is the generation of reactive oxygen species (ROS). Zinc activates 12-lipoxygenase (12-LOX) and NADPH oxidase to trigger ROS generation (Noh & Koh, 2000; Zhang *et al.*, 2004). Subsequently, ROS can activate mitogen-activated protein kinase (MAPK) cascades including the Ras/Raf/MEK/ERK and p38 MAPK pathways (Figure 2). Zinc-induced ERK signaling causes toxicity in cortical cultures through poly(ADP-ribose) polymerase activation, DNA damage, ROS production via NADPH oxidase, and mitochondrial hyperpolarization and dysfunction (Du *et al.*, 2002; He & Aizenman, 2010). Zinc activation of p38 MAPK leads to phosphorylation of a c-terminal serine of the delayed rectifying voltage-gated potassium channel Kv2.1. Similarly zinc increases phosphorylation of

Kv2.1 at an n-terminal tyrosine through its activation of Src kinase and concurrent inhibition of cytoplasmic protein phosphatase ε (McLaughlin *et al.*, 2001; Redman *et al.*, 2007; Huang *et al.*, 2008; Redman *et al.*, 2009). Together, this dual phosphorylation leads to insertion of Kv2.1 into the membrane, increased Kv2.1 activity, and, subsequently to caspase activation and apoptotic cell death by decreasing intracellular potassium concentrations (Figure 2) (Redman *et al.*, 2009). Another zinc-regulated apoptotic signaling cascade is $p75^{NTR}$ mediated cell death in which $p75^{NTR}$ and $p75^{NTR}$-associated death executor induction leads to caspase activation and neuronal degeneration (Figure 2) (Park *et al.*, 2000). Intracellular zinc also triggers degeneration through mitochondrial dysfunction and energy failure. Following increases in the cytoplasm, zinc can accumulate in the mitochondria via the mitochondrial calcium uniporter (Malaiyandi *et al.*, 2005; Medvedeva & Weiss, 2014). Zinc accumulation is associated with a loss of mitochondrial membrane potential, subsequent mitochondrial dysfunction, and ROS production (Sensi *et al.*, 2003; Dineley *et al.*, 2005; Medvedeva & Weiss, 2014). Additionally zinc-mediated signaling has been linked to opening of the mitochondrial permeability transition pore, which triggers mitochondrial failure (Jiang *et al.*, 2001; Bonanni *et al.*, 2006). Zinc also disrupts energy production through its inhibition of GAPDH, thus impairing glycolysis (Sheline *et al.*, 2000).

Intracellular zinc also triggers neuroprotective signaling mechanisms at concentrations that are insufficient for toxicity. This process, in which a sub-lethal insult protects cells against subsequent lethal ones, is called preconditioning. Treating neuronal cultures with metal chaperones to increase intracellular zinc protects neuron against subsequent excitotoxic and ischemic insults, suggesting zinc itself can drive preconditioning (Wang *et al.*, 2010; Johanssen *et al.*, 2015). In fact, studies in cortical cultures found that preconditioning with sub-lethal potassium cyanide leads to

transient increases in labile zinc that are necessary and sufficient for neuroprotection against subsequent excitotoxicity. Zinc transients are triggered by protein kinase C (PKC)-facilitated release of zinc from metallothionein 1 and subsequent upregulation of gene expression (Figure 2) (Aras *et al.*, 2009). Similarly, ischemic preconditioning in rats leads to transient zinc increases in the cortex and striatum. Chelation of zinc is sufficient to abolish the neuroprotective effect. Furthermore, zinc induced preconditioning in cortical cultures is associated with activation of the $p75^{NTR}$ pathway and upregulation of heat-shock protein 70, via p38 and extracellular regulated kinase MAPK signaling (Figure 2) (Lee *et al.*, 2008). Sub-lethal zinc signaling also triggers ryanodine receptor- mediated calcium release from the endoplasmic reticulum which drives calcineurin-dependent redistribution of Kv2.1 channels, thus preventing apoptotic insertion of additional Kv2.1 channels into the membrane (Figure 2) (Schulien *et al.*, 2016; Justice *et al.*, 2017). Together these findings highlight the essential role of zinc as an intermediate in both neurotoxic and neuroprotective signaling cascades.

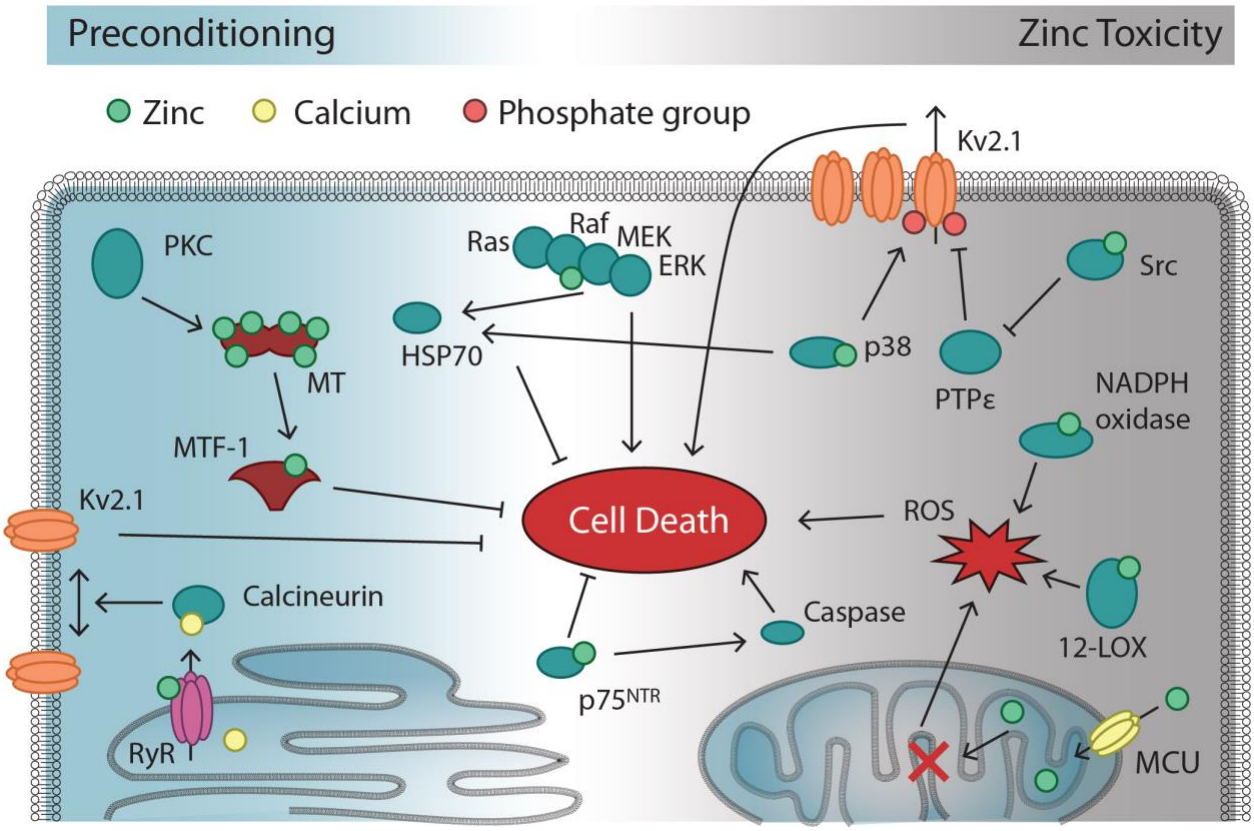

Figure 2 Zinc Signaling Cascades mediating Preconditioning and Cell Death

Legend for Figure 2: Increases in intracellular zinc trigger both protective (light blue) and toxic (gray) signaling cascades. (A) Preconditioning: Sublethal increases in intracellular zinc protect against subsequent cell death. PKC driven release of zinc from metallothioneins triggers upregulation of zinc sensitive genes. Zinc binding to ryanodine receptors (RyRs) triggers calcium release from ER stores and subsequent activation of calcineurin, which leads to the dispersal of Kv2.1 channels, thus preventing Kv2.1 insertion. ERK and p38 both activate protective HSP70 signaling. (B) Zinc Toxicity: Kv2.1 dual phosphorylation and insertion into the membrane is driven by p38 and Src-driven inhibition of PTPε, leading to apoptotic potassium efflux through Kv2.1. Zinc also activates NADPH oxidase and 12-LOX which drives the generation of toxic reactive oxygen species (ROS). Similarly zinc import into the mitochondria through the mitochondrial cation uniporter (MCU) leads to dysfunction, ROS generation, and neuronal death.

1.6 Regulation of Neuronal Zinc

Intracellular and extracellular labile zinc is normally maintained at low concentrations, despite fluctuations that result from release from synaptic terminals. This hints towards the dynamic processes that regulate zinc localization and concentration. However cellular zinc is not static, but is regulated by complex mechanisms involving transporters, ion channels, and metalloproteins. These systems work in tandem to spatially and temporally regulate cellular zinc signaling while protecting against the activation of injurious, zinc-activated cascades. In fact, metal binding proteins and at least twenty-four distinct zinc transporters tightly regulate the spatial and temporal distribution of the metal.

Metallothioneins are metal binding proteins that buffer intracellular zinc. There are four isoforms of metallothionein, three of which (MT-I through MT-III) are expressed in the central nervous system, with MT-III the primary form expressed in neurons (Aschner *et al.*, 1997). These proteins contain 20 cysteine residues that can bind up to 7 zinc ions via metal-thiolate clusters (Maret & Krezel, 2007). MTs release zinc in response to oxidative stimuli (Maret, 1994; 1995). For example, the thiol oxidant 2,2'-dithiodipyridine (DTDP) causes intracellular zinc release and subsequent zinc-dependent cell death in cortical neurons *in vitro* (Aizenman *et al.*, 2000). Nitric oxide, an endogenous gas, also triggers zinc release from MTs (Lin *et al.*, 2007), likely as a result of its interaction with superoxide and production of peroxynitrite (Zhang *et al.*, 2004). Inhibitors of NO synthase can prevent the accumulation of intracellular zinc following ischemia reperfusion injury, suggesting that NO endogenously mobilizes zinc from intracellular stores (Wei *et al.*, 2004).

Zinc transporters are responsible for transport of zinc across membranes. There are two families of zinc transporters, ZIP and ZnTs, both of which are part of the broader solute carrier family of transporters. Zrt, Irt-like proteins (ZIPs) are zinc transporters named for the first homologs of the broad family of metal transports discovered in *Saccharomyces cerevisiae (Zhao & Eide, 1996a; b)* and *Arabidopsis thaliana* respectively (Eide *et al.*, 1996). There are 14 ZIP transporters in mammals encoded by the genes SLC39A1-14, which transport zinc from the extracellular space or subcellular organelles into the cytoplasm. They are predicted to have 8 transmembrane domains with extracytoplasmic N- and C-termini, and form homo- and heterodimers in the membrane. Initial characterization of ZIPs suggested that they transport zinc in a temperature- and concentration-dependent manner (Gaither & Eide, 2000). ZIP sequences lack ATP-binding sites, which suggests that they are not active transporters, but instead act through secondary transport or facilitated diffusion (Gaither & Eide, 2001). From the structure of the bacterial homolog BbZIP, it was hypothesized that zinc transport by the ZIP family is mediated via a rigid rocking mechanism that alternatively exposes the binuclear metal center to the cytoplasm and extracellular space (Zhang *et al.*, 2017).

ZnTs transport zinc from the cytoplasm to the extracellular space or subcellular organelles. They are part of the cation diffusion facilitator (CDF) family of proteins. Since the initial discovery of ZnT1, an additional 9 ZnTs have been identified (ZnT2-ZnT10). Recently the protein TMEM163, also known as synaptic vesicle 31, was found to extrude zinc. Furthermore, sequence alignment and phylogenetic analysis place TMEM163 in the CDF family of proteins. Therefore TMEM163 has been proposed to be a new member of the ZnT family, ZnT11 (Sanchez *et al.*, 2019). ZnTs are thought to function as proton antiporters. In agreement with this, disruption of the

vacuolar-type H^+ ATPase blocks ZnT-mediated zinc transport into intracellular vesicles, suggesting that ZnT function requires a proton gradient. Furthermore, ZnT expression increases the rate of alkalization of intracellular vesicles, indicating that ZnTs promote efflux of protons (Ohana *et al.*, 2009; Golan *et al.*, 2019). A recent study has provided a high-resolution structure of human ZnT8, revealing, for the first time, a plausible mechanism for the Zn^{2+}/H^+ exchange mechanism in a mammalian zinc transporter (Xue *et al.*, 2020). By resolving both the inward (cytosolic) and outward (luminal) facing states of the transporter, the results from this study suggest a simple two-state model for zinc transport. In this model, ZnT8, functions as a dimer and alternates between inward and outward facing states via large structural rearrangements of the transmembrane domain, housing the zinc ion in a differential, pH-dependent manner. The lower luminal pH induces the release of zinc from the outward-facing side, while the higher pH of the cytosolic environment increases the affinity of the primary binding site of the outward-facing state for the metal (Xue *et al.*, 2020).

Intracellular zinc regulates transcription of zinc regulatory proteins, including transporters. Metal-regulated gene transcription was first observed with metallothionein-1 (MT-1), a metal-binding protein involved in zinc homeostasis and protection against oxidative stress. Mice injected with zinc or cadmium exhibited increased MT-1 mRNA expression in multiple tissues (Durnam & Palmiter, 1981). Further characterization of the MT-1 gene identified a 12 base pair DNA motif in the promoter region that was necessary for metal responsiveness, and thus was named metal response element (MRE) (Carter *et al.*, 1984; Stuart *et al.*, 1984; Searle *et al.*, 1985). Shortly thereafter, a zinc-inducible transcription factor was found that bound MRE to induce gene transcription (Westin & Schaffner, 1988). Upon zinc binding, this metal regulatory transcription

factor (MTF-1) rapidly translocates to the nucleus and binds to DNA (Dalton *et al.*, 1997; Smirnova *et al.*, 2000). MTF-1 upregulates transcription of multiple gene targets including MT-II, MT-III and ZnT1. This transcriptional pathway allows the cell to maintain stable zinc concentrations in the face of fluctuating zinc levels.

1.7 Zinc Transporter 1

ZnT1 was the first mammalian zinc transporter identified based on its ability to confer protection against zinc toxicity (Palmiter & Findley, 1995). It is an essential gene for development, as homozygous knockout of ZnT1 is embryonic lethal (Andrews *et al.*, 2004). It is located in the plasma membrane and protects cells against zinc toxicity through its extrusion of zinc out of the cell (Palmiter, 2004). Furthermore, it dynamically responds to intracellular zinc concentrations to increase or decrease zinc efflux. When intracellular zinc increases it binds MTF-1 to upregulate ZnT1 expression (Langmade *et al.*, 2000). Conversely, ZnT1 surface expression is downregulated via endocytosis and degradation of the transporter under zinc-deficient conditions, leading to decreased efflux from the cytoplasm. ZnT1 endocytosis is regulated, in part, through N-glycosylation of asparagine 299 of the protein (Nishito & Kambe, 2019).

ZnT1, in addition to its role in transporting zinc, also regulates voltage gated calcium channels. The C-terminal domain of ZnT1 binds to the β subunit of L-type calcium channels (LTCC). This association reduces in LTCC current by decreasing trafficking of the α_1 subunit to the membrane (Levy *et al.*, 2009). Furthermore, expression of the C-terminal domain of ZnT1 is

sufficient to drive this reduction in LTCC current, indicating that this effect is independent of zinc transport (Shusterman *et al.*, 2017). Given that LTCCs mediate zinc influx, ZnT1-dependent reduction in LTCC suggests a unique mechanism in which the same protein that removes zinc from the cytoplasm also prevents further influx. In addition to its modulation of LTCCs, ZnT1 also regulates Ras/Raf/MEK/ERK signaling (Jirakulaporn & Muslin, 2004) by promoting Raf-1 signaling through ZnT1's interaction with the N-terminal regulatory domain. This enhancement of Raf-1 signaling upregulates T-type calcium channel expression on the plasma membrane and subsequently increases calcium currents (Mor *et al.*, 2012). These findings show that ZnT1 protein interactions are associated with functional changes in both calcium and zinc signaling.

ZnT1 is found throughout the brain with significant overlap in expression with high zinc concentration and ZnT3 expression (Sekler *et al.*, 2002). This suggests that ZnT1 may contribute to zinc homeostasis at synapses. Indeed, ZnT1 is localized to the postsynaptic density in hippocampal neurons (Sindreu *et al.*, 2014b). Furthermore, ZnT1 binds directly to the C-terminal domain of the GluN2A subunit of NMDARs (Mellone *et al.*, 2015). Overexpression or silencing of ZnT1 leads to an increase or decrease in spine size, respectively. Given that NMDAR activation is a significant regulator of synaptic strength and spine dynamics (Segal, 2005; Sala & Segal, 2014), ZnT1's association with NMDAR may be driving changes in spine morphology by regulating NMDAR function.

1.8 Dissertation Goal

The majority of studies of zinc signaling in synapses have focused on the vesicular transporter ZnT3, despite the complex system of transporters that regulate zinc localization and concentration in neurons. Indeed, there is evidence that ZnT3-independent zinc pools influence synaptic functions, including glycinergic and NMDAR-mediated transmission (Anderson *et al.*, 2015; Perez-Rosello *et al.*, 2015). ZnT1 is located postsynaptically and directly binds to the highly zinc-sensitive GluN2A subunit of NMDARs, thus positioning ZnT1 to directly regulate zinc inhibition of NMDARs (Mellone *et al.*, 2015). The goal of this dissertation is to determine the role of ZnT1 in zinc inhibition of NMDARs. To address this question, we developed a peptide to specifically interfere with the interaction between ZnT1 and the GluN2A subunit. Using this peptide, we determined that ZnT1 is crucial for endogenous zinc inhibition of NMDARs in cortical cultures and acute slices of the DCN (Chapter 2). Furthermore, we revealed a zinc-dependent mechanism that regulates zinc inhibition of NMDARs via upregulation of ZnT1 (Chapter 3). These results challenge the conventional understanding of how zinc inhibits synaptic NMDARs and demonstrates that presynaptic release and a postsynaptic transporter organize zinc into distinct microdomains to modulate NMDAR neurotransmission.

2.0 Chapter 2: Synaptic Zinc Inhibition of NMDA Receptors Depends on the Association of GluN2A with Zinc Transporter ZnT1

2.1 Overview

The NMDA receptor (NMDAR) is inhibited by synaptically released zinc. This inhibition is thought to be the result of zinc diffusion across the synaptic cleft, and subsequent binding to the extracellular domain of the NMDAR. However, this model fails to incorporate the observed association of the highly zinc-sensitive NMDAR subunit GluN2A to the postsynaptic zinc transporter ZnT1, which moves intracellular zinc to the extracellular space. Here, we report that disruption of ZnT1-GluN2A association by a cell-permeant peptide strongly reduced NMDAR inhibition by synaptic zinc in mouse dorsal cochlear nucleus synapses. Moreover, synaptic zinc inhibition of NMDARs required postsynaptic intracellular zinc, suggesting that cytoplasmic zinc is transported by ZnT1 to the extracellular space in close proximity to the NMDAR. These results demonstrate that presynaptic release and a postsynaptic transporter organize zinc into distinct microdomains to modulate NMDAR neurotransmission.

2.2 Introduction

Zinc is a neuromodulator that regulates glutamatergic, GABAergic and glycinergic synaptic transmission (Xie & Smart, 1991; Vogt *et al.*, 2000; Hirzel *et al.*, 2006; Vergnano *et al.*, 2014; Anderson *et al.*, 2015; Kalappa *et al.*, 2015; Perez-Rosello *et al.*, 2015), short- and long-

term synaptic plasticity (Huang *et al.*, 2008; Pan *et al.*, 2011; Perez-Rosello *et al.*, 2013; Vergnano *et al.*, 2014; Kalappa & Tzounopoulos, 2017; Eom *et al.*, 2019), auditory processing, and acuity for sensory stimulus discrimination (Patrick Wu & Dyck, 2018; Kumar *et al.*, 2019). The zinc transporter ZnT3 (Slc30a3) packages zinc into presynaptic vesicles of large populations of excitatory neurons in many brain regions, including the cerebral cortex, hippocampus, amygdala, and dorsal cochlear nucleus, (McAllister & Dyck, 2017). During synaptic activity, vesicular zinc is released from ZnT3-containing terminals (Assaf & Chung, 1984; Vogt *et al.*, 2000) and diffuses across the synaptic cleft (Anderson *et al.*, 2015) to modulate a number of postsynaptic receptors (Ruiz *et al.*, 2004; Besser *et al.*, 2009; Kalappa *et al.*, 2015; Perez-Rosello *et al.*, 2015), including the highly zinc-sensitive N-methyl-D-aspartate glutamatergic receptor (NMDAR) (Peters *et al.*, 1987; Paoletti *et al.*, 1997; Jo *et al.*, 2008; Vergnano *et al.*, 2014; Anderson *et al.*, 2015).

GluN2A-containing NMDARs are the major postsynaptic targets of synaptically-released zinc due to their sensitivity to nanomolar concentrations of extracellular zinc, which inhibit receptor function (Paoletti *et al.*, 1997). It is generally accepted that zinc release alone provides sufficient accumulation of the metal in the synaptic cleft to account for the observed zinc inhibition of GluN2A-containing NMDARs (Pan *et al.*, 2011; Vergnano *et al.*, 2014; Anderson *et al.*, 2015). However, this model only takes into account ZnT3's contribution to activity-dependent vesicular zinc inhibition of NMDARs, when, in fact, there are 24 known unique zinc transporters (10 Slc30a and 14 Slc39a) (Kambe *et al.*, 2014) that may be involved in zinc's spatial distribution in synapses. Little is known, however, how zinc transporters other than ZnT3 influence synaptic zinc's actions upon its receptor targets.

ZnT1 (Slc30a1), a cell membrane transporter that shuttles zinc from the cytoplasm to the extracellular space, not only localizes to the postsynaptic density (Sindreu *et al.*, 2014a), but also binds directly to the GluN2A subunit of NMDARs (Mellone *et al.*, 2015). This positions ZnT1, in concert with the presynaptic ZnT3 transporter, as a likely co-regulator of synaptic zinc concentration and function in the synaptic cleft. Here, we developed a peptide to disrupt ZnT1-GluN2A binding and used ZnT3 null mice and zinc chelation to assess the contribution of ZnT1 into synaptic actions of zinc. Our studies reveal a novel interplay between ZnT3- and ZnT1-dependent zinc transport to inhibit NMDAR-mediated neurotransmission.

2.3 Results

2.3.1 N2AZ disrupts the binding of ZnT1 to GluN2A

To study the effect of ZnT1 on zinc inhibition of NMDARs, we designed a peptide aimed at disrupting the ZnT1-GluN2A interaction. We first constructed a peptide spot array spanning 74 amino acids of the C-terminal domain (residues 1390-1464) of mouse GluN2A (Uniprot# P35436), previously shown to be necessary for ZnT1-GluN2A binding (Mellone *et al.*, 2015). The array consisted of sixty-one 15-mers, each sequentially overlapping by 14 amino acids, similar to procedures described earlier by our groups for other protein-protein interaction systems (Brittain *et al.*, 2011; Yeh *et al.*, 2017). Next, we probed the peptide spot arrays with flag-tagged ZnT1-enriched cell lysates and then visualized and quantified ZnT1 binding with immunofluorescence against the flag tag (Figure 3A). This approach identified three regions of significant ZnT1 binding, spanning peptide numbers 2-8, 40-42, and 48-52 in Fig. 3A, B. We focused on the

broadest binding peak (peptides 2-8, Figure 3B, in red), which included a common 9 amino acid sequence among the peptides with high ZnT1 binding (NDSYLRSSL, corresponding to GluN2A residues 1397-1406). Notably, this 9 amino acid sequence from the mouse GluN2A is conserved in both the rat and human GluN2A sequences (isoform 1, Uniprot# rat: Q00959, human: Q12879). This peptide and its scrambled control (SNLSDSYLR; Figure 3B, inset) were conjugated to the **t**rans-**a**ctivator of **t**ranscription (TAT) cell-penetrating peptide (YGRKKRRQRRR) to endow them with membrane permeability. As it was designed to prevent ZnT1-GluN2A binding, the peptide, and its scrambled control, will herein be referred to as N2AZ and scN2AZ, respectively. To confirm that N2AZ prevents GluN2A-derived sequences from binding to ZnT1, the peptide spot assay was repeated in the presence of either N2AZ or scN2AZ (100 µM). We noted that N2AZ significantly reduced ZnT1 binding to the spot array, when compared to scN2AZ control (Figure 4). These results indicate that N2AZ can disrupt the ZnT1-GluN2A association.

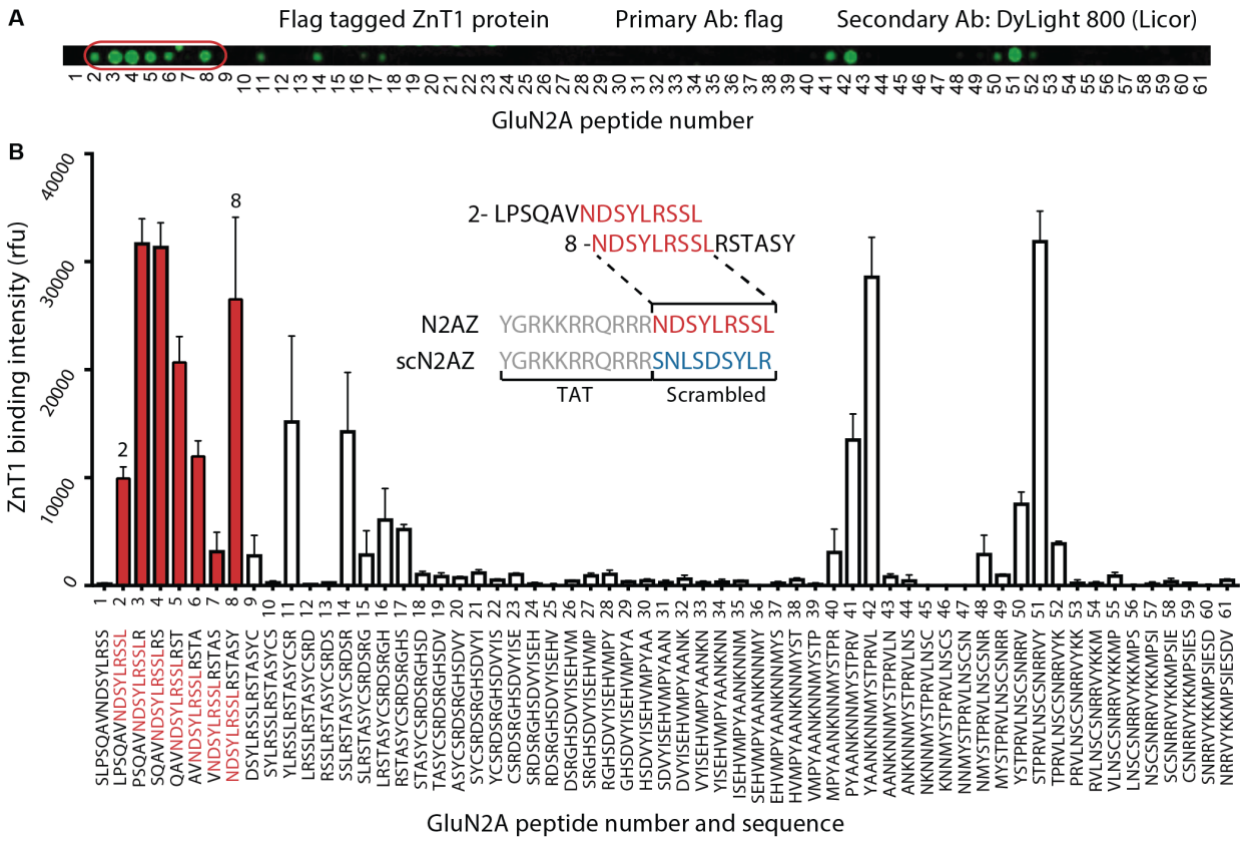

Figure 3 Generation of a ZnT1-binding Peptide (N2AZ) derived from the GluN2A C-terminal domain.

Legend for Figure 3: (**A**) A peptide spot array was composed of sixty-one 15-mers spanning the GluN2A C-terminus region (residues 1390–1464) with 14 amino acid overlapping sequential sequences used to identify regions of high ZnT1 binding. A representative array is shown with corresponding peptide numbers denoted below the blot. Sequences for each peptide number are shown in (B). The peptides denoting the broadest ZnT1 binding region are outlined in red. (**B**) Mean ± SEM (n=4) of ZnT1 binding intensity for each GluN2A-derived peptide. **Inset**: Peptide sequences flanking a region of high ZnT1 binding (peptide numbers 2-8, in red) were used to determine the shared peptide sequence of the ZnT1 binding peptides. Sequence in light gray represents the cell-permeable HIV trans-activator of transcription domain (TAT) sequence. The red sequence represents final peptide, and the blue represents its scrambled control. Both peptides were conjugated to TAT to create our experimental (N2AZ) and control (scN2AZ) peptides.

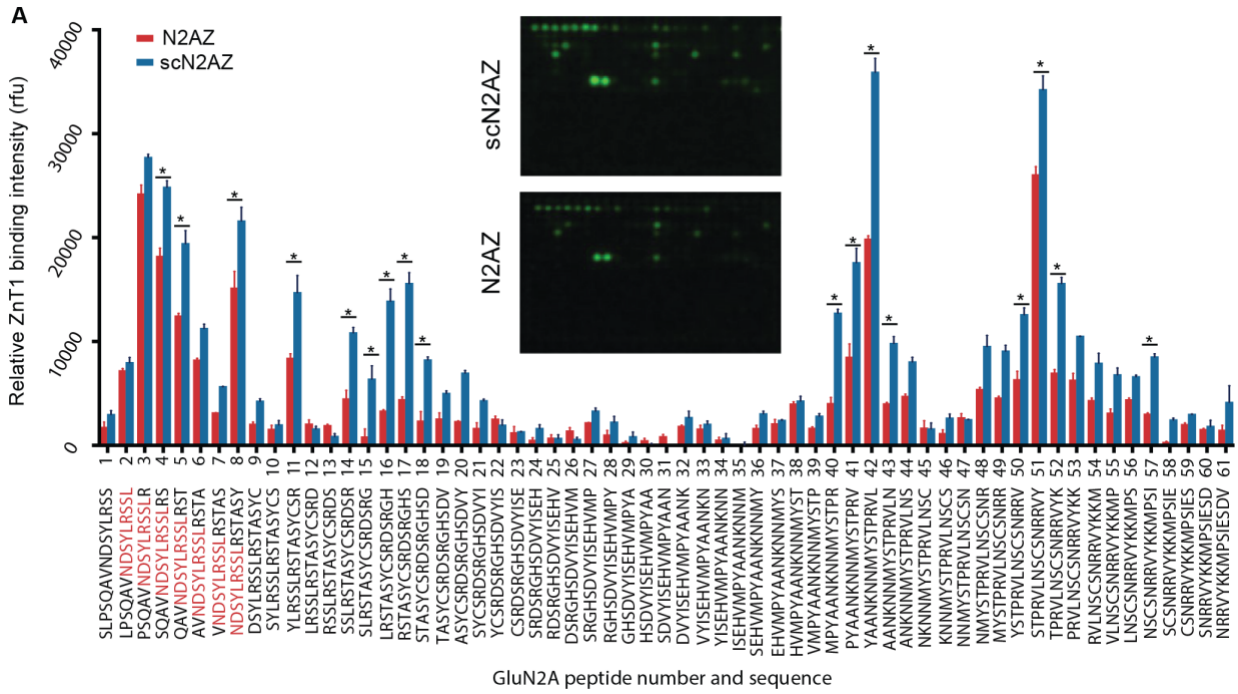

Figure 4 N2AZ disrupts ZnT1-GluN2A C-terminal peptide binding

Legend for Figure 4: Quantification of peptide spot arrays of GluN2A C-terminus region (residues 1390-1464) using the same peptide segments as in **Fig. 3** Bar graphs show the summary of ZnT1 binding intensity for each GluN2A-derived peptide in the presence of either N2AZ (red, 100 µM) or scN2AZ (blue, 100 µM). *Significant differences in ZnT1 binding for each peptide number are noted (multiple unpaired t-test, $p < 0.05$, multiple comparisons, Holm-Sidak method). Mean ± SEM (n=4) (Inset) Representative peptide spot-array in scN2AZ (top) and N2AZ (bottom).

Next, we utilized rat cortical cultures to determine whether N2AZ treatment was sufficient to disrupt ZnT1-GluN2A association in neurons. First, we verified that ZnT1 mRNA was indeed expressed in cortical cultures using quantitative PCR. We observed that ZnT1 mRNA expression increased over the first four weeks *in vitro* (Figure 5), paralleling the established developmental profile of GluN2A expression previously obtained in the same preparation by our group (Sinor *et al.*, 2000). Next, we quantified ZnT1-GluN2A interactions in the cultures using a proximity ligation assay (PLA, see Materials and Methods). This method results in fluorescent puncta when target proteins are within 40 nm of one another, thus revealing protein-protein interactions (Zhu *et al.*, 2017). Cultures (21 - 25 days *in vitro*, DIV) were treated overnight in either scN2AZ or N2AZ (3 µM) prior to performing PLA. To visualize neurons, cultures were immunostained against MAP2. We observed that PLA puncta localized along neuronal dendrites, consistent with previous findings localizing ZnT1 to the postsynaptic density (Figure 6A) (Sindreu *et al.*, 2014a; Mellone *et al.*, 2015). Importantly, we found that N2AZ treatment significantly reduced the number of PLA puncta, when compared to sister cultures treated with scN2AZ (Figure 6B, paired t-test, $p = 0.004$; n= 4 coverslips). These results indicate that N2AZ effectively disrupts ZnT1-GluN2A interactions in cultured neurons.

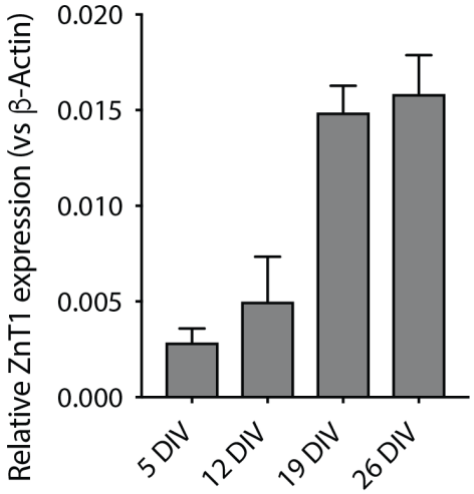

Figure 5 Developmental profile of ZnT1 expression in cortical cultures

Legend for Figure 5: qPCR measurements of ZnT1 RNA expression in mouse cortical cultures over the first 4 weeks in vitro (DIV = days in vitro). Error bars indicate mean ± SEM across 3 experiments.

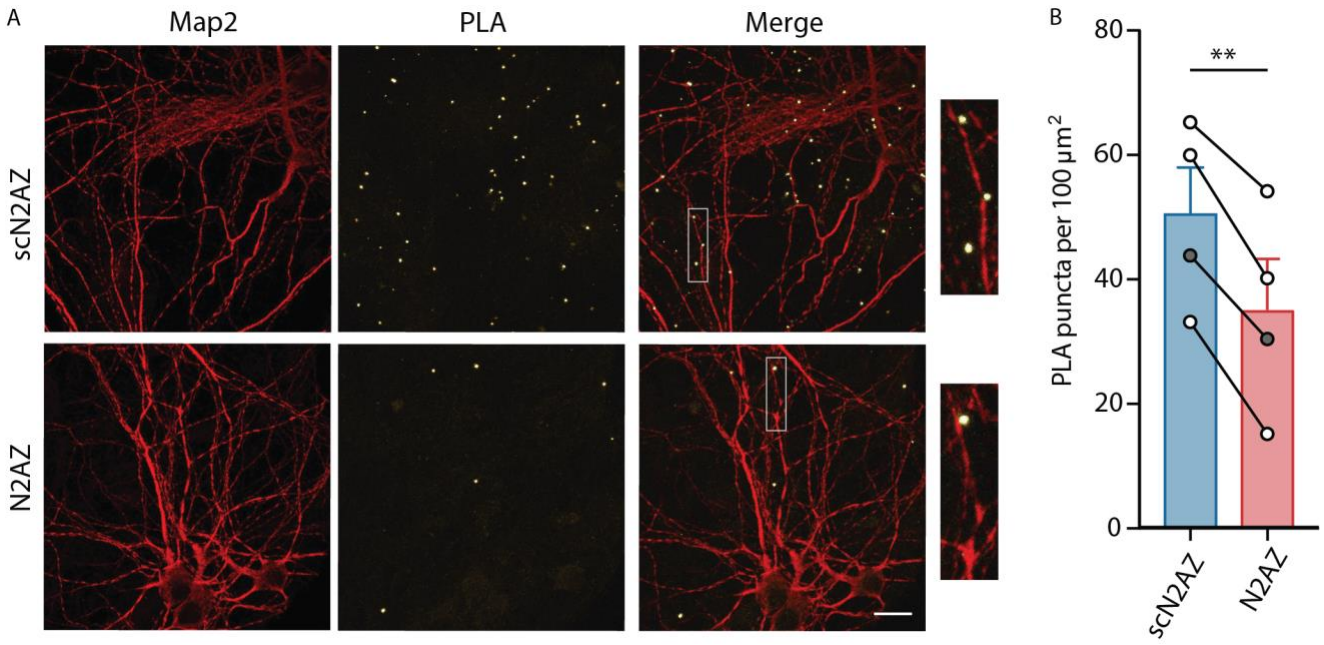

Figure 6 N2AZ disrupts ZnT1-GluN2A association

Legend for Figure 6: (**A**) Representative images of rat cortical cultures following proximity ligation assay (PLA) between GluN2A and ZnT1. The PLA immunofluorescently labeled sites of interaction between GluN2A and ZnT1 (white puncta). Additionally, MAP2 is immunofluorescently labeled in red to visualize neuron morphology. Scale bar: 20 µm. Top row shows PLA assay following overnight exposure to 3 µM scN2AZ, while bottom row shows PLA assay following 3 µM N2AZ treatment. Insets show the localization of PLA puncta along a MAP2 stained dendrite. (**B**) Quantification of PLA puncta per 100 μm^2 in sister cortical cultures treated overnight with 3 µM N2AZ or scN2AZ show that N2AZ significantly reduced the number of ZnT1-GluN2A interactions compared to scN2AZ (Paired t-test, $p = 0.0044$, $n = 4$). Gray filled circles indicate the quantification of representative images in A. Error bars indicate mean ± SEM.

2.3.2 Disrupting the ZnT1-GluN2A association reduces zinc inhibition of NMDAR currents in cortical neurons

Zinc inhibits GluN2A-containing NMDARs through its high-affinity binding site on the extracellular, N-terminal domain of the GluN2A subunit (Paoletti *et al.*, 1997; Nozaki *et al.*, 2011; Anderson *et al.*, 2015). As ZnT1 shuttles neuronal intracellular zinc to the extracellular space (Shusterman *et al.*, 2014), we hypothesized that ZnT1 functionally localizes zinc in close proximity to its GluN2A binding site, and thereby, contributes to the inhibition of NMDARs by the metal. To test this hypothesis, we treated cortical cultures (DIV 18-22) overnight with N2AZ or scN2AZ (3 µM) prior to recording NMDAR-receptor mediated currents. These currents were evoked by photolytic uncaging of caged glutamate (4-Methoxy-7-nitroindolinyl-caged-L-glutamate, 40 µM) along the dendrites of neurons (Figure 7A). Neurons were held at -70 mV in the absence of extracellular Mg^{2+} to prevent block of NMDARs, and in the presence of DNQX (20 µM) to block AMPAR currents. Zinc inhibition was determined by measuring the extent of NMDAR EPSC potentiation following application of the fast, high affinity, zinc-specific cell-impermeant (extracellular) zinc chelator ZX1 (3 µM) (Pan *et al.*, 2011; Anderson *et al.*, 2015; Kalappa *et al.*, 2015). We observed that in cells previously treated with the scN2AZ control, extracellular zinc chelation with ZX1 produced a potentiation of NMDAR-mediated currents (Figure 7B-C, 37.40 ± 11.63%, n=10, p = 0.02, paired t-test of peak responses before and after ZX1), likely reflective of background tonic zinc present in the cultures. In contrast, N2AZ prevented ZX1 potentiation of NMDAR-mediated currents (Figure 7B-C, 1.34 ± 3.48%, n=9, p = 0.62, paired t-test of peak responses before and after ZX1; scN2AZ versus N2AZ, p = 0.01, unpaired t-test). This result indicates that ZnT1 binding to GluN2A is critical for endogenous zinc inhibition of NMDAR-mediated currents in cortical neuronal cultures.

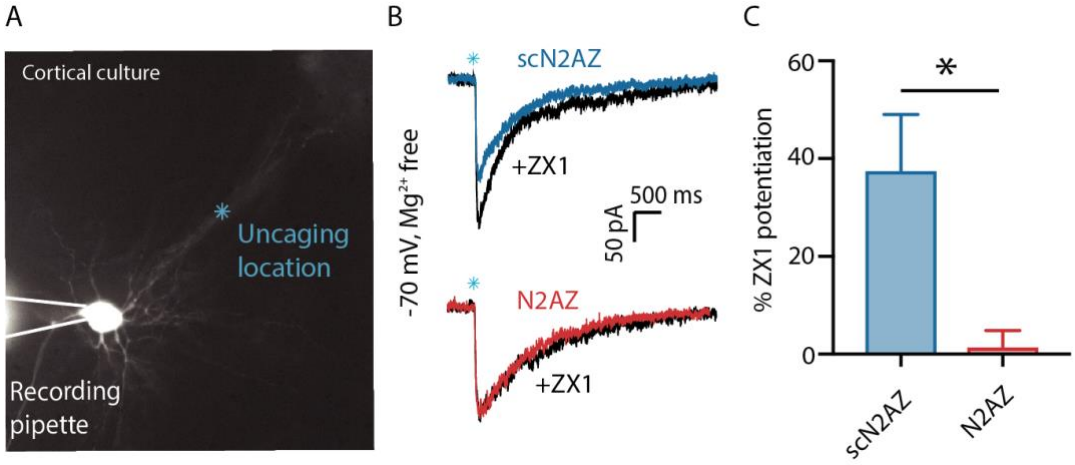

Figure 7 N2AZ reduces zinc inhibition of NMDAR currents in cortical cultures

Legend for Figure 7: (**A**) Representative image of a neuron in cortical culture filled with Alexa 548 during whole cell recording. Blue asterisk represents one example location of laser photolysis of MNI-caged glutamate (40 µM, 1 ms pulse) used to evoke EPSCs. (**B**) Sample traces of NMDAR currents, averaged over 4 sweeps, evoked by photolysis of MNI-caged glutamate in cultured cortical neurons held at -70 mV in Mg^{2+} free solution, before (blue scN2AZ, red N2AZ; 3 µM, treated overnight) and after application of ZX1 (black; 100 µM). (**C**) ZX1 potentiation of NMDAR currents was significantly diminished in N2AZ-treated cells versus scN2AZ control (unpaired t-test, $p = 0.01$, $n = 10,9$). Bar graphs represent the average potentiation of responses 5 minutes after ZX1 application. Error bars indicate mean ± SEM.

2.3.3 N2AZ reduces zinc inhibition in dorsal cochlear nucleus synapses

In order to investigate whether ZnT1 contributes to synaptic zinc mediated inhibition of NMDARs, we performed electrophysiological recordings in acutely-prepared brain slices of the dorsal cochlear nucleus (DCN), an auditory brainstem nucleus containing parallel fibers with zinc-

rich synaptic terminals (Frederickson *et al.*, 1988). In response to parallel fiber stimulation, synaptic zinc inhibits both NMDA and AMPA-mediated synaptic currents in cartwheel cells (Anderson *et al.*, 2015; Kalappa *et al.*, 2015), interneurons in the molecular layer of the DCN. NMDAR excitatory postsynaptic currents (EPSCs) were isolated by voltage-clamping cartwheel cells at +40 mV to relieve the Mg^{2+} block, while recording in the presence of DNQX (20 µM). Slices were incubated with either scN2AZ or N2AZ (3 µM) for at least 1 hour prior to ZX1 (100 µM) application. We stimulated parallel fibers at 20 Hz, a frequency where zinc inhibition of NMDARs is entirely ZnT3-dependent in DCN parallel fiber synapses (Anderson *et al.*, 2015). We found that N2AZ reduced the ZX1 potentiation of NMDAR EPSCs, when compared to scN2AZ (Figure 8A-C; N2AZ: 19.39 ± 5.82%, n=14 vs. scN2AZ: 47.30 ± 10.14% n = 9, unpaired t-test, p= 0.02). This result indicates that, contrary to the current model, synaptically-released zinc release alone cannot account for the inhibition of NMDARs by the metal. Instead, this result suggests that the ZnT1-GluN2A association is crucial for the synaptic zinc inhibition of NMDARs.

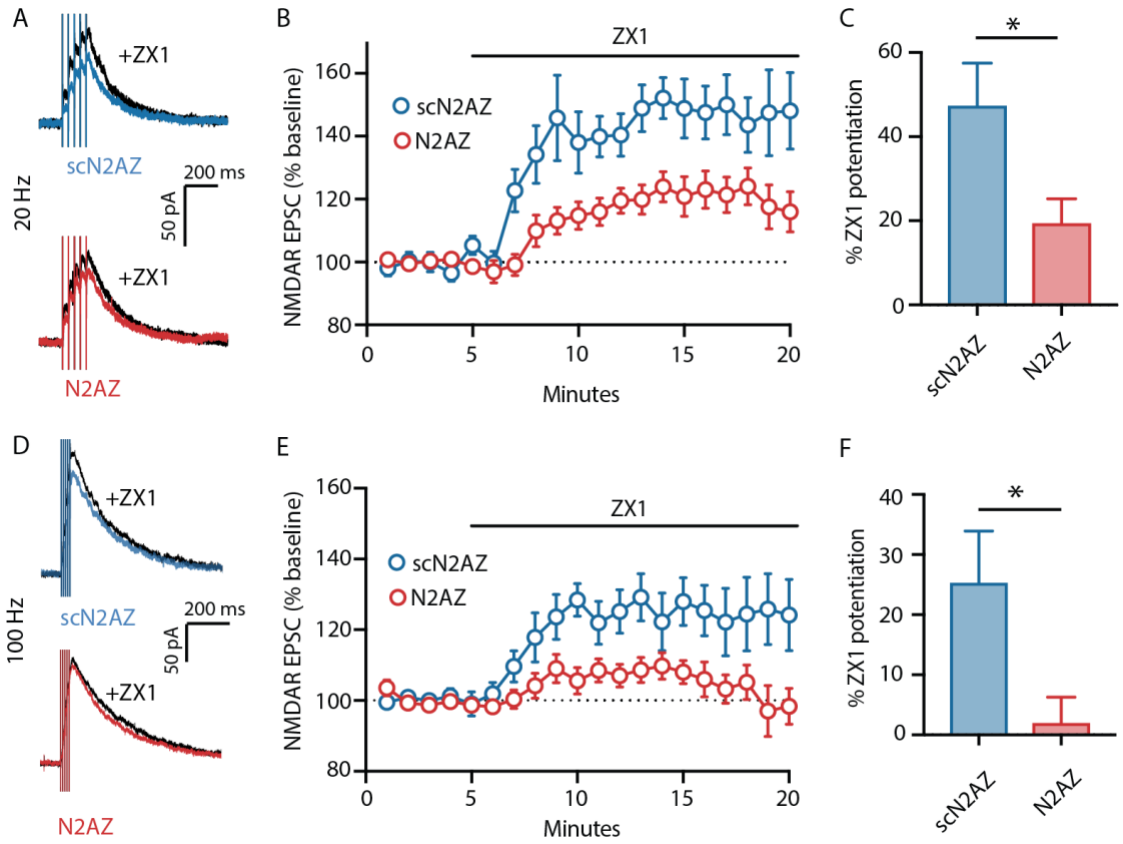

Figure 8 N2AZ reduces ZnT3-dependent and ZnT3-independent inhibition of NMDAR EPSCs in DCN cartwheel cells

Legend for Figure 8: (**A, D**) Sample traces of NMDAR EPSCs, averaged over 5 sweeps, evoked in cartwheel cells in response to five pulses at 20 Hz (A) or 100 Hz (D) stimulation frequency of parallel fibers. Before (blue scN2AZ, red N2AZ; 3 µM, treated ≥1 hour prior to recording) and after application of ZX1 (black; 100 µM). (**B, E**) Time course of NMDAR EPSCs, normalized to a 5-minute baseline prior to addition of ZX1. Dotted line marks 100% of baseline. (**C, F**) Group data show ZX1 potentiation of EPSCs was significantly reduced in N2AZ- versus scN2AZ-treated slices for 20 Hz stimulation (unpaired t-test, p= 0.02, n = 14,9) and 100 Hz stimulation (unpaired t-test, p = 0.02, n = 14,9). Bar graphs represent the average potentiation of responses 10-15 minutes after ZX1 application. Error bars indicate mean ± SEM.

To control for potential off-target actions of N2AZ, we next validated that the actions of the peptide on synaptic zinc inhibition of NMDAR depend on ZnT3. To do this, we tested the effects of ZX1 on NMDAR EPSCs in N2AZ-treated slices obtained from ZnT3 null (KO) mice, lacking synaptic zinc, and wild-type (WT) littermates. As expected (Anderson *et al.*, 2015), ZX1 had similar, albeit very modest, effects on NMDAR EPSCs in both KO and WT N2AZ-treated slices (Figure 9, KO: 11.9 ± 6.90% potentiation, n=6; WT: 5.60 ± 4.38% potentiation, n=8). This finding indicates that in the absence of vesicular zinc, dissociating Glun2A from ZnT1 is of no consequence to zinc inhibition of NMDAR EPSCs.

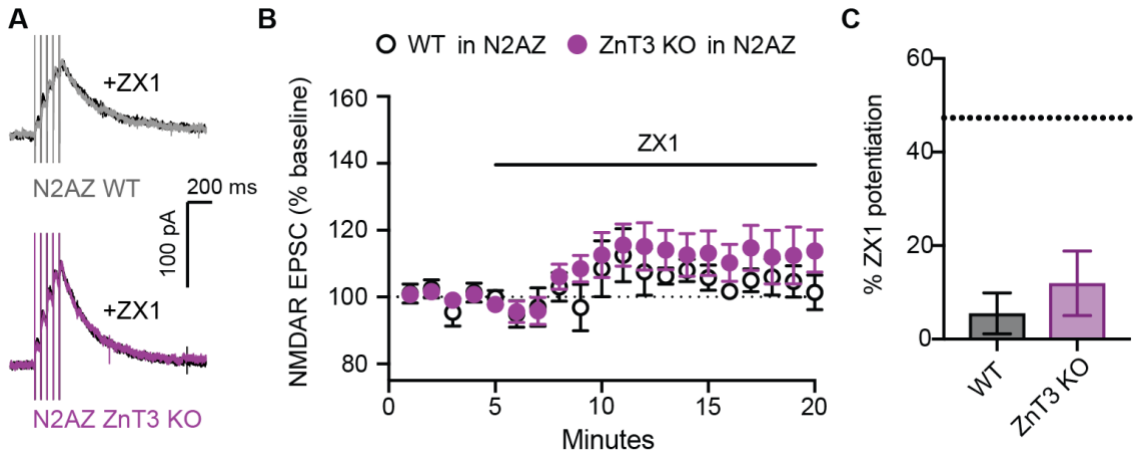

Figure 9 ZX1 has no significant effects on NMDAR EPSCs in either KO or WT N2AZ-treated slices

Legend for Figure 9: **(A)** Sample traces of NMDAR EPSCs at +40 mV, average of 5 sweeps, evoked in N2AZ treated slices (3 µM, treated ≥1 hour prior to recording) with 20 Hz stimulation of parallel fibers before (gray WT, purple ZnT3 KO) and after application of ZX1 (black, 100 µM). **(B)** Time courses of NMDAR EPSCs normalized to a 5-minute baseline in WT and ZnT3 KOs showing the effect of ZX1 on NMDAR EPSCs. Dotted line marks 100% of baseline. **(C)** Group data show ZX1 potentiation of EPSCs was not significantly different between WT (n = 8) and KOs (n = 6). Bar graphs represent the average potentiation of responses 10-15 minutes after ZX1 application. Dotted line indicates average potentiation measured following treatment of WT mice with scN2AZ as reported in **Figure 8**. Error bars indicate mean ± SEM.

Interestingly, stimulation of parallel fibers at higher frequencies (100 Hz – 150 Hz) previously uncovered a residual, ZnT3-independent component of zinc inhibition of NMDAR EPSCs (Anderson *et al.*, 2015). As such, we next evaluated the contribution of the ZnT1-GluN2A interaction to this additional mode of zinc inhibition. We found that N2AZ treatment indeed eliminated ZX1 potentiation of NMDAR EPSCs at 100 Hz stimulation frequency, suggesting that ZnT1-GluN2A interaction is also required for high stimulation frequency, ZnT3-independent zinc

inhibition (Figure 8D-F, 1.95 ± 4.33%, n=14, p = 0.45, paired t-test of responses before and after ZX1). Taken together, our results indicate ZnT1-GluN2A binding is critical for both ZnT3-dependent and high stimulus frequency, ZnT3-independent inhibition of NMDARs.

2.3.4 N2AZ effects are limited to the ZnT1-GluN2A association

In addition to blocking NMDAR, synaptically released zinc inhibits AMPAR EPSCs in cartwheel cells (Kalappa *et al.*, 2015). To test whether the aforementioned actions of N2AZ are specific for NMDAR ESPCs, we measured the effect of N2AZ and scN2AZ on zinc inhibition of AMPAR EPSCs. ZX1 potentiated AMPAR EPSCs to a similar extent regardless of the treatment with either scN2AZ or N2AZ (Figure 10; scN2AZ : 30.3 ± 10.24%, n=6; N2AZ : 29.3 ± 6.70, n=6; unpaired t-test p = 0.93), with the extent of AMPAR-mediated current potentiation being comparable to that observed in previous studies (Kalappa *et al.*, 2015). These results indicate that N2AZ reduces zinc inhibition of NMDAR ESPCs without affecting AMPAR EPSCs.

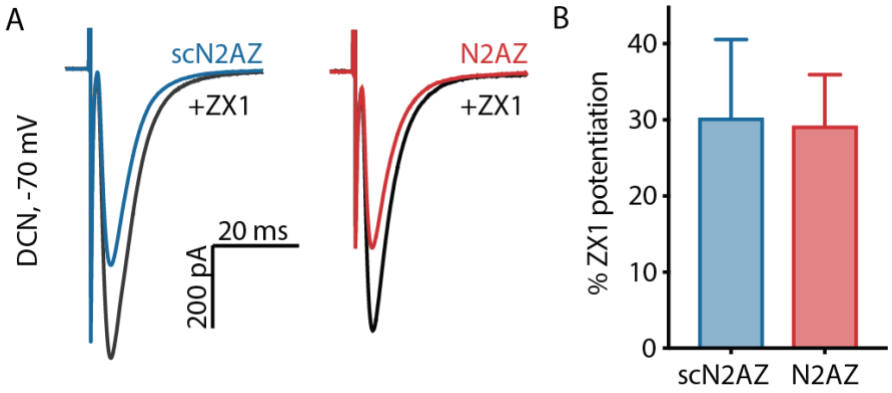

Figure 10 N2AZ does not affect zinc inhibition of AMPARs

Legend for Figure 10: (**A**) Sample traces of AMPAR EPSCs in cartwheel cells held at -70 mV, average of 5 sweeps, in response to single pulse parallel fiber stimulation (blue scN2AZ, red N2AZ; 3 µM, treated ≥ 1 hour prior to recording) and after application of ZX1 (black; 100 µM) (**B**) Group data of ZX1 potentiation of AMPAR EPSCs (n = 3) in scN2AZ and N2AZ treated groups. Bar graphs represent the average potentiation of responses 10-15 minutes after addition of ZX1. There were no differences in ZX1 potentiation of AMPAR EPSCs between these groups.

We also evaluated whether a change in presynaptic release of glutamate contributes to the observed actions of N2AZ on NMDAR-mediated synaptic currents. We used two independent measures of release probability, paired-pulse ratio (PPR) and the coefficient of variance (CV). We measured PPR by applying two stimuli in rapid succession (50 ms interpulse interval) and obtaining the amplitude ratio of the second EPSC to the first. We calculated CV as the standard deviation of a series of EPSCs divided by their mean amplitude. Both measures vary inversely with probability of release. We found that scN2AZ and N2AZ altered neither PPR nor CV (Figure 11, PPR; scN2AZ: 2.18 ± 0.26, n=3; N2AZ: 2.29 ± 0.07, n=5; unpaired t-test, p = 0.59, CV; scN2AZ: 0.28 ± 0.030, n=3; N2AZ: 0.26 ± 0.031, n=5; unpaired t-test, p = 0.76). As such, N2AZ's

effects on zinc inhibition of NMDAR-mediated synaptic currents are not associated with changes in presynaptic release probability.

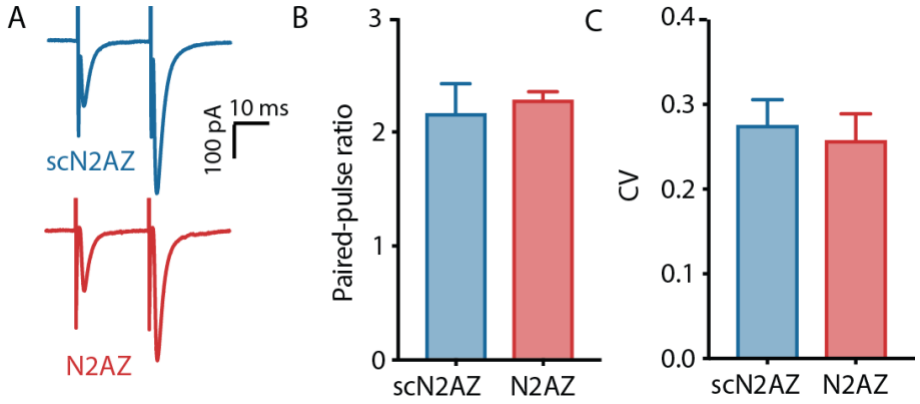

Figure 11 N2AZ does not affect probability of glutamate release

Legend for Figure 11 (**A**) Sample traces of paired-pulse of AMPAR EPSCs (50 ms interstimulus interval) showing similar facilitation in scN2AZ- (blue, top) and N2AZ- treated slices (red, bottom). (**B, C**) Group data of paired pulse ratio (PPR, D) and coefficient of variance (CV, E) show no effects in presynaptic glutamate release between scN2AZ- and N2AZ-treated slices (n = 3).

To control for potential effects of the peptide on the ZnT1 transporter activity, we next examined whether N2AZ modifies transport itself. Following intracellular zinc loading, we measured decreases in intracellular zinc levels over time as a readout of zinc transport in HEK293 cells previously transfected with a plasmid encoding ZnT1, or with an empty vector. We used FluoZin-3 fluorescence to measure intracellular zinc levels. FluoZin-3-loaded cells were briefly treated with zinc pyrithione (1 µM Zn^{2+}, 5 µM sodium pyrithione) to increase intracellular zinc concentrations until the fluorescent signal reached a maximum, steady-state level (Figure 12A). Zinc efflux was then measured as the decrease in FluoZin-3 fluorescence (Devinney *et al.*, 2005)

(Figure 12A). As expected, ZnT1-expressing cells showed significantly more zinc efflux than vector transfected controls (Figure 12B, one-way ANOVA, $p = <0.0001$, Tukey multiple comparisons N2AZ versus vector, scN2AZ versus vector, $p = <0.0001$). However, the rate of zinc efflux was not different in ZnT1-expressing cells treated with either scN2AZ or N2AZ (-0.0002273 (F/F0)/s, n=5) or scN2AZ (-0.0002327 (F/F0)/s, n=4) (Tukey multiple comparisons, N2AZ versus scN2AZ, $p = 0.97$), indicating that N2AZ's actions on zinc inhibition of NMDARs cannot be explained by alterations in ZnT1 zinc transport activity.

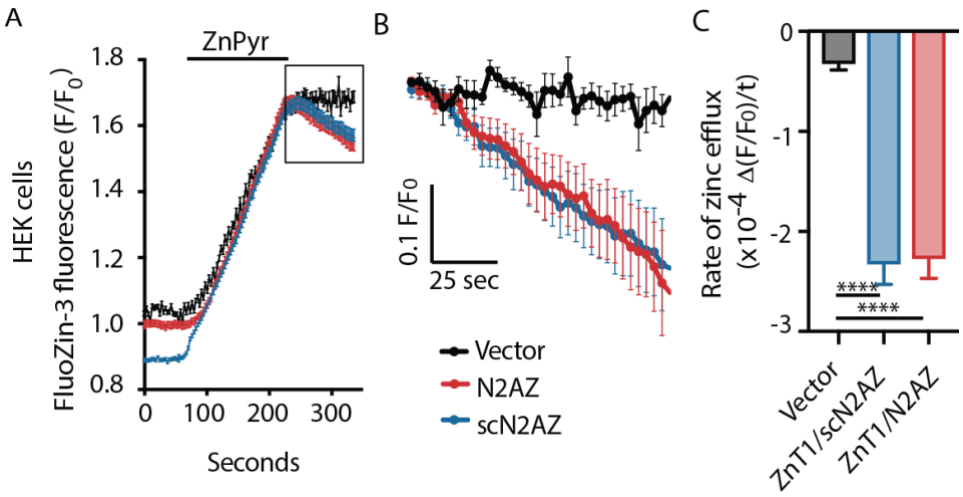

Figure 12 N2AZ does not affect ZnT1 transport activity

Legend for Figure 12: (**A**) Example traces of zinc-sensitive FluoZin-3 fluorescence from one set of coverslips of HEK293 cells transfected with vector (black), transfected with ZnT1 in addition to scN2AZ treatment (blue), or transfected with ZnT1 in addition to N2AZ treatment (red). After initial baseline fluorescence was obtained, zinc pyrithione (1 µM Zn^{2+}, 5 µM pyrithione) was added to increase intracellular zinc (black bar, above). Then zinc pyrithione was washed out and zinc efflux was measured as the decrease in FluoZin-3 fluorescence. Box indicates time epoch where zinc efflux was measured. (**B**) Average of all experiments showing the change in FluoZin-3 fluorescence following washout of zinc pyrithione (**C**) The rates of zinc efflux were determined by the slope of the average fluorescence traces in G. As expected, ZnT1-transfected N2AZ and scN2AZ treated cells exhibited greater zinc efflux compared to vector-transfected controls (one-way ANOVA, p = <0.0001, Tukey multiple comparisons N2AZ (n =4) versus vector (n=5), scN2AZ (n=4) versus vector, p = <0.0001); however, there was no difference in zinc efflux between scN2AZ and N2AZ (Tukey multiple comparisons, N2AZ versus scN2AZ, p = 0.97).

To control for potential effects of N2AZ on NMDAR affinity for zinc itself, we measured NMDAR inhibition by exogenous zinc application onto tsa201 cells previously transfected with plasmids encoding GluN1 and GluN2A. Exogenous, extracellular zinc was applied across a wide range of concentrations (1-300 µM) using a multi-barreled rapid-perfusion system while recording glutamate (1 mM)-evoked steady-state GluN1/2A receptor current. The calculated IC_{50}'s for zinc block in vehicle, scN2AZ-, or N2AZ-treated cells were not different across the three treatments (Figure 13, IC_{50} in nM; Vehicle: 21.8 ± 2.1, n = 5; scN2AZ: 23.4 ± 2.4, n = 5; N2AZ = 25.6 ± 2.2 n = 5, Ordinary one-way ANOVA, p = 0.4996), indicating that N2AZ does not affect zinc's affinity for GluN1/2A receptors. Taking all of these results together, we conclude that N2AZ reduces zinc inhibition of NMDARs by disrupting the ZnT1-GluN2A interaction, without affecting glutamate release, ZnT1-dependent zinc transport, or zinc affinity for GluN1/2A receptors. Moreover, these results suggest that N2AZ does not have either toxic or non-specific effects.

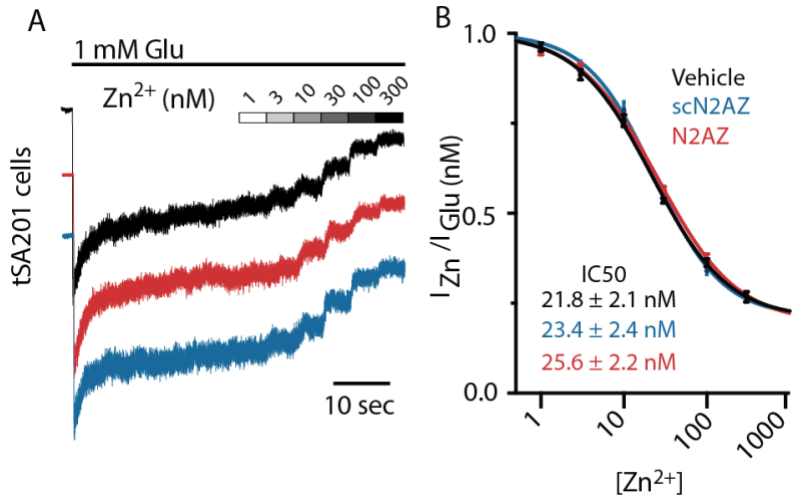

Figure 13 N2AZ does not affect exogenous zinc-mediated inhibition of GluN1/2A NMDARs

Legend for Figure 13 (**A**) Sample traces of NMDAR currents following fast application of glutamate (1 mM, Glu, black bar, above) in tsA201 cells transfected with GluN1/2A with stepwise decreases in current resulting from addition of increasing concentrations of zinc (1-300 nM). (**B**) Zinc inhibition curves showing the current measured at each concentration of zinc (I_{Zn}) divided by the current measured with glutamate application alone (I_{Glu}). Inset shows the IC_{50} for each treatment, which indicates the concentration of zinc that reduces NMDAR current in half. The IC_{50}s for vehicle (black), scN2AZ (blue), and N2AZ (red) treated cells (3 μM, ≥ 1 hour prior to recording) are not different from one another (one-way ANOVA, $p = 0.4996$, $n = 5$). Error bars indicate mean ± SEM.

2.3.5 Postsynaptic intracellular zinc is necessary for synaptic zinc inhibition of NMDARs

The simplest model to explain our results thus far is that the ZnT1-GluN2A interaction is necessary for zinc inhibition by transporting zinc from the cytoplasm of the postsynaptic cell to the extracellular space and in close proximity to the NMDAR. This model predicts that postsynaptic intracellular zinc contributes to synaptic zinc inhibition of NMDARs. Because ZX1 is cell-impermeant, we opted to selectively chelate intracellular zinc by including ZX1 in the recording pipette to test the contribution of intracellular zinc to synaptic zinc inhibition of NMDARs. ZX1 (100 μM) in the recording pipette was allowed to diffuse into the patched cell for at least 30 minutes prior to applying extracellular ZX1. We observed that intracellular ZX1 blocked extracellular ZX1 potentiation of NMDAR ESPCs (Figure 14A,B, 5.23 ± 4.22%, n=6, p = 0.64, paired t-test of responses before and after ZX1), in contrast to control experiments (no ZX1 in the recording pipette), which showed robust potentiation of NMDAR EPSCs (Figure 14A,B: 32.10 ± 6.36%, n=6, p = 0.009, paired t-test of responses before and after ZX1; Figure 14C: intracellular ZX1 versus control, p = 0.006, unpaired t-test). This result indicates that intracellular postsynaptic zinc is required for synaptic zinc inhibition of NMDARs.

We next examined whether the well-established routes of entry for zinc into neurons, including calcium-permeable AMPAR (Weiss *et al.*, 1993), and L-type calcium channels (Kerchner *et al.*, 2000b), mediate potential translocation of synaptic zinc into the cytoplasm of cartwheel cells. AMPAR were immediately ruled out by the fact that all our experiments were performed in the presence of DNQX. As prior reports have shown that L-type calcium channels can also bind to ZnT1 (Levy *et al.*, 2009; Shusterman *et al.*, 2017), we examined whether these channels contribute to synaptic zinc inhibition of NMDARs. We applied nimodipine (20 μM) for

at least 20 minutes prior to recordings, to inhibit L-type calcium channels and measured zinc inhibition of NMDAR responses. We observed no significant differences in ZX1 potentiation of NMDAR EPSCs between nimodipine-treated slices (Figure 14D-F, 23.6 ± 6.9%, n = 4) and vehicle-treated (DMSO) slices (23.6 ± 9.4% n = 6, unpaired t-test, p = 0.997), indicating that L-type calcium channels do not significantly contribute to zinc inhibition of NMDARs.

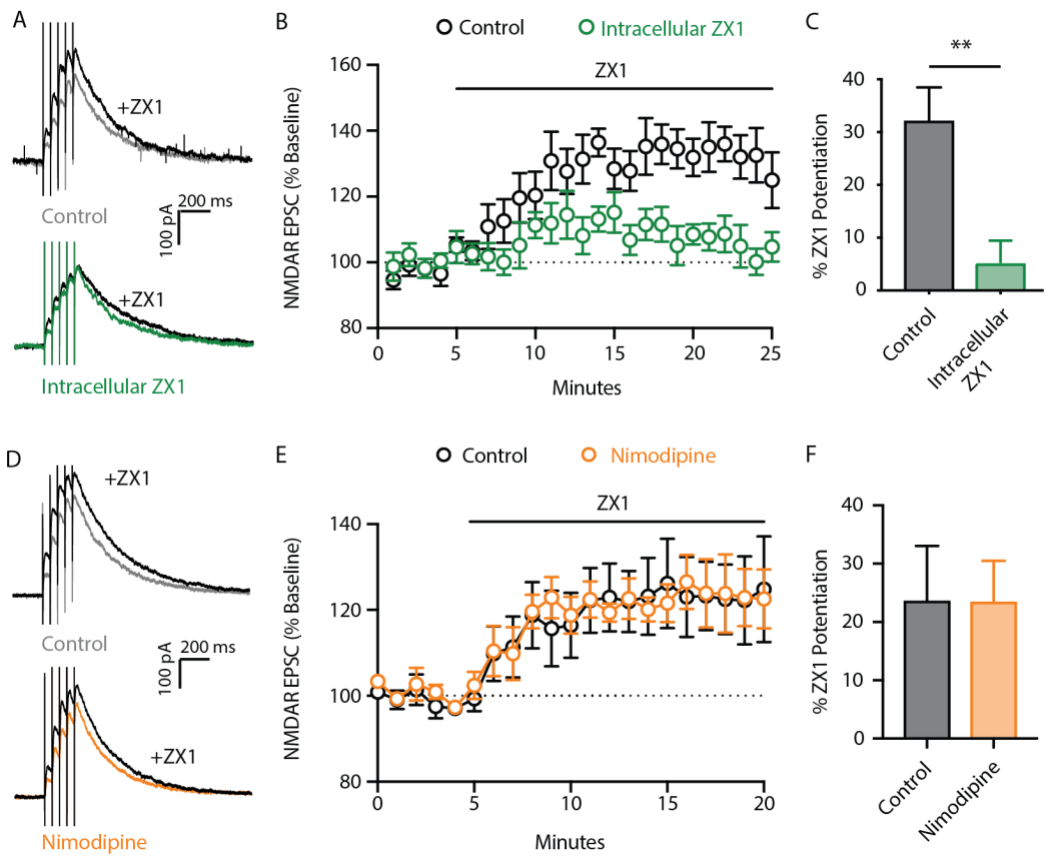

Figure 14 Chelating intracellular zinc reduces zinc inhibition of NMDAR EPSCs

Legend for Figure 14: (**A**) Sample NMDAR EPSCs at +40 mV, average of 5 sweeps, in response to five pulses at 20Hz stimulation frequency, before and after application of extracellular ZX1 (100 µM) in control (no intracellular ZX1) and in 100 µM intracellular ZX1. (**B**) Time course of NMDAR EPSCs normalized to a 5-minute baseline in control (black) and intracellular ZX1 (green) showing the effect of ZX1 on NMDAR EPSCs. Dotted line marks 100% of baseline. (**C**) Group data show that intracellular ZX1 significantly reduced extracellular ZX1 potentiation of NMDAR EPSCs compared to control (unpaired t-test, $p = 0.049$, $n = 4$ (control), 8 (intracellular ZX1)). Bar graphs represent the average potentiation of responses 15-20 minutes after ZX1 application. (**D**) Sample traces of NMDAR EPSCs at +40 mV, average of 5 sweeps, in response to five pulses at 20Hz stimulation frequency, before and after application of extracellular ZX1 (100 µM) in control (0.01% DMSO) and nimodipine (20 µM nimodipine in 0.01% DMSO, ≥ 20

minutes prior to beginning of recordings. (**E**) Time course of NMDAR EPSCs normalized to 5-minutes baseline in control (black) and extracellular nimodipine (orange) prior before and after ZX1 application (black bar, above). Dotted line marks 100% of baseline. (**F**) Group data show ZX1 potentiation was not significantly different between nimodipine and control (unpaired t-test, $p = 0.99$, $n = 6$ (control), 4 (nimodipine)). Bar graphs represent the average potentiation of responses 10-15 minutes after ZX1 application. Error bars indicate mean ± SEM.

2.4 Discussion

Current models suggest that zinc inhibition of synaptic NMDARs depends exclusively on presynaptically-released zinc. In contrast, our results indicate that zinc inhibition of NMDAR EPSCs also requires postsynaptic zinc and the presence of GluN2A-ZnT1 association. Our results demonstrate that the physical dissociation of GluN2A and ZnT1 by the newly developed peptide N2AZ diminished the inhibitory actions of synaptic zinc on NMDAR EPSCs. Moreover, chelation of postsynaptic intracellular zinc abolished zinc inhibition of NMDARs. Prior to the work presented here, it had been generally assumed that zinc cleft concentrations following its synaptic release are sufficient to directly inhibit NMDAR function (Vogt *et al.*, 2000; Pan *et al.*, 2011; Vergnano *et al.*, 2014; Anderson *et al.*, 2015; McAllister & Dyck, 2017), without involvement of the transport pathway uncovered by our work. However, here we show that ZnT1-GluN2A association is necessary for zinc to be rapidly localized to physiologically relevant microdomains in very close proximity to the GluN2A-containing NMDARs. Indeed, this is highly reminiscent of calcium microdomains that have been postulated for a number of synaptic functions, including

rapid synaptic release of neurotransmitters (Berridge, 2006). Whether similar transport processes are in place for synaptic zinc to activate or modify other known postsynaptic targets for the metal, including the metabotropic zinc receptor GPR39 (Besser *et al.*, 2009) or AMPAR-mediated synaptic currents (Kalappa *et al.*, 2015), remains to be determined.

Why is such an indirect signaling path necessary for synaptic zinc inhibition of NMDARs? This may be the result of the complex nature of zinc as a signaling molecule itself (Kay & Toth, 2008; Paoletti *et al.*, 2009; Pan *et al.*, 2011). As alluded to earlier, zinc is a promiscuous ligand that acts on a variety of postsynaptic targets (Hershfinkel *et al.*, 2001; Ruiz *et al.*, 2004; Perez-Rosello *et al.*, 2013; Kalappa *et al.*, 2015; Perez-Rosello *et al.*, 2015). Moreover, not all vesicles at zinc-rich synaptic terminals contain zinc (Wenzel *et al.*, 1997; Lavoie *et al.*, 2011), and zinc-containing vesicle release probability can change with varying levels of activity (Quinta-Ferreira & Matias, 2005; Lavoie *et al.*, 2011). Therefore, maintaining adequate signaling requires precise spatial zinc regulation, in addition to presynaptic release. The interaction between ZnT1 and GluN2A may be reflective of a system that harnesses and directs zinc's signaling properties, while supplying and maintaining specificity of action for a given activity level. As NMDAR function is regulated by subunit composition (Cull-Candy & Leszkiewicz, 2004), as well as by its localization in postsynaptic structures (Parsons & Raymond, 2014), ZnT1 may endow the zinc-containing synapse with a dynamic form of regulation specific for GluN2A-containing NMDAR signals.

ZnT1 expression is also tightly coupled to fluctuations in free intracellular zinc levels (Nishito & Kambe, 2019). Rises in intracellular zinc concentrations are quickly detected by the metal regulatory element (MRE) transcription factor 1 (MTF1) (Zhao *et al.*, 2014) to induce

upregulation of MRE-driven genes, including ZnT1 (Hardyman *et al.*, 2016). As increases in intracellular zinc levels have been prominently detected following neuronal depolarization (Li *et al.*, 2001; Sheline *et al.*, 2002), it is also conceivable that the ZnT1-GluN2A complex is a key component of activity-dependent synaptic processes, perhaps even in synapses that do not express ZnT3, and thereby, vesicular zinc. In fact, robust NMDAR activation can lead to intracellular zinc liberation from metal binding proteins such as metallothionein (Aizenman *et al.*, 2000) independent of synaptic zinc (Vander Jagt *et al.*, 2009), likely as a consequence of glutamate-stimulated production of oxygen-derived reactive species (Reynolds & Hastings, 1995). We suggest that the observed actions of N2AZ on ZnT3-independent zinc inhibition of NMDAR-mediated responses (i.e. caged glutamate responses in cortical neurons in culture and 100 Hz stimulation of parallel fibers, Figures 7 and 8E-G), may be reflective of increases of intracellular zinc in response to robust NMDAR activation produced under our experimental conditions. Interestingly, manipulations that enhance or diminish ZnT1 expression in cultured neurons have yielded subsequent increases or decreases in dendritic spine length, respectively (Mellone *et al.*, 2015). As NMDAR activation is a significant regulator of synaptic strength and spine dynamics (Segal, 2005; Sala & Segal, 2014), ZnT1-mediated zinc inhibition may provide unique forms of synaptic plasticity through its regulation of NMDAR function.

One remaining question not successfully addressed in our study is how presynaptic release of zinc and postsynaptic transport of intracellular zinc by ZnT1 cooperate to regulate NMDARs. It is tempting to assume that the source of the intracellular pool of zinc necessary for NMDAR block is derived from the synaptically released pool, translocating to the postsynaptic neuron. However, the predominant routes of entry for zinc (LTCC and AMPARs) do not appear to

contribute to zinc inhibition of NMDAR inhibition. SLC39A (ZIP) transporters, which move zinc into the cytoplasm, may serve as the route for synaptic zinc translocation, and both ZIP1 and ZIP3 have been previously observed to influence synaptic uptake of zinc, albeit under injurious conditions (Qian *et al.*, 2011). However, further experiments will be necessary to fully assess the complex interplay between ZnT3 and ZnT1 to regulate zinc's actions at the NMDAR.

In summary, we developed a cell-permeant peptide that dissociates the zinc transporter ZnT1 from the highly zinc sensitive NMDAR subunit GluN2A. This novel tool allowed us to uncover the mechanism via which zinc inhibits NMDAR function, which involves not only extracellular ZnT3-dependent zinc but also intracellular zinc and ZnT1-GluN2A complexes. We propose that the ZnT1-GluN2A association allows the synapse to direct zinc to its high affinity binding site within the GluN2A-containing NMDAR by creating a physiologically- and spatially-distinct extracellular zinc microdomain in the synapse.

2.5 Materials and Methods

2.5.1 Experimental Design and materials

All animal procedures used in experiments were approved by the Institutional Animal Care and Use Committee of the University of Pittsburgh School of Medicine. Experiments in dorsal cochlear nucleus slices were performed blind to the treatment. Experiments using ZnT3 knockout and wildtype animals were performed blind to the genotype of the animal. All key materials utilized are summarized below (Table 1).

Table 1 Key Resources

Reagent type (species) or resource	Designation	Source or reference	Identifiers
antibody	Mouse anti-GluN2A	Sigma	Cat #: SAB5200888
antibody	Chicken anti-Map2	Abcam	Cat #: ab5392
antibody	Rabbit anti-ZnT1	Alomone Labs	Cat #: AZT-011
antibody	goat anti-Flag	Sigma	Cat #: F1804
antibody	goat anti-mouse	Thermo Fisher Scientific	Cat #: SA5-10176
commercial assay or kit	Invitrogen PureLink RNA Mini Kit	Thermo Fisher Scientific	Cat #: 12183018A
commercial assay or kit	iScript Select cDNA Synthesis kit	BioRad	Cat #: 1708896
commercial assay or kit	iTaq Universal SYBR Green	BioRad	Cat #: 1725120
commercial assay or kit	Duolink® In Situ Orange Starter Kit Mouse/Rabbit	Sigma	Cat #: DUO92102
chemical compound, drug	Chelex 100 Resin	BioRad	Cat #: 1422822
chemical compound, drug	TTX	Alomone Labs	Cat #: T-550
chemical compound, drug	FuGENE 6	Promega	Cat #: E2691
chemical compound, drug	DNQX	Hello Bio	Cat #: HB0261
chemical compound, drug	QX-314	Tocris Biosciences	Cat #: 2313
chemical compound, drug	SR95531	Hello Bio	Cat #: HB0901
chemical compound, drug	Strychnine	Abcam	Cat #: ab120416
chemical compound, drug	ZX1	Strem Chemicals	Cat #: 07-0350
chemical compound, drug	MNI-caged glutamate	Tocris Biosciences	Cat #: 1490
chemical compound, drug	FluoZin-3	Thermo Fisher Scientific	Cat #: F24195

2.5.2 Neuronal Cultures

Cortical cultures were prepared from embryonic day 16 rats. Briefly, pregnant rats (Charles River Laboratory) were sacrificed via CO_2 inhalation. Embryonic cortices were dissociated with trypsin and plated at 670,000 cells per well on glass coverslips in six-well plates. Non-neuronal cell proliferation was inhibited after 2 weeks in culture with cytosine arabinoside (1–2 μM). Cultures were utilized at 3–4 weeks *in vitro* for PLA and electrophysiology experiments.

2.5.3 Cell line culture and transfection

Human embryonic kidney tsa201 cells were maintained in DMEM supplemented with 10% fetal bovine serum, 1% GlutaMAX. Cells were plated in 35 mm petri dishes with three 15 mm glass coverslips treated with poly D-lysine (0.1 mg/ml) and rat-tail collagen (0.1 mg/ml) at a density of 1 x 10^5 cells/dish. Eighteen to 30 hours after plating, the cells were co-transfected using FuGENE 6 Transfection Reagent with cDNA coding for enhanced green fluorescent protein (eGFP) for identification of transfected cells and the WT rat NMDAR subunits GluN1-1a (GluN1; GenBank X63255) and GluN2A (GenBank M91561 in pcDNA1). GluN1-1a and eGFP were expressed using a specialized pCl-neo vector with cDNA encoding eGFP inserted between the CMV promoter and the GluN1 open reading frame to express eGFP and GluN1 as separate proteins. At the time of transfection, 200 μM dl-APV was added to culture medium to prevent NMDAR-mediated cell death. For experiments testing the effect of N2AZ and scN2AZ, cells were incubated with 3 μM peptide for at least 1 hr prior to recording.

2.5.4 Proximity ligation assay

Proximity ligation assays were performed using Duolink PLA kit. Cortical cultures (3–4 weeks in vitro) were treated overnight with either N2AZ or scN2AZ (3 µM, dissolved in water). Coverslips were fixed in ice cold methanol for 5 minutes, rinsed in phosphate buffered saline (PBS) then permeabilized with 0.1% Triton-X in PBS. Coverslips were then incubated with primary antibodies: rabbit anti-ZnT1, mouse anti-GluN2A, and chicken anti-MAP2. Coverslips were incubated with a donkey anti-chicken fluorescent secondary antibody targeting MAP2 antibodies to visualize neuron morphology. The PLA reaction was then completed according to DuoLink PLA protocol. Briefly, coverslips were incubated in DuoLink secondary antibodies (anti-rabbit and anti-mouse) which are conjugated with complementary oligonucleotides. Ligation solution was added to hybridize connector oligonucleotides and PLA probes, allowing the oligonucleotides to join in a closed loop when secondary antibodies were in close proximity. Next, the reaction was amplified with rolling-circle amplification (RCA) using the closed loop hybridized probes as a template. PLA probes were fluorescently labeled with oligonucleotides which hybridized to the RCA product during amplification. Coverslips from sister cultures were treated with either scN2AZ or N2AZ and reactions were run simultaneously using the same preparation of reagents. Coverslips were mounted on glass slides using DuoLink mounting media and 4 random fields of view were imaged from each coverslip using a 60x oil objective on a Nikon A1R laser scanning confocal. PLA puncta were counted automatically with Fiji ImageJ (Version 2.0) software. We used maximum intensity projection of 8 sequential images in the z plane. All images were normalized to the same intensity threshold using the Yen threshold setting prior to automated quantification of puncta.

2.5.5 Brain Slices

Male and female mice (postpartum days 18-28) were anesthetized with isoflurane and sacrificed. Brains were rapidly dissected and sectioned with a vibratome (Leica, VT1000S) into 210 µm thick coronal slices of the brainstem containing dorsal cochlear nucleus (DCN). Slices were incubated in ACSF containing (in mM) NaCl 130, KCl 3, $CaCl_2$ 2.4, $MgCl_2$ 1.3, $NaHCO_3$ 20, HEPES 3, and glucose 10, saturated with 95% O_2/5% CO_2 (vol/vol), pH ~7.3, ~300 mOsm at 35 °C for 1 h before being moved to room temperature. During preparation, ACSF was treated with Chelex 100 resin to remove any contaminating zinc. After applying Chelex to the ACSF, high-purity calcium and magnesium salts were added (99.995% purity). All plastic and glassware were washed with 5% high-purity nitric acid.

2.5.6 Electrophysiology

Whole-cell voltage-clamp recordings from tsa201 cells were performed 18-30 hours after transfection. Pipettes were fabricated from borosilicate capillary tubing (OD = 1.5 mm, ID = 0.86) using a Flaming Brown P-97 electrode puller (Sutter Instruments) and fire-polished to a resistance of 2.5 – 4.5 MΩ with an in-house fabricated microforge. Intracellular pipette solutions consisted of (in mM): 130 CsCl, 10 HEPES, 10 BAPTA, and 4 MgATP with pH balanced to 7.2 ± 0.05 using CsOH and final osmolality of 280 ± 10 mOsm. Extracellular recording solution contained (in mM): 140 NaCl, 2.8 KCl, 1 $CaCl_2$, 10 HEPES, 10 tricine, and 0.1 glycine and was balanced to pH 7.2 ± 0.05 and osmolality 290 ± 10 mOsm with NaOH and sucrose, respectively. Glutamate (Glu), and $ZnCl_2$ were diluted from concentrated stock solutions in extracellular solution each day of

experiments. Buffered Zn^{2+} solutions were prepared as previously described (Paoletti *et al.*, 1997) via serial dilution. Extracellular solutions were delivered to the cell using a fast perfusion system. Whole-cell currents were recorded using an Axopatch 200A patch-clamp amplifier (Molecular Devices), low-pass filtered at 5 kHz, and sampled at 20 kHz in pClamp10.7 (Molecular Devices). In all recordings from tsa201 cells, series resistance was compensated 85-90% and an empirically determined -6 mV liquid junction potential between the intracellular pipette solution and the extracellular recording solution was corrected.

The effect of the N2AZ on Zn^{2+} inhibition of GluN1/2A receptors was determined using the protocol shown in Fig 5I. 1 mM Glu was applied for 30 s until current reached steady-state, followed by sequential applications (5 s each) of 1 mM Glu and Zn^{2+} at 1, 3, 10, 30, 100, and 300 nM. A final 30 s application of Glu in the absence of Zn^{2+} was then performed to allow recovery from inhibition. Zn^{2+} IC_{50} was estimated by fitting the following equation to data:

$$\frac{I_{Zn}}{I_{Glu}} = A + \frac{1 - A}{1 + (\frac{[Zn^{2+}]}{IC_{50}})^{n_H}}$$

where I_{Zn}/I_{Glu} was calculated as the mean current over the final 1 s of Zn^{2+} application divided by the average of the mean steady state currents (final 1 s) elicited by Glu before and after Zn^{2+} application. A (I_{Zn}/I_{Glu} at saturating Zn^{2+}), IC_{50}, and n_H (Hill coefficient) were free parameters during fitting. Curve fitting and statistical comparisons were performed in Prism 8. IC_{50}s were compared by one-way ANOVA.

Whole-cell recordings from cultured cortical neurons were obtained with glass micropipettes (3-6 MΩ) containing (in mM): 140 CsF, 10 CsEGTA, 1 $CaCl_2$, 10 HEPES, pH =

7.2, 295 mOsm. Extracellular recording solution contained (in mM): 150 NaCl, 2.8 KCl, 1.0 $CaCl_2$, 10 HEPES, 10 µM glycine, pH = ~7.2, ~300 mOsm. Using *Ephus* (Suter *et al.*, 2010) and a Multiclamp 700B amplifier (Molecular Devices), NMDAR EPSCs were recorded in voltage clamp (held at -70 mV) in the presence of TTX (300 nM, sodium channel blocker), DNQX (20 µM, AMPA and kainate receptor antagonist), and 4-Methoxy-7-nitroindolinyl (MNI)-caged glutamate (40 µM). Neurons were visualized by including 10 µM Alexa 594 in the internal solution. To evoke NMDAR EPSCs, we photolytically uncaged MNI-caged glutamate onto dendrites at four locations 0, 40, 80, and 120 µm from the cell soma using 1 ms pulses of UV-laser light (355 nm, DPSS Lasers). The ZX1-mediated potentiation for each cell was calculated as the average percent increase in responses following application of the metal chelator across these 4 uncaging locations.

For brain slice recordings, whole-cell recordings of NMDAR EPSCs of DCN cartwheel cells were obtained with micropipettes (3-6 MΩ) containing (in mM) 128 $Cs(CH_3O_3S)$, 4 $MgCl_2 \cdot 6H_2O$, 4 Na_2ATP, 10 HEPES, 0.3 Tris-GTP, 10 Tris-phosphocreatine, 1 CsEGTA, 1 QX-314, 3 sodium ascorbate, pH = ~7.2, 300 mOsm in chelexed ACSF with the following composition: (in mM) NaCl 130, KCl 3, $CaCl_2$ 2.4, $MgCl_2$ 1.3, $NaHCO_3$ 20, HEPES 3, and glucose 10, saturated with 95% O_2/5% CO_2 (vol/vol), pH ~7.3, ~300 mOsm. Cartwheel cells were identified by the presence of complex spikes (Tzounopoulos *et al.*, 2004) in cell-attached configuration before break-in or in response to current injections in current-clamp mode immediately after break-in. NMDAR EPSCs were recorded in voltage clamp mode, at a holding potential of +40 mV, in the presence of DNQX (20 µM), SR95531 (20 µM, $GABA_AR$ antagonist), and strychnine (1 µM, GlyR antagonist). ZX1 (100 µM) was included in the pipette in experiments where noted. Whole-cell recordings of AMPAR EPSCs were obtained with micropipettes containing (in mM) 113 K-

gluconate, 4.5 $MgCl_2$•6 H_2O, 14 Tris-phosphocreatine, 9 HEPES, 0.1 EGTA, 4 Na_2ATP, 0,3 Tris-GTP, 10 sucrose, pH = 7.3, 295 mOsm. AMPAR EPSCs were recorded in voltage clamp mode at a holding potential of -70 mV in the presence of SR9551 (20 μM) and strychnine (1 μM). Both NMDAR and AMPAR EPSCs were evoked using an Isoflex stimulator (A.M.P.I, 0.1 ms pulses) stimulating parallel fibers with voltage pulses through a theta glass electrode. For paired-pulse experiments, inter-stimulus interval was 50 ms. Once a stable response was established, ZX1 (100 μM) was added to the recording solution to measure the effect of zinc chelation on EPSCs. The series resistance was not compensated because the currents measured were relatively small, therefore there was minimum voltage clamp error. The cell parameters were monitored during the recording by delivering −5 mV voltage steps for 50 msec at each sweep. The peak current value (ΔI_{peak}) generated immediately after the step in the command potential was used to calculate series resistance (R_{series}) using the following formula: R_{series} = -5 mv/ ΔI_{peak}. The difference between baseline and steady-state current (ΔI_{ss}) was used to calculate input resistance (R_I) using the following formula: $R_I = -5\ mV/\Delta I - R_{series}$. Recordings were excluded from further analysis if the series resistance or input resistance changed by more than 20% compared to the baseline period. Data were low-pass-filtered at 4 kHz and sampled at 10 kHz. NMDAR EPSC peak values were averaged over a 20-ms time window using custom Matlab 2012a software. All values reported are animal-based values, in cases where multiple cells were recorded from the same animal preparation, the average of cells is presented. All recordings were performed at room temperature.

2.5.7 Quantitative real-time PCR (qPCR)

For qPCR analysis of rat cortical cultures, cells were harvested at 5, 12, 19, and 26 DIV and RNA was isolated using Invitrogen PureLink RNA Mini Kit. cDNA was synthesized from RNA transcripts using iScript Select cDNA Synthesis kit using Eppendorf Thermocycler. qRT-PCRs were performed on a Bio-Rad CFX qRT-PCR machine using iTaq Universal SYBR Green Supermix. Relative expression was calculated using α-actin as a reference gene. Custom primers against rat β-actin (Forward: TTCAACACCCCAGCCATGT Reverse: GCATACAGGGACAACACAGCC; Invitrogen) and rat ZnT1 (Forward: TGGGCGCTGACGCTTACT; Reverse: GTCAGCCGTGGAGTCAATAGC; Invitrogen) were designed using NCBI Primer-BLAST.

2.5.8 Zinc efflux assay

HEK293 cells were grown in Dulbecco's modified Eagle's medium (DMEM) containing: 100 units/ml penicillin, 0.1 mg/ml streptomycin, 2 mm glutamine, and 10% (v/v) fetal calf serum in a 5% CO2 humidified atmosphere at 37 °C. To express ZnT1, HEK 293 cells were transfected with ZnT1 or empty plasmid (control) using $CaPO_4$ precipitation. Briefly,1 μg mouse ZnT-1 (pCMV6; ZnT1 GenBank Q60738) or empty vector plasmid (pCMV6, Origene) were incubated with 2 M calcium chloride in HEPES buffered solution containing 1.5 mM Na_2HPO_4 to generate a co-precipitate, this solution was then dispersed onto cultured cells for 6 hours. Twenty-four hours later, cells were treated overnight with N2AZ or scN2AZ (3 μM). To visualize intracellular zinc, cells were loaded with the fluorescent zinc indicator FluoZin-3 (2 μM) for 25 min at room

temperature before imaging. Cells were imaged using 480 nm excitation filter and an emission 525 nm long pass filter on a Zeiss Axiovert 100 inverted microscope with a Polychrome IV monochromator (T.I.L.L. Photonics) and a cooled CCD camera (PCO). To measure zinc efflux, cells were superfused with Ringer's solution (composition in mM: NaCl 120, MgCl 0.8, KCl 5.4, CaCl 1.8, HEPES 20, glucose 15) and 1 μM Zn^{2+} with 5 μM pyrithione were added for 150 seconds. The FluoZin-3 signal was normalized to 10 second baseline in each experiment. Rates of initial decrease of the fluorescent signal following removal of Zn^{2+} pyrithione were determined during a 100 second period. For each experiment, at least 30 cells were imaged per coverslip and rates were averaged for 3-5 coverslips performed as 3 independent experiments. Fluorescence imaging measurements were acquired using Axon Imaging Workbench 5.2 (INDEC BioSystems) and analyzed using Excel and Prism GraphPad.

2.5.9 Peptide spot array and far-Western assay

Far-Western protein-binding affinity assays were performed as previously described (Yeh *et al.*, 2017). Peptide spot arrays (15-mers) spanning the proximal C-terminus residues 1390–1464 of mouse GluN2A (Uniprot# P35436) in overlapping 1 residue steps were constructed using the Spots-synthesis method. Standard 9-fluorenylmethoxy carbonyl (Fmoc) chemistry was used to synthesize the peptides and spot them onto nitrocellulose membranes, which were pre-derivatized with a polyethylene glycerol spacer (Intavis). Fmoc protected and activated amino acids were spotted in 20–30 arrays on 150 by 100 mm membranes using an Intavis MultiPep robot. The nitrocellulose membrane containing the immobilized peptides was soaked in N-cyclohexyl-3-aminopropanesulfonic acid (CAPS) buffer (10 mM CAPS, pH 11.0, with 20% v/v methanol) for

30 min, washed once with Tris-buffered 0.1% Tween 20 (TBST), and then blocked for 1 h at room temperature (RT) with gentle shaking in TBST containing 5% (w/v) nonfat milk and then incubated with enriched Flag-tagged ZnT1 (SLC30a1) protein overnight at 4°C with gentle shaking. Next, the membrane was incubated in primary antibody for Flag for 1 hr at RT with gentle shaking, followed by washing with TBST. Finally, the membrane was incubated in secondary antibody for 45 min, washed for 3 times 5 min in TBST, and then visualized by infrared fluorescence (Li-Cor). Four independent peptide spot arrays were used in this study. A second set of membranes (n = 4) was treated as above, but also in the presence of 100 µM of either N2AZ or scN2AZ and compared to 0.1% DMSO. For each experiment, an additional peptide array was done with omission of Flag-tagged ZnT1 (SLC30a1) protein to measure and correct for the background due to the primary and secondary antibodies.

2.5.10 Statistical Analyses

Slice electrophysiology experiments using N2AZ and scN2AZ were completed blind to the identity of the peptide. Experiments in ZnT3 knockout and wild type animals were completed blind to the genotype. Electrophysiology recordings in cortical cultures and DCN slices were obtained using *Ephus* (Suter *et al.*, 2010) software run in Matlab 2012a (MathWorks). Cell parameters and response peaks were calculated using custom Matlab scripts. For neuronal culture electrophysiology, ZX1 potentiation was measured as the percent increase in NMDAR amplitude 5 minutes after the application of ZX1. In slice experiments, ZX1 potentiation was calculated as the average percent increase over baseline of NMDAR or AMPAR EPSCs 10-15 minutes after the addition of ZX1 (Figures 8,9,10 & 14D-F) or 15-20 minutes after the addition of ZX1 (Figure

14A-C). Un-paired t-tests and ANOVAs were used to compare between treatments or genotypes. To determine if ZX1 significantly potentiated responses, paired t-tests were used to compare amplitude of peak responses before and after addition of ZX1. Statistical analysis was completed in Prism 8 (GraphPad).

3.0 Chapter 3: Zinc-dependent Upregulation of ZnT1 Enhances Zinc Inhibition of NMDA Receptors

3.1 Overview

Zinc is loaded into a subset of glutamate-containing presynaptic vesicles by the transporter ZnT3 and is synaptically released in an activity-dependent manner. Zinc modulates neurotransmission through its actions on postsynaptic receptors, including high-affinity inhibition of NMDA receptors. Recently, an additional postsynaptic mechanism of transport was identified that critically regulates endogenous zinc inhibition of NMDARs. In this new model of zinc regulation, the postsynaptic transporter ZnT1 mediates zinc inhibition of NMDARs through its interaction with the highly zinc-sensitive GluN2A subunit. This positions ZnT1, a transporter which moves zinc from the cytoplasm to the extracellular domain, as a direct regulator of NMDAR-mediated neurotransmission. ZnT1 expression is transcriptionally driven by the metal-responsive transcription factor 1 (MTF-1). When MTF-1 binds zinc, it translocates to the nucleus and engages metal response elements (MRE) on zinc-regulated genes, including ZnT1, to upregulate expression. In this study, we found that increasing intracellular zinc strongly drives the MRE/MTF-1 system in cortical neurons *in vitro*, increases the number of GluN2A-ZnT1 interactions, and enhances zinc inhibition of NMDARs. Importantly, this effect is absent when the interaction between GluN2A and ZnT1 is disrupted by a cell-permeable peptide. Together, these results suggest that alterations in intracellular zinc levels can dynamically regulate NMDAR transmission by upregulating ZnT1-mediated inhibition.

3.2 Introduction

Zinc is a neuromodulator with diverse roles in synaptic transmission, synaptic plasticity, and sensory processing (McAllister & Dyck, 2017). The majority of loosely bound, so-called 'labile' zinc in the brain is found in presynaptic vesicles in a subset of glutamatergic neurons throughout the cerebral cortex, hippocampus, amygdala, and auditory brainstem (Cole *et al.*, 1999). These zinc-containing neurons package zinc into vesicles using the transporter ZnT3 and release it in an activity-dependent manner (Palmiter *et al.*, 1996; Anderson *et al.*, 2015). The ion acts on multiple postsynaptic receptors to modulate both excitatory (Westbrook & Mayer, 1987; Kalappa *et al.*, 2015) and inhibitory (Bloomenthal *et al.*, 1994; Hosie *et al.*, 2003) transmission. Notably, zinc inhibits NMDA receptors through an allosteric binding site on the N-terminal domain of the GluN2 subunit (Paoletti *et al.*, 2000; Erreger & Traynelis, 2008). GluN2A-containing NMDARs are the most sensitive receptors and require just nanomolar concentrations of the metal for inhibition (Paoletti *et al.*, 1997).

Multiple mechanisms generate transient increases in intracellular zinc, including translocation of vesicular zinc into the postsynaptic cell (Li *et al.*, 2001), as well as liberation of zinc from intracellular stores (Dineley *et al.*, 2008; Kiedrowski, 2012; Sanford *et al.*, 2019). Intracellular zinc influences a variety of signaling pathways, including gene transcription (Smirnova *et al.*, 2000), kinase signaling cascades (Murakami *et al.*, 1987; Seo *et al.*, 2001), and cell death signaling cascades (Aizenman, 2019). To terminate signaling, zinc must be bound or sequestered away from its signaling targets. Indeed, a complex system of zinc transporters and metalloproteins work together to regulate the localization and concentration of zinc, including at

least twenty four different zinc transporters (Colvin *et al.*, 2000; Colvin *et al.*, 2010). However, it remains unclear how the regulation of zinc in neurons contributes to synaptic function.

Previously it was assumed that presynaptic release and diffusion across the cleft was sufficient to explain the modulatory actions of zinc (Vergnano *et al.*, 2014). However, recent work revealed an additional postsynaptic mechanism where the transporter ZnT1 is necessary for NMDARs inhibition (Krall *et al.*, 2020). ZnT1, which transports zinc from the cytoplasm to the extracellular space, binds directly to the GluN2A subunit of NMDARs (Mellone *et al.*, 2015). Disrupting this interaction between GluN2A and ZnT1 blocks endogenous zinc inhibition of NMDARs. Furthermore, chelating intracellular zinc, thus removing ZnT1's source, is also sufficient to prevent zinc inhibition of NMDARs (Krall *et al.*, 2020). Therefore, ZnT1 critically regulates the localization and concentration of zinc to drive endogenous NMDAR inhibition. This reveals that regulation of zinc in the synapse is more complex than previously assumed.

ZnT1 expression levels are not static, but instead dynamically respond to intracellular zinc state through transcriptional regulation. When intracellular zinc increases, it binds to the metal regulatory transcription factor 1 (MTF-1) (Dalton *et al.*, 1997). MTF-1 rapidly translocates to the nucleus where it binds to metal response elements (MRE) on target genes to regulate transcription (Westin & Schaffner, 1988; Smirnova *et al.*, 2000). The ZnT1 gene, SLC30A1, contains two MRE tandem sequences in its promotor region, such that ZnT1 is rapidly upregulated following MTF-1 activation (Langmade *et al.*, 2000). This zinc-induced upregulation of ZnT1 protects cells against zinc toxicity (Palmiter, 2004), suggesting that the MRE/MTF-1 system functionally increases zinc efflux in response to the zinc state. Given that ZnT1 also regulates zinc inhibition of NMDARs,

MTF-1 driven upregulation may be a novel mechanism regulating NMDAR-mediated neurotransmission. Here, we test the hypothesis that zinc-induced upregulation of ZnT1 enhances inhibition of NMDARs via its interaction with GluN2A.

3.3 Results

3.3.1 Zinc Pyrithione drives MRE-regulated expression

The aim of this study was to examine if ZnT1-mediated inhibition of NMDARs dynamically changes in response to cellular zinc state. Therefore, we first needed to identify a treatment to sufficiently increase zinc to activate MTF-1 without itself causing neuronal injury (Choi *et al.*, 1988). To rapidly increase intracellular zinc, we utilized the zinc ionophore pyrithione. This allowed for the use of lower, sub-lethal concentrations of zinc (10 µM) because it circumvents use of endogenous transport systems or ion channels for entry into the cell, thus reducing off target signaling that could be triggered by higher concentrations of zinc (Sensi *et al.*, 1997).

To determine if ZnPyr treatment is sufficient to activate MTF-1 driven gene expression, we used a MRE-luciferase assay, as described previously (Hara & Aizenman, 2004). In this assay, neurons are transfected with a plasmid encoding a firefly luciferase with an MRE sequence in the promoter. Firefly luciferase activity is then assayed and serves as a measure of MRE-driven gene upregulation. As a control for transfection efficacy, a non-inducible *Renilla* luciferase is also transfected and assayed. One day after transfection, neurons were treated with pyrithione (250 nM, Pyr) alone or in conjunction with zinc (10 µM, ZnPyr) overnight. Zinc-induced gene expression

was quantified by measuring both *Renilla* and firefly luciferase activity and taking the ratio of Firefly/*Renilla* activity. We observed that ZnPyr led to a significant increase in MRE-driven transcription and subsequent Firefly/*Renilla* luciferase activity (6.41 ± 0.90, n = 5) compared to Pyr (2.7 ± 0.18, n = 3;) and untreated controls (3.77 ± 0.29, n = 12) (Figure 15, One-way ANOVA: p = 0.0012, Sidak multiple comparisons: Control versus Pyr, p = 0.5; Control versus ZnPyr, p = 0.003; Pyr versus ZnPyr, p = 0.004). A significant level of MRE-driven luciferase expression was observed with this treatment protocol with no observable damage to the cells, therefore this treatment was utilized in subsequent experiments.

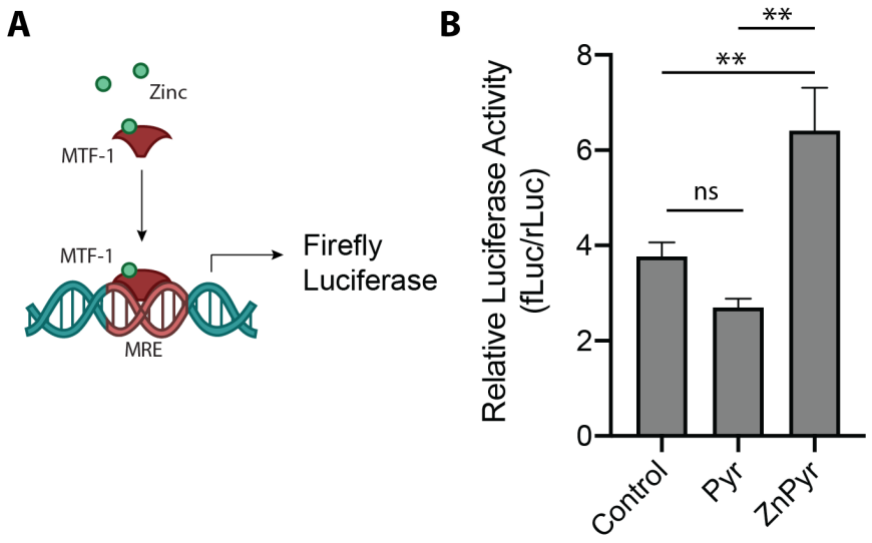

Figure 15 ZnPyr treatment induces MRE-drive gene transcription

Legend for Figure 15: (**A**) Schematic of the luciferase assay showing binding of zinc to MTF1 and subsequent upregulation of firefly luciferase. (**B**)The average ratio of MRE-driven firefly luciferase activity to *Renilla* luciferase activity for untreated, Pyr (250 nM), or ZnPyr (10 µM $ZnCl_2$, 250 nM Pyr) treated neurons (One-way ANOVA, p = 0.0012; Control, n =12; Pyr, n = 3; ZnPyr, n =5). ZnPyr treatment led to a significant increase in firefly/*Renilla* activity compared to control (Sidak multiple comparisons, p = 0.004) and Pyr (p = 0.003) No significant increase was observed with Pyr treatment compared to control (p = 0.5). Error bars indicate mean ± SEM.

3.3.2 ZnT1-GluN2A interactions are upregulated with increased intracellular zinc

Next we aimed to determine if intracellular zinc and MRE-driven gene expression leads to an upregulation of GluN2A-ZnT1 interactions in neurons. To accomplish this, we used a proximity ligation assay that fluorescently labels locations where GluN2A and ZnT1 are within 40 nm of each other (Krall *et al.*, 2020). Neurons were treated overnight either with ZnPyr (10 µM $ZnCl_2$, 250 nM Pyr) to increase intracellular zinc levels or Pyr alone as a control. We hypothesized that

ZnPyr would increase the number of PLA puncta by increasing the instances GluN2A-ZnT1 interactions. Alternatively, ZnPyr treatment could simply increase the likelihood of ZnT1 being in the proximity of GluN2A, with no change in its direct interaction with GluN2A. To distinguish between these two possibilities, neurons were treated overnight with a cell-permeant peptide that specifically disrupts GluN2A-ZnT1 interaction (N2AZ, 3 µM) or its scramble control (scN2AZ, 3 µM) (Krall *et al.*, 2020).

We found that in scN2AZ treated cells, ZnPyr led to an average 2.4-fold increase in PLA puncta compared to sister coverslips treated with Pyr (Figure 16A,C; 2.4 ± 0.23 ZnPyr puncta/Pyr puncta; n=4), suggesting that zinc upregulates ZnT1-GluN2A interactions. N2AZ treated cells exhibited no increase with ZnPyr treatment compared to Pyr control (Figure 16B,C; 0.986 ± 0.33 ZnPyr puncta/Pyr puncta ; n=3). The zinc-induced increase in PLA puncta was significantly different between N2AZ and scN2AZ treated neurons (Figure 16C, Unpaired t-test, $p = 0.017$). This indicates that zinc treatment upregulates the number of GluN2A-ZnT1 interactions in neurons. This upregulation is blocked by specific disruption of GluN2A-ZnT1 by N2AZ, suggesting that the increase is not an epiphenomenon of increased ZnT1 expression.

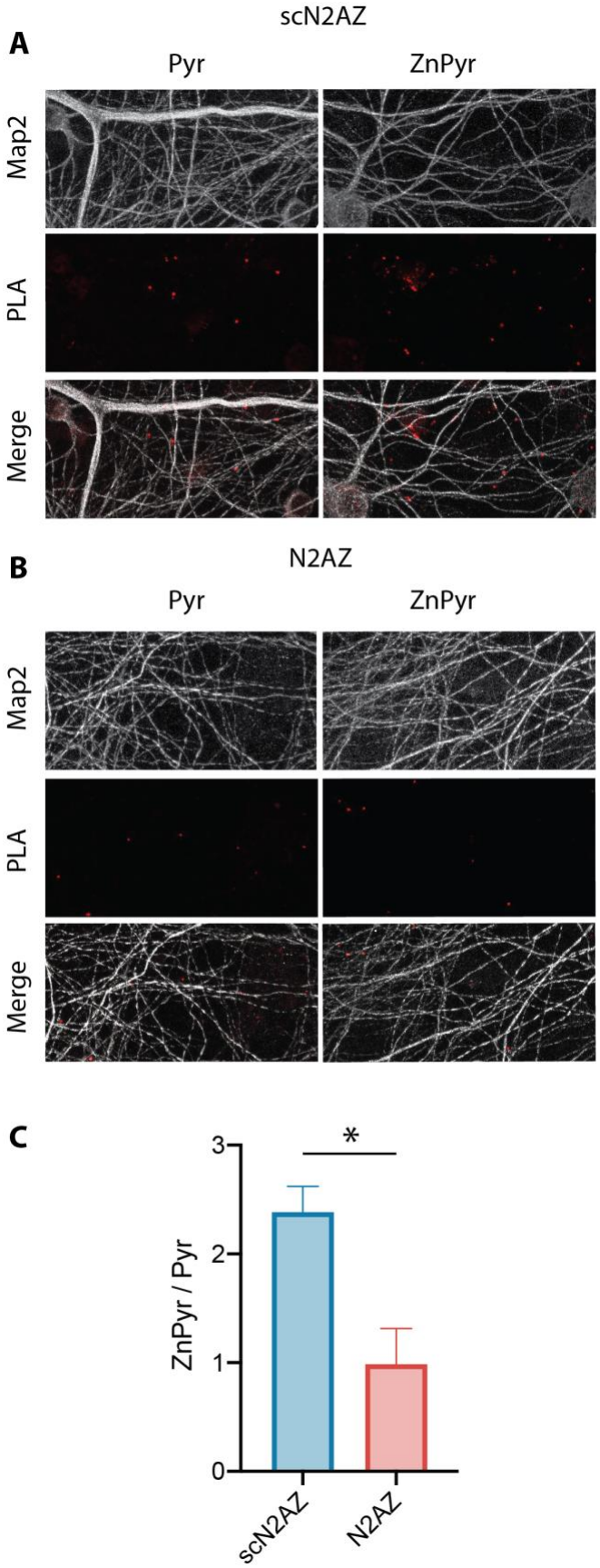
A
scN2AZ
Pyr
ZnPyr
Map2
PLA
Merge
B
N2AZ
Pyr
ZnPyr
Map2
PLA
Merge
C
*
ZnPyr / Pyr
0
1
2
3
scN2AZ
N2AZ

Figure 16 ZnPyr increases GluN2A-ZnT1 interactions in scN2AZ but not N2AZ treated neurons

Legend for Figure 16: Representative images of rat cortical cultures following proximity ligation assay (PLA) of GluN2A and ZnT1 in scN2AZ (**A**) and N2AZ (**B**) treated cultures, comparing Pyr (left column) to ZnPyr (right column) treated cells. Top row shows MAP2 immunofluorescently labeled in white to visualize neuron morphology. Middle row shows the PLA sites of interaction between GluN2A and ZnT1 (red puncta). Bottom row shows the merged images. (**C**) Quantification of the average ratio of ZnPyr to Pyr PLA puncta counts in scN2AZ (blue) and N2AZ (red) treated neurons. scN2AZ treated neurons exhibited a significantly higher ratio compared to N2AZ (unpaired t-test, $p = 0.017$, $n = 4,3$). Error bars indicate mean ± SEM.

3.3.3 Increasing intracellular zinc leads to enhanced ZnT1-mediated zinc inhibition of NMDARs

Previously, we showed that the interaction between GluN2A and ZnT1 is critical for endogenous zinc inhibition of NMDAR currents in cortical cultures (Krall *et al.*, 2020). We therefore hypothesized that upregulating the GluN2A-ZnT1 interaction would increase zinc inhibition of NMDARs. To test this, we used whole-cell recording of cultured neurons under voltage clamp, held at -70 mV in magnesium-free conditions, and evoked NMDAR responses by photolytically uncaging glutamate onto the cell. Similar to PLA experiments, neurons were previously treated overnight with either Pyr or ZnPyr, in the presence of scN2AZ or N2AZ to determine if increasing intracellular zinc increases ZnT1-dependent zinc inhibition of NMDARs. Zinc inhibition was determined by measuring the potentiation of NMDAR responses after the addition of the high affinity zinc chelator, ZX1 (100 µM). We found that in scN2AZ treated

neurons, ZnPyr led to a significant increase in ZX1-dependent NMDAR potentiation compared to Pyr controls (Figure 17A, Pyr: 14.65 ± 6.90 %; ZnPyr: 40.37 ± 9.04%, unpaired t-test, p = 0.04; n = 8). In contrast, NMDAR-mediated currents in N2AZ treated cells did not appear to potentiate following ZX1 treatment and there were no significant differences between Pyr and ZnPyr treated groups. (Figure 17C, Pyr: -3.12 ± 3.54 %; ZnPyr: 1.69 ± 10.00 %, unpaired t-test, p = 0.68, n = 7). Together, these data suggest that increasing intracellular zinc with ZnPyr upregulates ZnT1-mediated zinc inhibition of NMDARs.

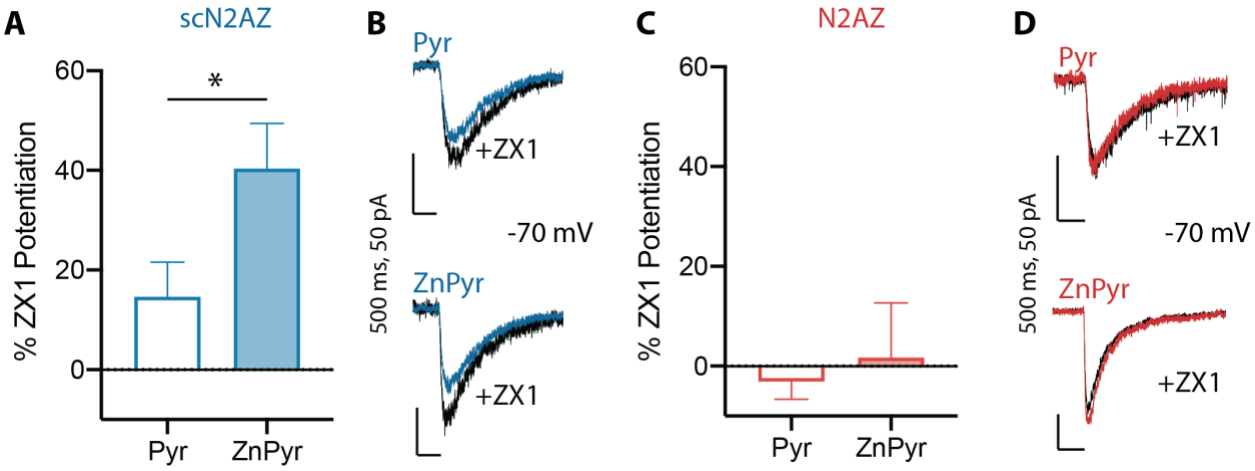

Figure 17 ZnPyr increases ZnT1-dependent zinc inhibition of NMDARs

Legend for Figure 17: (**A,C**) ZX1 potentiation of NMDAR currents was significantly increased between ZnPyr and Pyr groups in scN2AZ treated neurons (A, unpaired t-test, p = 0.04, n = 8). However, no significant differences were seen in N2AZ treated neurons (C, unpaired t-test, p = .068, n =7). Bar graphs represent the average potentiation of responses 10 minutes after ZX1 application. Error bars indicate mean ± SEM. (**B,D**) Sample traces of NMDAR currents from scN2AZ (B) and N2AZ (D) treated groups, averaged over 10 sweeps, evoked by photolysis of MNI-caged glutamate in cultured cortical neurons held at -70 mV in Mg^{2+} free solution, before (blue, scN2AZ; red, N2AZ, 3 µM) and after application of ZX1 (black; 100 µM).

3.4 Discussion

A growing body of literature is uncovering the diverse roles of zinc as a dynamic signaling ion with a complex system of regulation (McAllister & Dyck, 2017). In this study, we found a novel role of zinc-regulated gene expression, in which intracellular zinc enhances inhibition of NMDARs via increased interactions between the zinc transporter ZnT1 and the GluN2A subunit. This suggests that ZnT1's regulation of glutamatergic transmission can be strongly influenced by changes in intracellular zinc concentrations. Previous studies have shown that increases in intracellular zinc can drive ZnT1 expression to protect against zinc toxicity (Palmiter, 2004), consistent with its documented role for maintenance of zinc homeostasis (Palmiter & Findley, 1995). This study expands on the role of zinc-dependent regulation of ZnT1 to reveal an additional influence on NMDAR-mediated transmission. Glutamate, in addition to activating NMDARs, has been associated with postsynaptic increases in intracellular zinc (Dineley *et al.*, 2008). Therefore, intracellular zinc may act as a signal to increase NMDAR inhibition following activation through upregulation of ZnT1-mediated zinc transport.

Although this study used exogenous zinc to alter intracellular levels, multiple endogenous mechanisms increase postsynaptic zinc, as mentioned above. Chemical stimulation with either glutamate or KCl generates postsynaptic zinc transients in neurons (Dineley *et al.*, 2008; Ha *et al.*, 2018; Sanford *et al.*, 2019; Sanford & Palmer, 2020). These may occur either through uptake of synaptically released zinc or liberation of the ion from intracellular stores. Multiple channels conduct zinc into the cell, including calcium permeable AMPA receptors (Jia *et al.*, 2002), NMDARs (Koh & Choi, 1994; Marin *et al.*, 2000), L-type calcium channels (Kerchner *et al.*, 2000a), and TRP channels (Hu *et al.*, 2009; Inoue *et al.*, 2010). Zinc influx has been linked to zinc

toxicity in multiple pathological conditions including seizures (Frederickson *et al.*, 1989), ischemia (Koh *et al.*, 1996) and traumatic brain injury (Suh *et al.*, 2000), and, as such, the mechanism uncovered here may be a protective mechanism to minimize cell injury.

In addition to zinc influx, multiple studies have found that zinc transients are induced by neuronal stimulation even in the presence of extracellular zinc chelators, suggesting an intracellular origin (Dineley *et al.*, 2008; Sanford & Palmer, 2020). These transient can result from acidification driven by NMDAR-mediated calcium influxes and subsequent proton-dependent release of zinc from intracellular ligands. (Kiedrowski, 2012; 2014) Similarly intracellular zinc may arise from NMDAR-dependent generation of reactive oxygen species triggering zinc release from metallothioneins (Reynolds & Hastings, 1995; Aizenman *et al.*, 2000). Interestingly, zinc has also been shown to be released from thapsigargin-sensitive stores in an IP3 dependent manner, suggesting the G_q-coupled metabotropic receptors such as Type 1 mGluRs or mZnR, can trigger intracellular zinc transients (Stork & Li, 2010). Together this shows multiple convergent mechanisms can mediate increases in intracellular zinc in response to physiological or pathophysiological neuronal activity.

Although the full consequences of changes in postsynaptic intracellular zinc is not yet fully understood, a variety of synaptic functions have been identified that are modulated by zinc. Zinc transients induced by neuronal depolarization triggers differential expression of 931 genes, including those implicated in synaptic structure and transmission (Sanford *et al.*, 2019). Interestingly this change in transcription occurs when intracellular zinc levels increase to just 220 pM, suggesting that even modest concentrations of zinc can have broad influence on neurons

(Sanford *et al.*, 2019). Intracellular zinc also influences synaptic plasticity, including modulation of long-term potentiation at both CA1 and CA3 neurons in the hippocampus (Takeda *et al.*, 2015; Tamano *et al.*, 2017). The latter is mediated by activation of the TrkB receptor via zinc-dependent activation of Src family kinase activity (Huang *et al.*, 2008). Intracellular zinc has also been linked to structural organization and remodeling of the synapse. Notably, zinc stabilizes Shank2 and 3, postsynaptic density scaffolding proteins critical for synapse maturation and plasticity (Arons *et al.*, 2016; Ha *et al.*, 2018). Postsynaptic zinc treatment alters AMPAR composition at the synapse via a Shank-dependent recruitment of GluA2-containing receptors to the surface (Ha *et al.*, 2018). ZnT1 expression also influences synaptic morphology. Overexpression or knockdown of the transporter causes increase or decrease in dendritic spine length and width respectively (Mellone *et al.*, 2015). Although the mechanism of ZnT1-driven alteration in morphology are unknown, NMDAR activation is known to be a critical modulator of synaptic strength and morphology (Sala & Segal, 2014). Therefore, ZnT1 may mediate morphological changes through its regulation of NMDAR activation. However, further studies are needed to uncover how zinc-dependent regulation of ZnT1 contributes to downstream NMDAR signaling and subsequent synaptic remodeling. Together these various zinc-dependent signaling cascades point to the multifaceted impact of zinc, both intracellularly and extracellularly, as a regulator of synaptic function.

Beyond its role in zinc homeostasis, ZnT1 is associated with a variety of signaling functions. In addition to regulating inhibition of NMDARs, ZnT1 regulates Ras/Raf/MEK/ERK signaling (Jirakulaporn & Muslin, 2004) and voltage gated calcium channels (Levy *et al.*, 2009; Shusterman *et al.*, 2017). ZnT1 interacts directly with the N-terminal regulatory domain of Raf-1 to promote its activity. ZnT1 enhancement of Ras-ERK signaling leads to upregulation of T-type

calcium channel expression on the plasma membrane and subsequent increase in calcium currents (Mor *et al.*, 2012). ZnT1 also binds directly to L-type calcium channels to inhibit their activity (Levy *et al.*, 2009; Shusterman *et al.*, 2017). Therefore, alterations in ZnT1 may influence multiple signaling pathways beyond zinc inhibition of NMDARs. Finally, decreases in intracellular zinc levels reduce ZnT1 expression through endocytosis and degradation of the transporter (Nishito & Kambe, 2019), allowing for bidirectional regulation of ZnT1-mediated signaling. Together, this suggests that the intracellular zinc state may be a critical regulator of signaling pathways, including NMDAR activation, through its impact on ZnT1.

In summary, we determined that intracellular zinc upregulates NMDAR inhibition through the zinc transporter ZnT1. Furthermore, this zinc-dependent regulation depends on the association between the GluN2A subunit of NMDARs and ZnT1. Together these results reveal a novel mechanism by which intracellular zinc influences NMDAR signaling in which intracellular zinc drives upregulation of ZnT1-mediated inhibition of NMDARs (Figure 18).

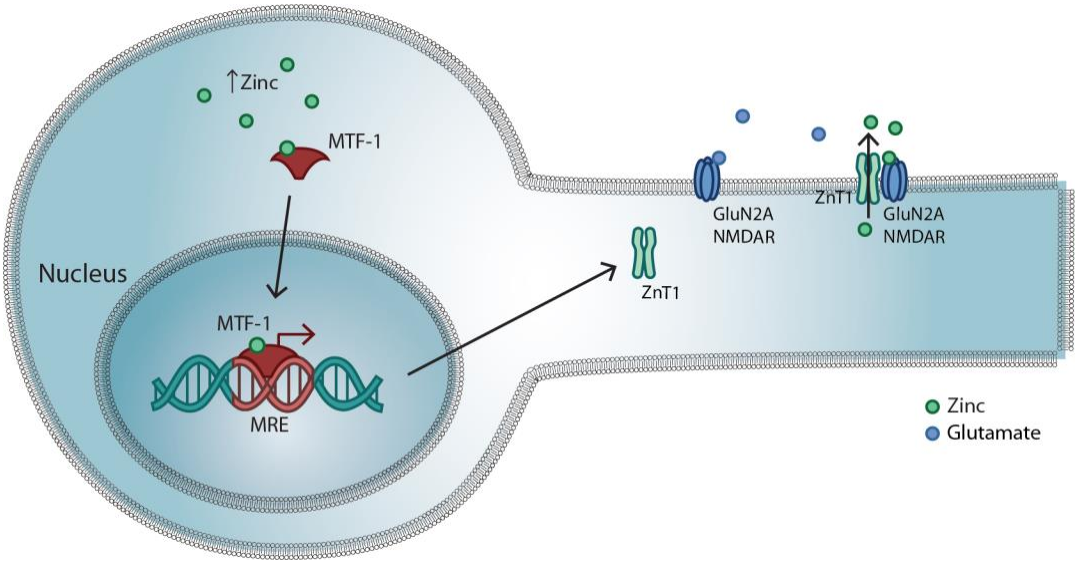

Figure 18 Proposed model of zinc-induced upregulation of ZnT1-mediated NMDAR inhibition

Legend for Figure 18: Increases in intracellular zinc bind to MTF-1 to drive MRE-driven gene expression. This leads to upregulation of expression of ZnT1, which associates with GluN2A subunits in the membrane. Increased GluN2A-ZnT1 interactions subsequently enhance zinc inhibition of NMDARs.

3.5 Material and Methods

3.5.1 Neuronal cultures

All animal procedures used in experiments were approved by the Institutional Animal Care and Use Committee of the University of Pittsburgh School of Medicine. Cortical cultures were prepared from embryonic day 16 rats. Briefly, pregnant rats (Charles River Laboratory) were sacrificed via CO2 inhalation. Embryonic cortices were dissociated with trypsin and plated at

670,000 cells per well on glass coverslips in six-well plates. Non-neuronal cell proliferation was inhibited after 2 weeks in culture with cytosine arabinoside (1–2 μM). Cultures were utilized at 3–4 weeks in vitro.

3.5.2 MRE-Luciferase reporter assay

Mixed cortical cultures were transfected at 19-20 DIV with MRE-firefly luciferase reporter (pLuc-MCS/4MREa), and *Renilla* luciferase reporter (pRLTK). *Renilla* was used as a non-inducible reporter as a control for transfection efficiency. Cells were transfected with the plasmids (1 μg pLuc-MSC/4MREa, 0.4 μg pRLTK, 0.1 μg pBK-CMV) using Lipofectamine 2000. Twenty-four hours later, cells were treated with 250 nM pyrithione (a zinc ionophore) or 250 nM pyrithione with 10 μM $ZnCl_2$ in DMEM containing 2% calf serum and 25 mM HEPES. Twenty-four hours after treatment, both firefly and *Renilla* luciferase expression were measured using the Dual-Glo Luciferase Assay System (Promega). Results were expressed as the ratio of firefly luciferase activity to *Renilla* luciferase activity, as described previously (Hara & Aizenman, 2004).

3.5.3 Proximity ligation assay

Proximity ligation assays were performed using Duolink PLA kit. Cortical cultures (3–4 weeks in vitro) were treated overnight with either N2AZ or scN2AZ (3 μM, dissolved in water), and pyrithione (250 nM), or zinc pyrithione (10 μM ZnCl, 250 nM pyrithione) . Coverslips were fixed in ice cold methanol for 5 minutes, rinsed in phosphate buffered saline (PBS) then permeabilized with 0.1% Triton-X in PBS. Coverslips were then incubated with primary antibodies: rabbit anti-ZnT1, mouse anti-GluN2A, and chicken anti-MAP2. Coverslips were

incubated with a donkey anti-chicken fluorescent secondary antibody targeting MAP2 antibodies to visualize neuron morphology. The PLA reaction was then completed according to DuoLink PLA protocol. Briefly, coverslips were incubated in DuoLink secondary antibodies (anti-rabbit and anti-mouse) which are conjugated with complementary oligonucleotides. Ligation solution was added to hybridize connector oligonucleotides and PLA probes, allowing the oligonucleotides to join in a closed loop when secondary antibodies were in close proximity. Next, the reaction was amplified with rolling-circle amplification (RCA) using the closed loop hybridized probes as a template. PLA probes were fluorescently labeled with oligonucleotides which hybridized to the RCA product during amplification. Coverslips from sister cultures were treated with either scN2AZ, N2AZ and pyrithione or zinc pyrithione and reactions were run simultaneously using the same preparation of reagents. Coverslips were mounted on glass slides using DuoLink mounting media and 4 random fields of view were imaged from each coverslip using a 60x oil objective on a Nikon A1R laser scanning confocal. PLA puncta were counted automatically with Fiji ImageJ (Version 2.0) software. We used maximum intensity projection of 15 sequential images in the z plane. All images were thresholded using Yen threshold setting prior to automated quantification of puncta. The ratio of puncta per field of view in ZnPyr versus Pyr treated conditions was taken between sister coverslips that were treated, fixed, and assayed with the same PLA preparation.

3.5.4 Electrophysiology

Whole-cell recordings from cultured cortical neurons were obtained with glass micropipettes (3-6 MΩ) containing (in mM): 140 CsF, 10 CsEGTA, 1 CaCl2, 10 HEPES, pH = 7.2, 295 mOsm. Extracellular recording solution contained (in mM): 150 NaCl, 2.8 KCl, 1.0 CaCl2, 10 HEPES, 60 µM glycine, pH = ~7.2 , ~300 mOsm. Using *Ephus* (Suter *et al.*, 2010) and

a Multiclamp 700B amplifier (Molecular Devices), NMDAR EPSCs were recorded in voltage clamp (holding potential -70 mV) in the presence of TTX (300 nM, sodium channel blocker), DNQX (20 µM, AMPA and kainate receptor antagonist), and 4-Methoxy-7-nitroindolinyl (MNI)-caged glutamate (40 µM). To evoke NMDAR EPSCs, we photolytically uncaged MNI-caged glutamate using 1 ms pulses of UV-laser light (355 nm, DPSS Lasers). The ZX1-mediated potentiation for each cell was calculated as the percent increase in average response (10 sweeps, before and after ZX1) following application of the metal chelator.

3.5.5 Statistical Analyses

Electrophysiology recordings were obtained using *Ephus* (Suter *et al.*, 2010) software run in Matlab 2012a (MathWorks). Cell parameters and response peaks were calculated using custom Matlab scripts. For electrophysiology, ZX1 potentiation was measured as the percent increase in NMDAR amplitude 10 minutes after the application of ZX1. Unpaired t-tests and ANOVAs were used to compare between treatments. Statistical analysis was completed in Prism 8 (GraphPad).

4.0 Discussion

This dissertation uncovered a novel postsynaptic mechanism that drives zinc inhibition of NMDARs. These findings challenge existing models that assume that diffusion of vesicular zinc across the synaptic cleft is sufficient to modulate postsynaptic NMDA receptors. We discovered that ZnT1's interaction with GluN2A is necessary for endogenous zinc inhibition, even in the presence of presynaptic release of vesicular zinc. Disrupting this association or chelating intracellular zinc is sufficient to significantly reduce endogenous inhibition. Furthermore, we found that increasing intracellular zinc content upregulates ZnT1-dependent zinc inhibition. Together these results reveal that multiple zinc-regulatory systems cooperate to maintain zinc inhibition of NMDARs. These findings expand on our understanding of the complex mechanisms that regulate zinc signaling within neurons.

Based on our results, we hypothesize a new model for zinc inhibition of NMDARs in which ZnT1 localizes zinc in the proximity of the receptor through its direct interaction with the GluN2A subunit (Figure 19). This model is supported by our finding that disrupting the association between GluN2A and ZnT1 reduces zinc inhibition, however there are some important caveats that should be noted. Our model assumes that N2AZ's action is specific to ZnT1's association with GluN2A. Although we determined that N2AZ did not alter presynaptic glutamate release, the IC_{50} of zinc, or ZnT1 transport, it is possible that N2AZ may disrupt other proteins' associations with GluN2A-containing NMDARs. The C-terminal domain of GluN2 subunits is a common site for protein interactions including those that contribute to receptor scaffolding and downstream signaling (Hardingham, 2019). The N2AZ sequence may overlap with regions where other proteins bind to

GluN2A, therefore disrupting their association and consequent signaling. Another caveat to our findings is we do not know how the association between GluN2A and ZnT1 influences either protein's surface expression. A previous study showed that silencing ZnT1 led to increased internalization of GluN2A subunits in hippocampal neurons (Mellone et al., 2015). This finding suggests that the interaction with ZnT1 may serve to stabilize GluN2A-containing NMDARs in the membrane, therefore N2AZ may influence zinc sensitivity of neurons by reducing the surface expression of GluN2A-containing NMDARs.

Another factor to consider for the interpretation of our findings is the broader impact of zinc chelation and genetic knockdown of ZnT3 on neuronal function. We used ZX1 for its high affinity and fast kinetics, which allows it to chelate zinc transients generated by presynaptic vesicular zinc release. However, this high affinity chelation may also serve to strip zinc from lower affinity protein binding sites, therefore influencing zinc-regulated signaling in neurons beyond its inhibition of NMDARs. In particular, intracellular ZX1 may disrupt zinc binding to signaling proteins, such as kinases such as Src (Huang et al., 2008), which can influence NMDAR expression through phosphorylation of GluN2 subunits (Manzerra et al., 2001). Another limitation to consider is the impact of ZnT3 knockout on neuronal zinc signaling. Although knockouts are the most direct means of disrupting vesicular zinc, it is unclear if or how these knockout animals compensate for the lack of ZnT3 over the course of their development. For example, it is possible that in the absence of vesicular zinc release, ZnT3 knockout animals differentially express ZnT1 or other transporters to maintain zinc signaling. Therefore, further investigations are necessary to validate our model and ZnT1's role in physiological zinc signaling.

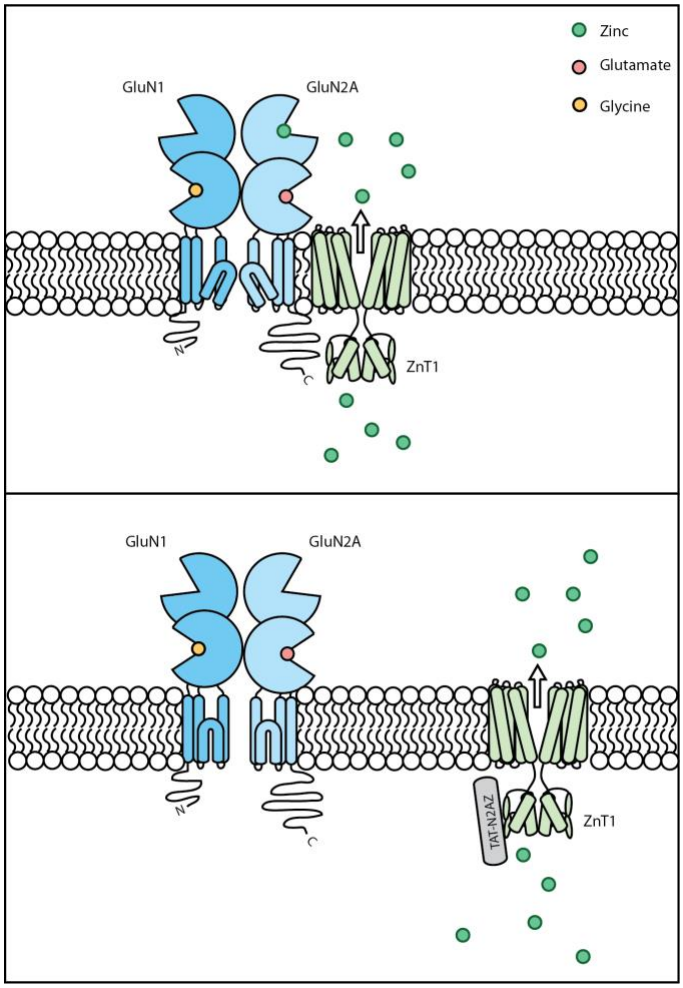

Figure 19 Model of N2AZ Action

Legend for Figure 19: Model of N2AZ Action. We propose that the association between ZnT1 and GluN2A localizes zinc in the proximity of NMDARs to drive zinc inhibition (top) through binding to the high affinity site on the N-terminal of GluN2A. When this association is disrupted using N2AZ (bottom), NMDARs are dissociated from the microdomain of zinc thus reducing endogenous zinc inhibition of the receptor.

4.1 Translocation of Vesicular Zinc

A significant unanswered question in our model is what is the relationship between ZnT3-dependent presynaptic release and postsynaptic transport by ZnT1. The simplest model to account for our observations is that vesicular zinc translocates into postsynaptic cells where it is then transported by ZnT1 to extracellular microdomains in the immediate vicinity of GluN2A. Consistent with this hypothesis, it has been shown that electrical or pharmacological stimulation of hippocampal neurons leads to transient increases in post-synaptic intracellular zinc that are dependent on extracellular zinc levels (Li *et al.*, 2001; Ha *et al.*, 2018). This suggests that vesicular zinc can translocate into the postsynaptic neuron following activity-dependent presynaptic release.

Multiple channels have been identified that mediate zinc translocation from vesicular stores to the postsynaptic neuron, including calcium-permeable AMPA receptors (CP-AMPARs), NMDA receptors (NMDARs), and voltage-gated calcium channels (VGCCs) (Figure 20). AMPARs were first linked to zinc transport with the observation that AMPAR activation increases zinc toxicity (Weiss *et al.*, 1993). Furthermore, zinc uptake selectively labels neurons that express CP-AMPARs and this subpopulation of neurons is more susceptible to zinc-toxicity (Yin & Weiss, 1995; Yin *et al.*, 1998). Direct measurement of zinc current through CP-AMPARs established that the receptor conducts zinc even in the presence of physiological calcium (Jia *et al.*, 2002). In addition to CP-AMPARs, voltage gated calcium channels mediate zinc-toxicity and zinc influx following depolarization with high potassium (Manev *et al.*, 1997; Sheline *et al.*, 2002). Electrophysiological recordings confirmed VGCCs conduct zinc (Kerchner *et al.*, 2000a), with L-type $Ca_V1.2$ and $Ca_V1.3$ isoforms, but not Ca_V2 or Ca_V3 isoforms, being permeable zinc to the ion (Park *et al.*, 2015). Zinc also permeates through NMDARs, but to a lesser extent than calcium

(Koh & Choi, 1994). NMDARs mediate increases in zinc following treatment with low micromolar zinc concentrations, suggesting that vesicular zinc released into the cleft reaches concentrations sufficient to permeate the receptor (Marin *et al.*, 2000). In this project, neither AMPARs or LTCCs were necessary for endogenous zinc inhibition of NMDARs, suggesting they are not essential links between ZnT3-dependent release and ZnT1 transport. However, it is possible that, under certain circumstances, zinc influx through these channels could activate MTF-1 to upregulate ZnT1 expression. In fact, zinc influx through LTCC was shown to drive expression of genes under the MRE-driven metallothionein promoter, albeit in a pituitary tumor cell line (Atar *et al.*, 1995). Therefore, LTCCs may indirectly alter ZnT1-dependent inhibition by driving zinc upregulation of ZnT1.

Transient receptor potential channels (TRPs) can also mediate zinc translocation into neurons. For example, TRPM7 channel inhibition or genetic knockdown reduces intracellular zinc and zinc toxicity in mouse cortical cultures (Inoue *et al.*, 2010). Interestingly, there are multiple examples of TRP channels coupling zinc influx to channel modulation. For instance, TRPM7 is necessary for extracellular zinc mediated activation of BK channels, which have intracellular zinc binding sites (Hou *et al.*, 2010). Similarly, zinc influx through TRPA1 mediates zinc inhibition of TRPV1 and subsequent reduction of acute nociception in dorsal root ganglion neurons (Luo *et al.*, 2018). TRPA1 itself mediates zinc influx required for its own activation by zinc binding to intracellular residues (Hu *et al.*, 2009). This suggests a shared mechanism in which TRP channels localize zinc influx to downstream signaling targets of zinc. Further studies are needed to determine if TRP channels directly contribute to zinc pools necessary for ZnT1-mediated inhibition of NMDARs.

Another possible conduit of vesicular zinc translocation into the postsynaptic neuron are ZIP transporters (Figure 20). Many ZIP transporters are localized in the plasma membrane suggesting they may play a role in postsynaptic import of vesicular zinc after release (Kambe *et al.*, 2015). In the brain, ZIP1 and ZIP3 contribute to zinc-mediated degeneration in the CA1 region of the hippocampus following kainate-induced seizures. Animals with ZIP1 and ZIP3 knockout exhibit reduced CA1 damage compared to controls resulting from decreased zinc uptake (Qian *et al.*, 2011). Similarly, ZIP1 and ZIP4 upregulation following kainate injections in the hippocampus leads to increased zinc import into neurons (Emmetsberger *et al.*, 2010). Little is known about ZIP transporter function in neurons under non-pathological conditions; therefore, further investigation is needed to understand if and how ZIP transporters contribute to regulation of zinc within the synaptic cleft.

4.2 Intracellular Zinc Release

Transient increases in intracellular zinc can also occur independent of translocation of vesicular zinc. For example, zinc accumulation in degenerating neurons occurs in regions of the brain that do not express ZnT3 (Lee *et al.*, 2000; Land & Aizenman, 2005; Medvedeva *et al.*, 2017). This suggests an additional pool of zinc can be mobilized to regulate synaptic function by supplying intracellular zinc for ZnT1 or to drive ZnT1 expression via MTF1. These ZnT3-independent intracellular zinc signals result from liberation of zinc from intracellular stores, such as zinc-binding proteins or subcellular organelles.

Intracellular zinc is buffered by intracellular proteins, notably metallothioneins. Metallothioneins are critical buffers of intracellular zinc with 20 cysteine residues per metallothionein protein that bind up to 7 zinc ions via metal-thiolate clusters (Maret & Krezel, 2007). Of the four metallothionein isoforms, three (MT-I through MT-III) are expressed in the central nervous system, with MT-III the primary form expressed in neurons (Aschner *et al.*, 1997). These proteins release zinc in response to oxidative stimuli (Maret, 1994; 1995). For example, the thiol oxidant 2,2'-dithiodipyridine (DTDP) triggers intracellular zinc release from MTs and subsequent zinc-dependent cell death in cortical neurons *in vitro* (Aizenman *et al.*, 2000). Glutamate also has been shown to trigger the generation of reactive oxygen species through NMDAR-mediated calcium influx and subsequent mitochondrial dysfunction. Therefore, glutamate-dependent reactive oxygen species generation may represent an activity-dependent mechanism driving zinc release from MTs (Reynolds & Hastings, 1995; Aizenman *et al.*, 2000). Nitric oxide, an endogenous gas, also liberates zinc from MTs (Lin *et al.*, 2007), likely through its interaction with superoxide and production of peroxynitrite (Zhang *et al.*, 2004). Following ischemic injury, inhibitors of NO synthase prevent the accumulation of intracellular zinc which suggests that NO endogenously mobilizes zinc from intracellular stores (Wei *et al.*, 2004). Notably, neuronal NO synthase (nNOS) activation is directly coupled to NMDAR-mediated calcium influx through nNOS's interaction with postsynaptic density protein 95, which suggests NMDAR activation itself can drive NO-mediated zinc release (Zhou *et al.*, 2010). Furthermore, glutamate-induced intracellular acidification drives proton-dependent release of zinc from zinc-binding proteins (Kiedrowski, 2012; 2014). Thus, multiple activity-dependent mechanisms liberate zinc from metal-binding proteins which may subsequently regulate postsynaptic zinc levels and ZnT1-mediated NMDAR inhibition.

Zinc can also be released from subcellular organelles, including the endoplasmic reticulum (ER) and Golgi apparatus. The ER sequesters zinc following increases in cytosolic levels in cortical neuron cultures (Qin *et al.*, 2011). Zinc can be released from the ER following activation of the IP_3 receptor or inhibition of the ER calcium pump with thapsigargin (Figure 20) (Stork & Li, 2010; Qin *et al.*, 2011). Therefore, IP_3 signaling through G_q-coupled metabotropic receptors, such as mZnR or metabotropic glutamate receptors, may trigger increases in intracellular zinc. Alternatively, zinc can be released from the ER and Golgi apparatus by the transporter ZIP7 (Figure 20). Phosphorylation of ZIP7 by protein kinase CK2 triggers intracellular zinc release (Taylor *et al.*, 2012; Nimmanon *et al.*, 2017). Interestingly, ZIP7 phosphorylation occurs following treatment of cells with 20 µM extracellular zinc, suggesting an additional possible mechanism by which release of vesicular zinc could drive intracellular zinc transients (Taylor *et al.*, 2012). Lysosomes also can accumulate zinc. Knockdown of TRPML1 leads to enlargement of and zinc accumulation in lysosomes, suggesting that TRPML1 may endogenously release zinc from these stores (Figure 20) (Eichelsdoerfer *et al.*, 2010; Kukic *et al.*, 2013). In fact, studies using the high-affinity zinc sensor GZnP3 found that activation of TRPML1 led to zinc release from endolysosomal compartments in neurites of hippocampal neuron cultures (Minckley *et al.*, 2019).

Together these examples illustrate that multiple mechanisms increase intracellular zinc without relying on direct transport of released vesicular zinc into the postsynaptic cell. This raises the intriguing possibility that ZnT1-mediated inhibition occurs at synapses that do not have presynaptic ZnT3. Indeed, we observed zinc inhibition in cortical cultures using glutamate uncaging, which does not engage presynaptic release mechanisms. However, this leads to the

question, why is ZnT3-dependent release necessary for zinc inhibition in the DCN (Anderson *et al.*, 2015)? One distinct possibility is that the dominant source of intracellular zinc arises from translocation of vesicular zinc to postsynaptic neurons, as discussed above. Another possibility is that zinc acts as a signal to elicit liberation of zinc from intracellular stores. For example, zinc is released from IP_3-sensitive stores (Stork & Li, 2010), suggesting that mZnR activation and subsequent IP_3 signaling is capable of eliciting intracellular zinc release. Alternatively, ZnT3 may be necessary for determining overall zinc content of intracellular stores in postsynaptic neurons. In this hypothesis, ZnT3-dependent release and translocation primes postsynaptic structures with sufficient levels of zinc that can be released from intracellular stores following physiological stimuli. Consistent with this, deletion of ZnT3 leads to a marked decrease in zinc staining throughout the brain (Cole *et al.*, 1999), suggesting that vesicular pools are an essential source of labile zinc in the brain. Therefore, a dynamic relationship between postsynaptic intracellular zinc and presynaptic zinc release may contributes to zinc signaling in the synapse.

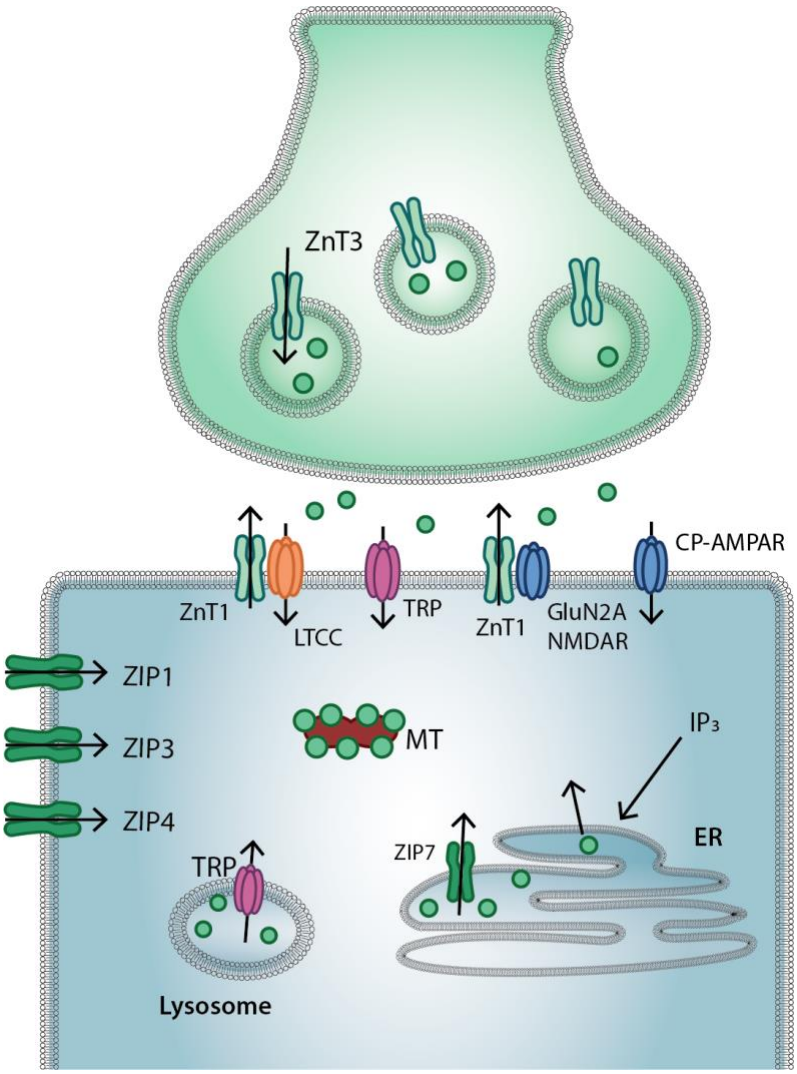

Figure 20 Model of Zinc Transport and Release at the Synapse

Legend for Figure 20: Model showing the various routes of entry of zinc into the cell and mechanisms of zinc release from intracellular stores.

4.3 Function of ZnT1-mediated Zinc Inhibition of NMDARs

Our experiments suggest that ZnT1 organizes zinc into distinct microdomains in the proximity of GluN2A-containing NMDARs to regulate inhibition. These microdomains may allow for precise control over zinc localization and concentration to target NMDARs without also affecting other zinc signaling pathways. Consistent with this, disrupting ZnT1's association with GluN2A had no effect on endogenous zinc inhibition of AMPARs. In recent years, investigation of the organization of pre- and postsynaptic protein complexes has revealed synaptic nanostructures can critically influence transmission and plasticity (Biederer *et al.*, 2017). For example, voltage gated calcium channels create microdomains of calcium in the proximity of synaptic vesicles to precisely control presynaptic release (Berridge, 2006). Furthermore, alignment of presynaptic vesicle release sites and postsynaptic AMPAR creates a trans-synaptic 'nanocolumn' that is hypothesized to precisely regulate neurotransmission (Tang *et al.*, 2016; Biederer *et al.*, 2017). It is reasonable to infer that zinc, which is co-released from glutamatergic vesicles, exhibits similar dynamics to preferentially targets receptors aligned to release sites, such as AMPARs. Therefore, postsynaptic ZnT1 may redistribute ZnT3-dependent zinc to receptors that are distal to release sites, such as peri- or extrasynaptic receptors. NMDARs are located extrasynaptically at the parallel fiber to cartwheel cell synapse in the DCN, where we observed ZnT1-dependent zinc inhibition (Anderson *et al.*, 2015). Extrasynaptic versus synaptic activation leads to differential activation of postsynaptic signaling cascades and gene expression. Notably, extrasynaptic NMDARs are hypothesized to mediate cell death signaling whereas synaptic activation is associated with pro-survival signaling (Hardingham & Bading, 2010; Parsons & Raymond, 2014). Therefore ZnT1-mediated inhibition may serve to preferentially modulate extrasynaptic NMDARs and subsequent downstream signaling.

NMDAR function is also influenced by subunit composition. NMDAR subunits exhibit differential expression patterns across development, brain regions, and cell types and are coupled to distinct signaling consequences (Paoletti *et al.*, 2013). Notably, subunit composition impacts the induction and direction of NMDAR-mediated plasticity. Subunit specific manipulations induce metaplasticity by shifting the ratio of GluN2A to GluN2B activation to influence the threshold for induction of plasticity (Yashiro & Philpot, 2008). Because ZnT1 specifically binds to the GluN2A C-terminal domain (Mellone *et al.*, 2015), it may mediate metaplasticity by driving preferential inhibition of GluN2A. Consistent with this hypothesis, it has been shown that zinc inhibition of GluN2A regulates the magnitude of LTP at the mossy fiber to CA1 synapse in the hippocampus (Vergnano *et al.*, 2014). ZnT1 overexpression or knockdown leads to a respective increase or decrease in spine length and width (Mellone *et al.*, 2015), which is a correlate of synaptic strength (Matsuzaki *et al.*, 2004). In this dissertation, we showed that ZnT1-mediated inhibition is dynamically regulated by intracellular zinc, which can increase in response to synaptic activity (Sanford & Palmer, 2020). Therefore, intracellular zinc, ZnT1, and subsequent GluN2A inhibition may cooperatively regulate activity-dependent changes in synaptic strength.

4.4 ZnT1 as a Target for Neuroprotection

NMDARs contribute to excitotoxic cell death in variety of pathological conditions, including ischemic stroke and neurodegenerative diseases (Hardingham & Bading, 2010). However, they are also essential for pro-survival signaling, synaptic transmission, and plasticity (Peters *et al.*, 1987). This dual role of the receptor makes blocking NMDAR for neuroprotection challenging. Therefore, the focus for therapeutic strategies has turned to targeting specific receptor

subpopulations and downstream signaling consequences (Wu & Tymianski, 2018). We found that ZnT1 drives zinc inhibition of extrasynaptic NMDARs, which are hypothesized to preferentially couple to cell death signaling (Hardingham & Bading, 2010). Therefore, ZnT1 may be a useful target for reducing excitotoxic cell death.

One effective mechanism that reduces excitotoxic cell death is preconditioning, a process in which sublethal insults trigger endogenous neuroprotective cascades that mitigate damage from subsequent injuries. Zinc signaling has been implicated in neuronal preconditioning. Zinc itself is sufficient to precondition neurons against NMDA-induced toxicity (Lee *et al.*, 2008; Lee *et al.*, 2015b). A rise in cytosolic zinc is necessary for an *in vitro* model of ischemic preconditioning in cortical cultures (Aras *et al.*, 2009). Furthermore, this preconditioning model also drives MRE-dependent gene expression. Together this suggests that zinc-driven proteins, such as ZnT1 may be critical for the expression of preconditioning. Consistent with this, ZnT1 is upregulated following sub-lethal transient ischemia in rat cerebral cortex and hippocampus (Aguilar-Alonso *et al.*, 2008). Together this points to ZnT1 upregulation and subsequent inhibition of NMDARs as a potential mechanism underlying preconditioning.

Beyond its role in excitotoxicity, zinc is also hypothesized to contribute to Alzheimer's disease (AD) through its interaction with Aβ, the primary component of amyloid plaques (Huang *et al.*, 2000). This 'Metal Hypothesis of Alzheimer's Disease' proposes that zinc, along with other transition metals such as copper, drive Aβ pathogenicity (Bush & Tanzi, 2008). This is based, in part, on the observation that vesicular zinc promotes the aggregation and accumulation of Aβ in the synapse (Bush *et al.*, 1994; Deshpande *et al.*, 2009) and modulating zinc levels, through

chelators or ZnT3 knockouts, reduces Aβ aggregation (Bush & Tanzi, 2008). Zinc binding to Aβ is also hypothesized to dysregulate neuronal zinc homeostasis (Sensi *et al.*, 2009), which is supported by the observation that localization and expression of zinc transporters are altered in AD models and postmortem brain tissue of AD patients (Xu *et al.*, 2019). Based on these findings, metal chaperones have been developed as potential therapeutics for the treatment of AD (Adlard & Bush, 2018). Metal chaperones bind extracellular zinc and transport it into the cytoplasm, and therefore serve to both reduce zinc-driven accumulation of Aβ and redistribute dysregulated zinc.

Metal chaperones drive pro-survival signaling via intracellular zinc-dependent cascades (Crouch *et al.*, 2011). Notably, treatment with the chaperone PBT2 preconditions cells against excitotoxic insults in a zinc-dependent manner (Johanssen *et al.*, 2015). NMDAR dysfunction and excitotoxicity have been linked to Aβ-driven pathology in Alzheimer's disease (Danysz & Parsons, 2012), therefore ZnT1-mediated inhibition of NMDARs may contribute to the protective effects of metal chaperones in AD models. A similar chaperone, clioquinol, was identified an activator of MTF-1, implicating chaperones in the upregulation of MRE-driven proteins, such as ZnT1 (Jackson *et al.*, 2020). Together this suggests that zinc driven ZnT1 expression and NMDAR inhibition may contribute to the efficacy of metal chaperones in the treatment of AD.

4.5 ZnT1 as a Target in NMDAR Dysfunction

Zinc and NMDAR signaling are both implicated for the regulation of pain. NMDARs contribute to regulation of pain sensitivity (Petrenko *et al.*, 2003) and reducing NMDAR signaling suppresses both inflammatory and neuropathic pain (Liu *et al.*, 2008). Mice with a knock-in

mutation on GluN2A that removes high affinity zinc binding exhibit hypersensitivity to pain stimuli, suggesting that endogenous zinc inhibition of NMDARs attenuates pain processing (Nozaki *et al.*, 2011). Consistent with this, a spinal nerve transection model of neuropathic pain leads to reduced ZnT3 expression and synaptic zinc in the spinal cord, correlated to increased pain sensitivity (Jo *et al.*, 2008). A similar model, partial sciatic nerve ligation, downregulates ZnT1 expression in the spinal cord, suggesting a correlation between ZnT1 expression and pain (Kitayama *et al.*, 2016). In fact, ZnT1 knockdown alone is sufficient to induce neuropathic pain symptoms (Kitayama *et al.*, 2016). Together, this suggests that ZnT1-mediated zinc inhibition of NMDARs in the spinal cord may regulate pain sensitivity. Furthermore, upregulation of ZnT1 via MTF1 may be a useful mechanism to investigate for the treatment of chronic pain.

Zinc dysregulation has been observed in patients and animal models of Autism Spectrum Disorder (ASD). Zinc deficiency is commonly observed in ASD patients (Yasuda *et al.*, 2011; Pfaender *et al.*, 2017). Furthermore, both maternal zinc deficiency and ZnT3 knockout leads to ASD-like phenotypes in mice (Grabrucker *et al.*, 2014; Grabrucker *et al.*, 2016; Yoo *et al.*, 2016). It is hypothesized that zinc contributes to ASD through to its role in stabilization of the post-synaptic density scaffolding proteins Shank2 and Shank3. Zinc binds to the sterile alpha motif (SAM; a putative protein interaction domain (Thanos *et al.*, 1999)) on the C-terminal of Shank2/3 to regulate its oligomerization and localization (Arons *et al.*, 2016). Dietary zinc supplementation is sufficient to ameliorate ASD-associated behaviors such as anxiety, repetitive behaviors, and social deficits in Shank 3 knockout models of ASD (Fourie *et al.*, 2018; Vyas *et al.*, 2020). In addition to these behavioral improvements, Shank 3 knockout models exhibit reductions in NMDAR currents and slower NMDAR decays (Fourie *et al.*, 2018). This may be indicative of a

reduction in GluN2A-mediated current, as GluN2A imparts fast decay kinetics on NMDARs (Paoletti *et al.*, 2013). Furthermore, clioquinol improves social interaction and modifies NMDAR activity in mouse models of ASD by increasing cytosolic zinc (Lee *et al.*, 2015a). Together this suggests that both cytosolic zinc availability and NMDARs are viable targets for modifying synaptic and behavioral dysfunction associated with ASD. ZnT1, which regulates both of these systems, stands out as a potential candidate for manipulating synaptic dysfunction associated with ASD.

Schizophrenia is also associated with dysregulation of both zinc and NMDAR signaling. The glutamatergic theory of schizophrenia hypothesizes that NMDAR hypofunction contributes to synaptic and circuit dysfunction in schizophrenia (Marek *et al.*, 2010). Consistent with this idea, NMDAR antagonists mimic schizophrenic symptoms in healthy adults and post-mortem tissue of schizophrenic patients exhibit decreased GluN1 expression (Hardingham & Do, 2016). Interestingly de novo mutations in GRIN2A, the gene encoding the GluN2A subunit, are associated with schizophrenia (Hardingham & Do, 2016). Single nucleotide polymorphisms associated with schizophrenia have been identified in multiple zinc transporters, including ZIP8, and ZIP13 (Fullard *et al.*, 2019) (Hess *et al.*, 2016) (Kranz *et al.*, 2015). Furthermore, post mortem tissue from patients with schizophrenia exhibit elevated ZIP12 expression in the cerebral cortex (Scarr *et al.*, 2016). This indicates that increased zinc import via ZIPs may be associated with the development of schizophrenia. We demonstrated that increases in intracellular zinc upregulate ZnT1-mediated NMDAR inhibition. Therefore, zinc-driven expression of ZnT1 and subsequent inhibition of NMDARs may be a unique mechanism linking zinc dysregulation and NMDAR hypofunction in schizophrenia.

4.6 Conclusion

There is a growing appreciation for the role of zinc signaling in both physiological and pathological functions in the brain. Despite zinc's widespread distribution and diversity of targets in the brain, much remains unclear about zinc's dynamics at the synapse. This dissertation reveals a novel mechanism of zinc regulation via postsynaptic ZnT1. ZnT1's association with the GluN2A of NMDAR critically contributes to endogenous zinc inhibition of NMDARs, which is further driven by intracellular zinc signals. This dynamic coupling of intracellular zinc, ZnT1, and GluN2A represent a complex mechanism of regulation that maintains NMDAR inhibition. Given the diverse functions of NMDARs, this system may serve as a novel target to modulate neuronal function in both health and disease.

Appendix A Endogenous extracellular zinc is neuroprotective against excitotoxicity

Appendix A.1 Overview

Excitotoxicity is a neurodegenerative process in which NMDAR overactivation leads to a lethal calcium influx and subsequent cell death. Excitotoxic cell death contributes to damage in a variety of disorders, including stroke, traumatic brain injury, and neurodegenerative diseases (Parsons & Raymond, 2014). Zinc is a potent inhibitor of NMDARs and application of zinc protects against excitotoxic damage (Peters *et al.*, 1987). In the brain, zinc is loaded into synaptic vesicles via the transporter ZnT3 and is co-released with glutamate to modulate neurotransmission (Sensi *et al.*, 2009). It has been shown that this vesicular zinc endogenously inhibits NMDARs (Pan *et al.*, 2011; Anderson *et al.*, 2015). Furthermore, an additional ZnT3-independent pool of zinc has been measured that endogenously inhibits extrasynaptic NMDARs (Anderson *et al.*, 2017). Given that extrasynaptic NMDARs receptors are thought to be preferentially linked to excitotoxicity (Parsons & Raymond, 2014), we investigated whether tonic zinc acts as an endogenous signal that limits excitotoxicity via its inhibition of NMDARs.

Appendix A.2 Results

To start investigating the role of tonic zinc in excitotoxicity and NMDAR inhibition, we first measured extracellular zinc concentrations in rat cortical cultures using the ratiometric fluorescent zinc probe, LZ9. This probe has both zinc sensitive (ZP1) and zinc insensitive (LRB)

fluorescence that are excited by blue and green light respectively (Figure 21A, B). Excitation of the zinc-sensitive ZPI domain was interleaved with excitation of the zinc-insensitive LRB domain to consistently measure the change fluorescence of both domains over time. The ratio of ZP1 fluorescence to LRB fluorescence provides a measure of zinc-dependent fluorescence. After measuring baseline fluorescence, the dynamic range of the probe is obtained by adding EDTA to get minimum fluorescence ratio followed by $ZnCl_2$ to get maximum fluorescence. Together these values can be used to calculate the concentration of extracellular zinc using the equation in Figure 21C. Using this method, we measured ~0.4 nM tonic zinc in cortical cultures, consistent with the level measured in slice preparations (Anderson *et al.*, 2015).

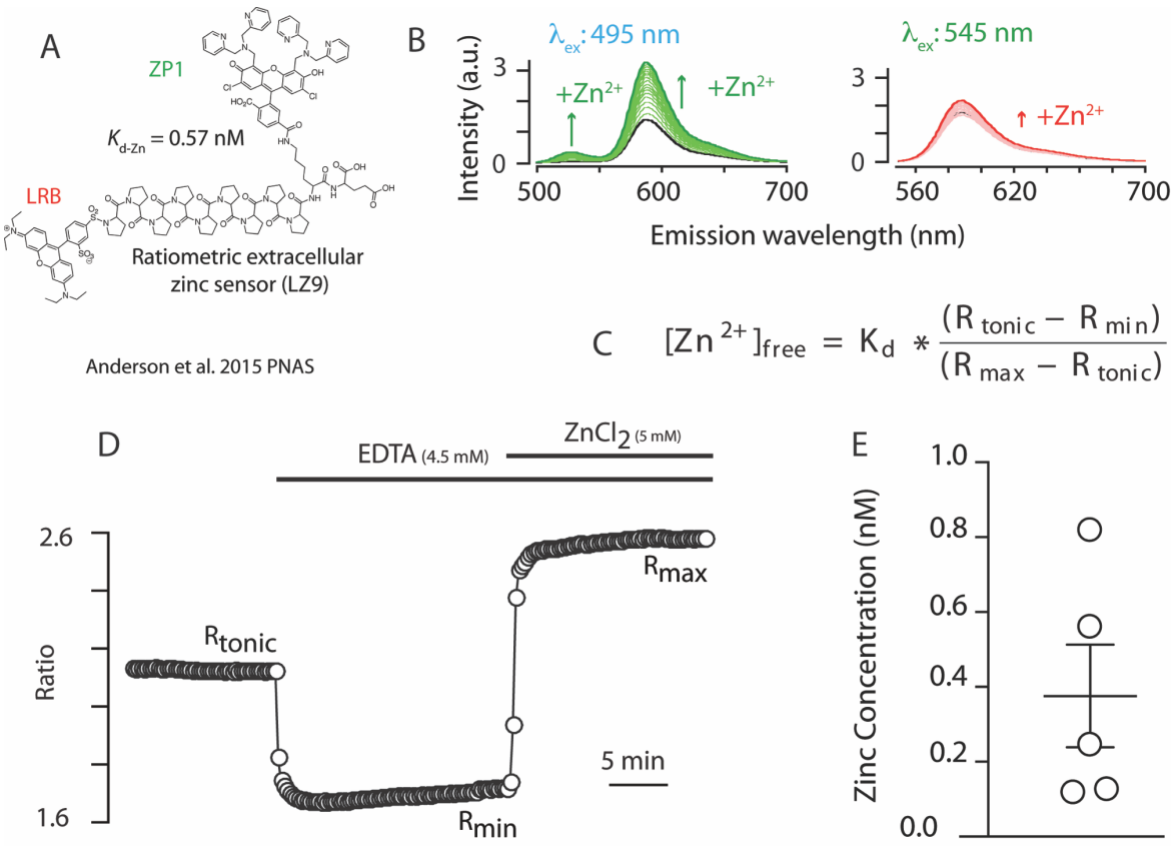

Figure 21 Nanomolar extracellular concentrations of zinc are present in cortical cultures

Legend for Figure 21: (A) Schematic of the ratiometric fluorescent probe, LZ9. (B) Emission profiles of the zinc-sensitive ZP1 and zinc-insensitive LRB domains of LZ9. Adapted from Anderson et al., 2015. (C) Equation used to determine the concentration of extracellular zinc using the baseline (R_{tonic}), maximum (R_{max}), and minimum (R_{min}) fluorescence in combination with the dissociation constant of LZ9. (D) Example trace of the ratio of ZP1:LRB fluorescence over time in an experiment. (E) Average zinc concentration in cortical culture preparations

Next, we tested whether endogenous extracellular zinc is protective during excitotoxicity. We used the glutamate uptake inhibitor DL-threo-β-benzyloxyaspartic acid (TBOA, 75 μM) to increase extracellular glutamate and thus promote excitotoxic cell death. TBOA treatment alone induced a significant increase in cell death compared to untreated controls as measured with LDH

assay (Figure 22B, Repeated measures one-way ANOVA, $p < 0.0001$, Bonferroni's Multiple comparisons, $p = 0.015$). Furthermore, TBOA induced cell death could be blocked with the NMDAR antagonist memantine (50 µM) indicating that TBOA-induced damage was NMDAR dependent (Figure 22C). We assessed if endogenous zinc protected against excitotoxicity by chelating extracellular zinc with the high-affinity, cell-impermeant chelator ZX1. ZX1 significantly increased TBOA-induced cell death compared to TBOA treatment alone (Figure 22B, $p = 0.048$), indicating that endogenous zinc protects against excitotoxicity. Furthermore, the cell death observed in all condition was completely blocked with memantine, indicating that cell death is NMDAR dependent (Figure 22C). To visualize the effect of these treatments, neurons were transfected with green fluorescent protein (GFP) prior to treatment (Figure 22A). These results indicate that endogenous zinc protects against excitotoxicity by inhibiting NMDARs.

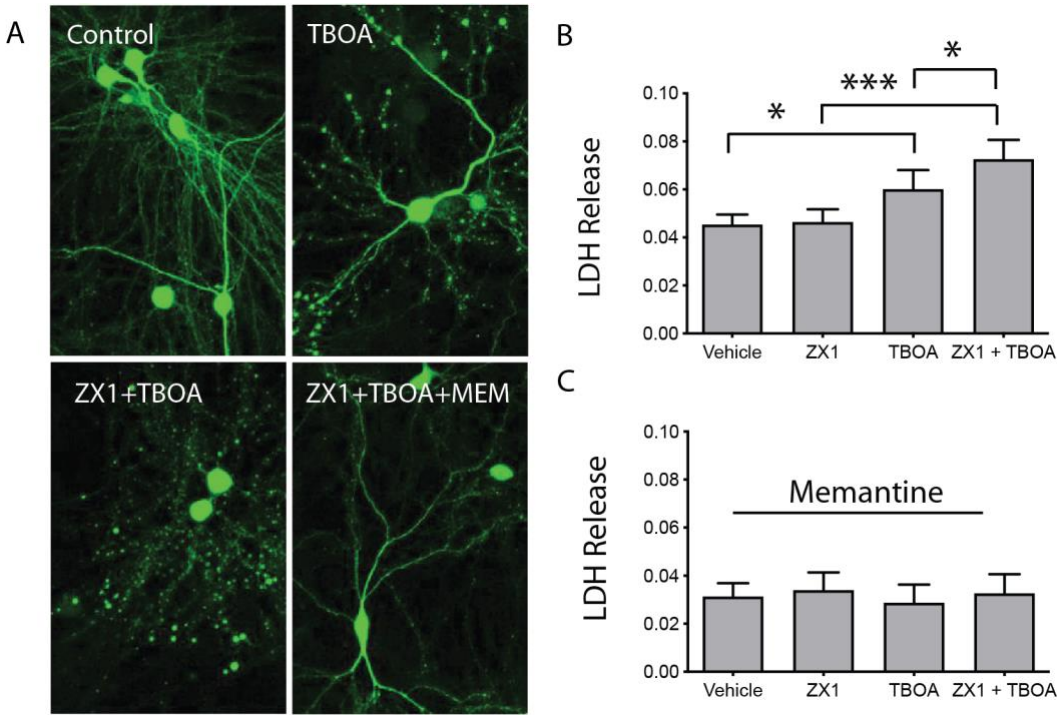

Figure 22 Extracellular zinc protects against excitotoxicity

Legend for Figure 22: (**A**) Representative images of GFP transfected neurons demonstrate excitotoxic damage for each treatment group. (**B**) LDH assay showing relative cell death across treatment groups. TBOA induced cell death compared to vehicle controls ($p = 0.015$) and significantly increased cell death when comparing ZX1 and ZX1+TBOA treated neurons ($p < 0.0001$). ZX1 treatment enhanced TBOA cell death compared to TBOA alone ($p = 0.048$) (**C**) LDH results for the same groups in the presence of NMDA receptor antagonist, memantine, indicating no significant differences between treatments (One-way ANOVA, $p = 0.418$)

Appendix A.3 Conclusions

These results indicate that tonic, nanomolar levels of zinc are present in cortical cultures and dampen excitotoxic damage through their inhibition of NMDARs. Although it is documented that application of zinc can reduce NMDAR-mediate toxicity (Peters *et al.*, 1987), these results suggest this protection also occurs with endogenous zinc pools. We measured low nanomolar concentrations of zinc present in our cortical culture preparation, which is sufficient to occupy the high-affinity zinc binding site on GluN2A-containing NMDARs. In light of our recent finding that ZnT1 regulates zinc inhibition of NMDARs, this nanomolar zinc measurement may represent an underestimation of zinc levels in the immediate vicinity of GluN2A (Chapter 2). We hypothesized that ZnT1 organizes zinc into microdomains that specifically concentrate zinc near NMDARs, and therefore the local concentration and subsequent inhibition may be higher than what is measured for the entire coverslip. Interestingly, ZnT1 expression and subsequent NMDAR inhibition is upregulated by intracellular zinc signals (Chapter 3). This suggests that endogenous extracellular zinc levels regulated by ZnT1 dynamically increases in response to intracellular zinc state. Together these results provide evidence that endogenous zinc signaling mechanisms may be useful targets for neuroprotection against excitotoxicity.

Appendix A.4 Methods

Appendix A.4.1 Ratiometric Zinc Imaging

To determine the concentration of extracellular zinc in cortical cultures described above, the ratiometric zinc probe LZ9 (2 µM) was used as previously described (Anderson *et al.*, 2015). Zinc sensitive (blue excitation) and zinc-insensitive (green excitation) fluorescence was evoked using an interleaved pattern of excitation. Fluorescence was monitored continually until a steady state (R_{tonic}) was observed, at which point EDTA (4.5 mM) was added to achieve minimum Zn^{2+} fluorescence (R_{min}), followed by $ZnCl_2$ (5 mM) to saturate the probe for maximum Zn^{2+} fluorescence (R_{max}). Ratiometric fluorescence was calculated by taking the ratio of Zn^{2+} sensitive: Zn^{2+} insensitive fluorescence. Total extracellular Zn^{2+} concentration was calculated using the following equation: $[Zn^{2+}] = K_d * \frac{R_{tonic} - R_{min}}{R_{max} - R_{tonic}}$.

Appendix A.4.2 Neuronal Cultures and LDH Assay

All animal procedures used in experiments were approved by the Institutional Animal Care and Use Committee of the University of Pittsburgh School of Medicine. Cortical cultures were prepared from embryonic day 16 rats. Briefly, pregnant rats (Charles River Laboratory) were sacrificed via CO2 inhalation. Embryonic cortices were dissociated with trypsin and plated at 670,000 cells per well on glass coverslips in six-well plates. Non-neuronal cell proliferation was inhibited after 2 weeks in culture with cytosine arabinoside (1–2 µM). Cultures were utilized at 3–4 weeks in vitro. Following overnight treatment with the glutamate uptake inhibitor TBOA (50

μM), the zinc chelator ZX1 (3 μM) and/or the NMDAR antagonist memantine (50 μM), cell viability was assessed using a lactate dehydrogenase (LDH) release assay (TOX-7 in vitro toxicology assay kit; Sigma). To visualize cell morphology, neurons were transfected with green fluorescent protein (GFP) using 2 μL Lipofectamine 2000, 100 μL Opti-MEM media, and 1.5 μg DNA per well.

Bibliography

Adlard, P.A. & Bush, A.I. (2018) Metals and Alzheimer's Disease: How Far Have We Come in the Clinic? *J Alzheimers Dis*, **62**, 1369-1379.

Aguilar-Alonso, P., Martinez-Fong, D., Pazos-Salazar, N.G., Brambila, E., Gonzalez-Barrios, J.A., Mejorada, A., Flores, G., Millan-Perezpeña, L., Rubio, H. & Leon-Chavez, B.A. (2008) The increase in zinc levels and upregulation of zinc transporters are mediated by nitric oxide in the cerebral cortex after transient ischemia in the rat. *Brain Res*, **1200**, 89-98.

Aizenman, E. (2019) Zinc Signaling in the Life and Death of Neurons. In Fukada, T., Kambe, T. (eds) *Zinc Signaling*. Springer Singapore, Singapore, pp. 165-185.

Aizenman, E., Stout, A.K., Hartnett, K.A., Dineley, K.E., McLaughlin, B. & Reynolds, I.J. (2000) Induction of neuronal apoptosis by thiol oxidation: putative role of intracellular zinc release. *J Neurochem*, **75**, 1878-1888.

Anderson, C.T., Kumar, M., Xiong, S. & Tzounopoulos, T. (2017) Cell-specific gain modulation by synaptically released zinc in cortical circuits of audition. *Elife*, **6**.

Anderson, C.T., Radford, R.J., Zastrow, M.L., Zhang, D.Y., Apfel, U.P., Lippard, S.J. & Tzounopoulos, T. (2015) Modulation of extrasynaptic NMDA receptors by synaptic and tonic zinc. *Proc Natl Acad Sci U S A*, **112**, E2705-2714.

Andreini, C., Banci, L., Bertini, I. & Rosato, A. (2006) Counting the zinc-proteins encoded in the human genome. *J Proteome Res*, **5**, 196-201.

Andrews, G.K., Wang, H., Dey, S.K. & Palmiter, R.D. (2004) Mouse zinc transporter 1 gene provides an essential function during early embryonic development. *Genesis*, **40**, 74-81.

Aras, M.A., Hara, H., Hartnett, K.A., Kandler, K. & Aizenman, E. (2009) Protein kinase C regulation of neuronal zinc signaling mediates survival during preconditioning. *J Neurochem*, **110**, 106-117.

Arons, M.H., Lee, K., Thynne, C.J., Kim, S.A., Schob, C., Kindler, S., Montgomery, J.M. & Garner, C.C. (2016) Shank3 Is Part of a Zinc-Sensitive Signaling System That Regulates Excitatory Synaptic Strength. *J Neurosci*, **36**, 9124-9134.

Aschner, M., Cherian, M.G., Klaassen, C.D., Palmiter, R.D., Erickson, J.C. & Bush, A.I. (1997) Metallothioneins in brain--the role in physiology and pathology. *Toxicol Appl Pharmacol*, **142**, 229-242.

Assaf, S.Y. & Chung, S.H. (1984) Release of endogenous Zn2+ from brain tissue during activity. *Nature*, **308**, 734-736.

Atar, D., Backx, P.H., Appel, M.M., Gao, W.D. & Marban, E. (1995) Excitation-transcription coupling mediated by zinc influx through voltage-dependent calcium channels. *J Biol Chem*, **270**, 2473-2477.

Barberis, A., Cherubini, E. & Mozrzymas, J.W. (2000) Zinc inhibits miniature GABAergic currents by allosteric modulation of GABAA receptor gating. *J Neurosci*, **20**, 8618-8627.

Berridge, M.J. (2006) Calcium microdomains: organization and function. *Cell Calcium*, **40**, 405-412.

Besser, L., Chorin, E., Sekler, I., Silverman, W.F., Atkin, S., Russell, J.T. & Hershfinkel, M. (2009) Synaptically released zinc triggers metabotropic signaling via a zinc-sensing receptor in the hippocampus. *J Neurosci*, **29**, 2890-2901.

Biederer, T., Kaeser, P.S. & Blanpied, T.A. (2017) Transcellular Nanoalignment of Synaptic Function. *Neuron*, **96**, 680-696.

Bloomenthal, A.B., Goldwater, E., Pritchett, D.B. & Harrison, N.L. (1994) Biphasic modulation of the strychnine-sensitive glycine receptor by Zn2+. *Mol Pharmacol*, **46**, 1156-1159.

Bonanni, L., Chachar, M., Jover-Mengual, T., Li, H., Jones, A., Yokota, H., Ofengeim, D., Flannery, R.J., Miyawaki, T., Cho, C.H., Polster, B.M., Pypaert, M., Hardwick, J.M., Sensi, S.L., Zukin, R.S. & Jonas, E.A. (2006) Zinc-dependent multi-conductance channel activity in mitochondria isolated from ischemic brain. *J Neurosci*, **26**, 6851-6862.

Bresink, I., Ebert, B., Parsons, C.G. & Mutschler, E. (1996) Zinc changes AMPA receptor properties: results of binding studies and patch clamp recordings. *Neuropharmacology*, **35**, 503-509.

Brittain, J.M., Chen, L., Wilson, S.M., Brustovetsky, T., Gao, X., Ashpole, N.M., Molosh, A.I., You, H., Hudmon, A., Shekhar, A., White, F.A., Zamponi, G.W., Brustovetsky, N., Chen, J. & Khanna, R. (2011) Neuroprotection against traumatic brain injury by a peptide derived from the collapsin response mediator protein 2 (CRMP2). *J Biol Chem*, **286**, 37778-37792.

Brown, C.E. & Dyck, R.H. (2002) Rapid, experience-dependent changes in levels of synaptic zinc in primary somatosensory cortex of the adult mouse. *J Neurosci*, **22**, 2617-2625.

Brown, C.E. & Dyck, R.H. (2005) Modulation of synaptic zinc in barrel cortex by whisker stimulation. *Neuroscience*, **134**, 355-359.

Bush, A.I., Pettingell, W.H., Multhaup, G., d Paradis, M., Vonsattel, J.P., Gusella, J.F., Beyreuther, K., Masters, C.L. & Tanzi, R.E. (1994) Rapid induction of Alzheimer A beta amyloid formation by zinc. *Science*, **265**, 1464-1467.

Bush, A.I. & Tanzi, R.E. (2008) Therapeutics for Alzheimer's disease based on the metal hypothesis. *Neurotherapeutics*, **5**, 421-432.

Carter, A.D., Felber, B.K., Walling, M.J., Jubier, M.F., Schmidt, C.J. & Hamer, D.H. (1984) Duplicated heavy metal control sequences of the mouse metallothionein-I gene. *Proc Natl Acad Sci U S A*, **81**, 7392-7396.

Celentano, J.J., Gyenes, M., Gibbs, T.T. & Farb, D.H. (1991) Negative modulation of the gamma-aminobutyric acid response by extracellular zinc. *Mol Pharmacol*, **40**, 766-773.

Choi, D.W., Yokoyama, M. & Koh, J. (1988) Zinc neurotoxicity in cortical cell culture. *Neuroscience*, **24**, 67-79.

Chorin, E., Vinograd, O., Fleidervish, I., Gilad, D., Herrmann, S., Sekler, I., Aizenman, E. & Hershfinkel, M. (2011) Upregulation of KCC2 activity by zinc-mediated neurotransmission via the mZnR/GPR39 receptor. *J Neurosci*, **31**, 12916-12926.

Christine, C.W. & Choi, D.W. (1990) Effect of zinc on NMDA receptor-mediated channel currents in cortical neurons. *J Neurosci*, **10**, 108-116.

Cole, T.B., Wenzel, H.J., Kafer, K.E., Schwartzkroin, P.A. & Palmiter, R.D. (1999) Elimination of zinc from synaptic vesicles in the intact mouse brain by disruption of the ZnT3 gene. *Proc Natl Acad Sci U S A*, **96**, 1716-1721.

Colvin, R.A., Davis, N., Nipper, R.W. & Carter, P.A. (2000) Zinc transport in the brain: routes of zinc influx and efflux in neurons. *J Nutr*, **130**, 1484s-1487s.

Colvin, R.A., Holmes, W.R., Fontaine, C.P. & Maret, W. (2010) Cytosolic zinc buffering and muffling: their role in intracellular zinc homeostasis. *Metallomics*, **2**, 306-317.

Crouch, P.J., Savva, M.S., Hung, L.W., Donnelly, P.S., Mot, A.I., Parker, S.J., Greenough, M.A., Volitakis, I., Adlard, P.A., Cherny, R.A., Masters, C.L., Bush, A.I., Barnham, K.J. & White, A.R. (2011) The Alzheimer's therapeutic PBT2 promotes amyloid-β degradation and GSK3 phosphorylation via a metal chaperone activity. *J Neurochem*, **119**, 220-230.

Cull-Candy, S.G. & Leszkiewicz, D.N. (2004) Role of distinct NMDA receptor subtypes at central synapses. *Sci STKE*, **2004**, re16.

Dalton, T.P., Bittel, D. & Andrews, G.K. (1997) Reversible activation of mouse metal response element-binding transcription factor 1 DNA binding involves zinc interaction with the zinc finger domain. *Mol Cell Biol*, **17**, 2781-2789.

Danysz, W. & Parsons, C.G. (2012) Alzheimer's disease, β-amyloid, glutamate, NMDA receptors and memantine--searching for the connections. *Br J Pharmacol*, **167**, 324-352.

Deshpande, A., Kawai, H., Metherate, R., Glabe, C.G. & Busciglio, J. (2009) A role for synaptic zinc in activity-dependent Abeta oligomer formation and accumulation at excitatory synapses. *J Neurosci*, **29**, 4004-4015.

Devinney, M.J., 2nd, Reynolds, I.J. & Dineley, K.E. (2005) Simultaneous detection of intracellular free calcium and zinc using fura-2FF and FluoZin-3. *Cell Calcium*, **37**, 225-232.

Dineley, K.E., Devinney, M.J., 2nd, Zeak, J.A., Rintoul, G.L. & Reynolds, I.J. (2008) Glutamate mobilizes [Zn2+] through Ca2+ -dependent reactive oxygen species accumulation. *J Neurochem*, **106**, 2184-2193.

Dineley, K.E., Richards, L.L., Votyakova, T.V. & Reynolds, I.J. (2005) Zinc causes loss of membrane potential and elevates reactive oxygen species in rat brain mitochondria. *Mitochondrion*, **5**, 55-65.

Du, S., McLaughlin, B., Pal, S. & Aizenman, E. (2002) In vitro neurotoxicity of methylisothiazolinone, a commonly used industrial and household biocide, proceeds via a zinc and extracellular signal-regulated kinase mitogen-activated protein kinase-dependent pathway. *J Neurosci*, **22**, 7408-7416.

Dufner-Beattie, J., Weaver, B.P., Geiser, J., Bilgen, M., Larson, M., Xu, W. & Andrews, G.K. (2007) The mouse acrodermatitis enteropathica gene Slc39a4 (Zip4) is essential for early development and heterozygosity causes hypersensitivity to zinc deficiency. *Hum Mol Genet*, **16**, 1391-1399.

Durnam, D.M. & Palmiter, R.D. (1981) Transcriptional regulation of the mouse metallothionein-I gene by heavy metals. *J Biol Chem*, **256**, 5712-5716.

Eichelsdoerfer, J.L., Evans, J.A., Slaugenhaupt, S.A. & Cuajungco, M.P. (2010) Zinc dyshomeostasis is linked with the loss of mucolipidosis IV-associated TRPML1 ion channel. *J Biol Chem*, **285**, 34304-34308.

Eide, D., Broderius, M., Fett, J. & Guerinot, M.L. (1996) A novel iron-regulated metal transporter from plants identified by functional expression in yeast. *Proc Natl Acad Sci U S A*, **93**, 5624-5628.

Emmetsberger, J., Mirrione, M.M., Zhou, C., Fernandez-Monreal, M., Siddiq, M.M., Ji, K. & Tsirka, S.E. (2010) Tissue plasminogen activator alters intracellular sequestration of zinc through interaction with the transporter ZIP4. *J Neurosci*, **30**, 6538-6547.

Eom, K., Hyun, J.H., Lee, D.G., Kim, S., Jeong, H.J., Kang, J.S., Ho, W.K. & Lee, S.H. (2019) Intracellular Zn(2+) Signaling Facilitates Mossy Fiber Input-Induced Heterosynaptic Potentiation of Direct Cortical Inputs in Hippocampal CA3 Pyramidal Cells. *J Neurosci*, **39**, 3812-3831.

Erreger, K. & Traynelis, S.F. (2008) Zinc inhibition of rat NR1/NR2A N-methyl-D-aspartate receptors. *J Physiol*, **586**, 763-778.

Fourie, C., Vyas, Y., Lee, K., Jung, Y., Garner, C.C. & Montgomery, J.M. (2018) Dietary Zinc Supplementation Prevents Autism Related Behaviors and Striatal Synaptic Dysfunction in Shank3 Exon 13-16 Mutant Mice. *Front Cell Neurosci*, **12**, 374.

Frederickson, C.J., Hernandez, M.D. & McGinty, J.F. (1989) Translocation of zinc may contribute to seizure-induced death of neurons. *Brain Res*, **480**, 317-321.

Frederickson, C.J., Howell, G.A., Haigh, M.D. & Danscher, G. (1988) Zinc-containing fiber systems in the cochlear nuclei of the rat and mouse. *Hear Res*, **36**, 203-211.

Fullard, J.F., Charney, A.W., Voloudakis, G., Uzilov, A.V., Haroutunian, V. & Roussos, P. (2019) Assessment of somatic single-nucleotide variation in brain tissue of cases with schizophrenia. *Transl Psychiatry*, **9**, 21.

Gaither, L.A. & Eide, D.J. (2000) Functional expression of the human hZIP2 zinc transporter. *J Biol Chem*, **275**, 5560-5564.

Gaither, L.A. & Eide, D.J. (2001) The human ZIP1 transporter mediates zinc uptake in human K562 erythroleukemia cells. *J Biol Chem*, **276**, 22258-22264.

Golan, Y., Alhadeff, R., Warshel, A. & Assaraf, Y.G. (2019) ZnT2 is an electroneutral proton-coupled vesicular antiporter displaying an apparent stoichiometry of two protons per zinc ion. *PLoS Comput Biol*, **15**, e1006882.

Grabrucker, S., Boeckers, T.M. & Grabrucker, A.M. (2016) Gender Dependent Evaluation of Autism like Behavior in Mice Exposed to Prenatal Zinc Deficiency. *Front Behav Neurosci*, **10**, 37.

Grabrucker, S., Jannetti, L., Eckert, M., Gaub, S., Chhabra, R., Pfaender, S., Mangus, K., Reddy, P.P., Rankovic, V., Schmeisser, M.J., Kreutz, M.R., Ehret, G., Boeckers, T.M. & Grabrucker, A.M. (2014) Zinc deficiency dysregulates the synaptic ProSAP/Shank scaffold and might contribute to autism spectrum disorders. *Brain*, **137**, 137-152.

Ha, H.T.T., Leal-Ortiz, S., Lalwani, K., Kiyonaka, S., Hamachi, I., Mysore, S.P., Montgomery, J.M., Garner, C.C., Huguenard, J.R. & Kim, S.A. (2018) Shank and Zinc Mediate an AMPA Receptor Subunit Switch in Developing Neurons. *Front Mol Neurosci*, **11**, 405.

Hara, H. & Aizenman, E. (2004) A molecular technique for detecting the liberation of intracellular zinc in cultured neurons. *J Neurosci Methods*, **137**, 175-180.

Hardingham, G. (2019) NMDA receptor C-terminal signaling in development, plasticity, and disease. *F1000Res*, **8**, F1000 Faculty Rev-1547.

Hardingham, G.E. & Bading, H. (2010) Synaptic versus extrasynaptic NMDA receptor signalling: implications for neurodegenerative disorders. *Nat Rev Neurosci*, **11**, 682-696.

Hardingham, G.E. & Do, K.Q. (2016) Linking early-life NMDAR hypofunction and oxidative stress in schizophrenia pathogenesis. *Nat Rev Neurosci*, **17**, 125-134.

Hardyman, J.E., Tyson, J., Jackson, K.A., Aldridge, C., Cockell, S.J., Wakeling, L.A., Valentine, R.A. & Ford, D. (2016) Zinc sensing by metal-responsive transcription factor 1 (MTF1) controls metallothionein and ZnT1 expression to buffer the sensitivity of the transcriptome response to zinc. *Metallomics*, **8**, 337-343.

Haug, F.M. (1967) Electron microscopical localization of the zinc in hippocampal mossy fibre synapses by a modified sulfide silver procedure. *Histochemie*, **8**, 355-368.

He, K. & Aizenman, E. (2010) ERK signaling leads to mitochondrial dysfunction in extracellular zinc-induced neurotoxicity. *J Neurochem*, **114**, 452-461.

Hershfinkel, M., Moran, A., Grossman, N. & Sekler, I. (2001) A zinc-sensing receptor triggers the release of intracellular Ca2+ and regulates ion transport. *Proc Natl Acad Sci U S A*, **98**, 11749-11754.

Hess, J.L., Tylee, D.S., Barve, R., de Jong, S., Ophoff, R.A., Kumarasinghe, N., Tooney, P., Schall, U., Gardiner, E., Beveridge, N.J., Scott, R.J., Yasawardene, S., Perera, A., Mendis, J., Carr, V., Kelly, B., Cairns, M., Tsuang, M.T. & Glatt, S.J. (2016) Transcriptome-wide mega-analyses reveal joint dysregulation of immunologic genes and transcription regulators in brain and blood in schizophrenia. *Schizophr Res*, **176**, 114-124.

Hirzel, K., Müller, U., Latal, A.T., Hülsmann, S., Grudzinska, J., Seeliger, M.W., Betz, H. & Laube, B. (2006) Hyperekplexia phenotype of glycine receptor alpha1 subunit mutant mice identifies Zn(2+) as an essential endogenous modulator of glycinergic neurotransmission. *Neuron*, **52**, 679-690.

Holst, B., Egerod, K.L., Schild, E., Vickers, S.P., Cheetham, S., Gerlach, L.O., Storjohann, L., Stidsen, C.E., Jones, R., Beck-Sickinger, A.G. & Schwartz, T.W. (2007) GPR39 signaling is stimulated by zinc ions but not by obestatin. *Endocrinology*, **148**, 13-20.

Hosie, A.M., Dunne, E.L., Harvey, R.J. & Smart, T.G. (2003) Zinc-mediated inhibition of GABA(A) receptors: discrete binding sites underlie subtype specificity. *Nat Neurosci*, **6**, 362-369.

Hou, S., Vigeland, L.E., Zhang, G., Xu, R., Li, M., Heinemann, S.H. & Hoshi, T. (2010) Zn2+ activates large conductance Ca2+-activated K+ channel via an intracellular domain. *J Biol Chem*, **285**, 6434-6442.

Howell, G.A., Welch, M.G. & Frederickson, C.J. (1984) Stimulation-induced uptake and release of zinc in hippocampal slices. *Nature*, **308**, 736-738.

Hu, H., Bandell, M., Petrus, M.J., Zhu, M.X. & Patapoutian, A. (2009) Zinc activates damage-sensing TRPA1 ion channels. *Nat Chem Biol*, **5**, 183-190.

Huang, X., Cuajungco, M.P., Atwood, C.S., Moir, R.D., Tanzi, R.E. & Bush, A.I. (2000) Alzheimer's disease, beta-amyloid protein and zinc. *J Nutr*, **130**, 1488s-1492s.

Huang, Y.Z., Pan, E., Xiong, Z.Q. & McNamara, J.O. (2008) Zinc-mediated transactivation of TrkB potentiates the hippocampal mossy fiber-CA3 pyramid synapse. *Neuron*, **57**, 546-558.

Inoue, K., Branigan, D. & Xiong, Z.G. (2010) Zinc-induced neurotoxicity mediated by transient receptor potential melastatin 7 channels. *J Biol Chem*, **285**, 7430-7439.

Jackson, A.C., Liu, J., Vallanat, B., Jones, C., Nelms, M.D., Patlewicz, G. & Corton, J.C. (2020) Identification of novel activators of the metal responsive transcription factor (MTF-1) using a gene expression biomarker in a microarray compendium. *Metallomics*, **12**, 1400-1415.

Jia, Y., Jeng, J.M., Sensi, S.L. & Weiss, J.H. (2002) Zn2+ currents are mediated by calcium-permeable AMPA/kainate channels in cultured murine hippocampal neurones. *J Physiol*, **543**, 35-48.

Jiang, D., Sullivan, P.G., Sensi, S.L., Steward, O. & Weiss, J.H. (2001) Zn(2+) induces permeability transition pore opening and release of pro-apoptotic peptides from neuronal mitochondria. *J Biol Chem*, **276**, 47524-47529.

Jirakulaporn, T. & Muslin, A.J. (2004) Cation diffusion facilitator proteins modulate Raf-1 activity. *J Biol Chem*, **279**, 27807-27815.

Jo, S.M., Danscher, G., Schrøder, H.D. & Suh, S.W. (2008) Depletion of vesicular zinc in dorsal horn of spinal cord causes increased neuropathic pain in mice. *Biometals*, **21**, 151-158.

Johanssen, T., Suphantarida, N., Donnelly, P.S., Liu, X.M., Petrou, S., Hill, A.F. & Barnham, K.J. (2015) PBT2 inhibits glutamate-induced excitotoxicity in neurons through metal-mediated preconditioning. *Neurobiol Dis*, **81**, 176-185.

Justice, J.A., Schulien, A.J., He, K., Hartnett, K.A., Aizenman, E. & Shah, N.H. (2017) Disruption of K(V)2.1 somato-dendritic clusters prevents the apoptogenic increase of potassium currents. *Neuroscience*, **354**, 158-167.

Kalappa, B.I., Anderson, C.T., Goldberg, J.M., Lippard, S.J. & Tzounopoulos, T. (2015) AMPA receptor inhibition by synaptically released zinc. *Proc Natl Acad Sci U S A*, **112**, 15749-15754.

Kalappa, B.I. & Tzounopoulos, T. (2017) Context-Dependent Modulation of Excitatory Synaptic Strength by Synaptically Released Zinc. *eNeuro*, **4**, ENEURO.0011-0017.2017.

Kambe, T., Hashimoto, A. & Fujimoto, S. (2014) Current understanding of ZIP and ZnT zinc transporters in human health and diseases. *Cell Mol Life Sci*, **71**, 3281-3295.

Kambe, T., Tsuji, T., Hashimoto, A. & Itsumura, N. (2015) The Physiological, Biochemical, and Molecular Roles of Zinc Transporters in Zinc Homeostasis and Metabolism. *Physiol Rev*, **95**, 749-784.

Kay, A.R. & Toth, K. (2008) Is zinc a neuromodulator? *Sci Signal*, **1**, re3.

Kerchner, G.A., Canzoniero, L.M., Yu, S.P., Ling, C. & Choi, D.W. (2000a) Zn2+ current is mediated by voltage-gated Ca2+ channels and enhanced by extracellular acidity in mouse cortical neurones. *J Physiol*, **528 Pt 1**, 39-52.

Kerchner, G.A., Canzoniero, L.M., Yu, S.P., Ling, C. & Choi, D.W. (2000b) Zn2+ current is mediated by voltage-gated Ca2+ channels and enhanced by extracellular acidity in mouse cortical neurones. *J Physiol*, **528 Pt 1**, 39-52.

Kiedrowski, L. (2012) Cytosolic acidification and intracellular zinc release in hippocampal neurons. *J Neurochem*, **121**, 438-450.

Kiedrowski, L. (2014) Proton-dependent zinc release from intracellular ligands. *J Neurochem*, **130**, 87-96.

Kitayama, T., Morita, K., Motoyama, N. & Dohi, T. (2016) Down-regulation of zinc transporter-1 in astrocytes induces neuropathic pain via the brain-derived neurotrophic factor - K(+)-Cl(-) co-transporter-2 signaling pathway in the mouse spinal cord. *Neurochem Int*, **101**, 120-131.

Kodirov, S.A., Takizawa, S., Joseph, J., Kandel, E.R., Shumyatsky, G.P. & Bolshakov, V.Y. (2006) Synaptically released zinc gates long-term potentiation in fear conditioning pathways. *Proc Natl Acad Sci U S A*, **103**, 15218-15223.

Koh, J.Y. & Choi, D.W. (1994) Zinc toxicity on cultured cortical neurons: involvement of N-methyl-D-aspartate receptors. *Neuroscience*, **60**, 1049-1057.

Koh, J.Y., Suh, S.W., Gwag, B.J., He, Y.Y., Hsu, C.Y. & Choi, D.W. (1996) The role of zinc in selective neuronal death after transient global cerebral ischemia. *Science*, **272**, 1013-1016.

Kouvaros, S., Kumar, M. & Tzounopoulos, T. (2020) Synaptic Zinc Enhances Inhibition Mediated by Somatostatin, but not Parvalbumin, Cells in Mouse Auditory Cortex. *Cereb Cortex*, **30**, 3895-3909.

Krall, R.F., Moutal, A., Phillips, M.B., Asraf, H., Johnson, J.W., Khanna, R., Hershfinkel, M., Aizenman, E. & Tzounopoulos, T. (2020) Synaptic zinc inhibition of NMDA receptors depends on the association of GluN2A with the zinc transporter ZnT1. *Science Advances*, **6**, eabb1515.

Kranz, T.M., Harroch, S., Manor, O., Lichtenberg, P., Friedlander, Y., Seandel, M., Harkavy-Friedman, J., Walsh-Messinger, J., Dolgalev, I., Heguy, A., Chao, M.V. & Malaspina, D. (2015) De novo mutations from sporadic schizophrenia cases highlight important signaling genes in an independent sample. *Schizophr Res*, **166**, 119-124.

Kukic, I., Lee, J.K., Coblentz, J., Kelleher, S.L. & Kiselyov, K. (2013) Zinc-dependent lysosomal enlargement in TRPML1-deficient cells involves MTF-1 transcription factor and ZnT4 (Slc30a4) transporter. *Biochem J*, **451**, 155-163.

Kumar, M., Xiong, S., Tzounopoulos, T. & Anderson, C.T. (2019) Fine Control of Sound Frequency Tuning and Frequency Discrimination Acuity by Synaptic Zinc Signaling in Mouse Auditory Cortex. *J Neurosci*, **39**, 854-865.

Laitaoja, M., Valjakka, J. & Jänis, J. (2013) Zinc coordination spheres in protein structures. *Inorg Chem*, **52**, 10983-10991.

Laity, J.H., Lee, B.M. & Wright, P.E. (2001) Zinc finger proteins: new insights into structural and functional diversity. *Curr Opin Struct Biol*, **11**, 39-46.

Land, P.W. & Aizenman, E. (2005) Zinc accumulation after target loss: an early event in retrograde degeneration of thalamic neurons. *Eur J Neurosci*, **21**, 647-657.

Langmade, S.J., Ravindra, R., Daniels, P.J. & Andrews, G.K. (2000) The transcription factor MTF-1 mediates metal regulation of the mouse ZnT1 gene. *J Biol Chem*, **275**, 34803-34809.

Lauwers, E., Landuyt, B., Arckens, L., Schoofs, L. & Luyten, W. (2006) Obestatin does not activate orphan G protein-coupled receptor GPR39. *Biochem Biophys Res Commun*, **351**, 21-25.

Lavoie, N., Jeyaraju, D.V., Peralta, M.R., 3rd, Seress, L., Pellegrini, L. & Toth, K. (2011) Vesicular zinc regulates the Ca2+ sensitivity of a subpopulation of presynaptic vesicles at hippocampal mossy fiber terminals. *J Neurosci*, **31**, 18251-18265.

Lee, E.J., Lee, H., Huang, T.N., Chung, C., Shin, W., Kim, K., Koh, J.Y., Hsueh, Y.P. & Kim, E. (2015a) Trans-synaptic zinc mobilization improves social interaction in two mouse models of autism through NMDAR activation. *Nat Commun*, **6**, 7168.

Lee, J.Y., Cole, T.B., Palmiter, R.D. & Koh, J.Y. (2000) Accumulation of zinc in degenerating hippocampal neurons of ZnT3-null mice after seizures: evidence against synaptic vesicle origin. *J Neurosci*, **20**, Rc79.

Lee, J.Y., Kim, Y.J., Kim, T.Y., Koh, J.Y. & Kim, Y.H. (2008) Essential role for zinc-triggered p75NTR activation in preconditioning neuroprotection. *J Neurosci*, **28**, 10919-10927.

Lee, J.Y., Oh, S.B., Hwang, J.J., Suh, N., Jo, D.G., Kim, J.S. & Koh, J.Y. (2015b) Indomethacin preconditioning induces ischemic tolerance by modifying zinc availability in the brain. *Neurobiol Dis*, **81**, 186-195.

Legendre, P. & Westbrook, G.L. (1990) The inhibition of single N-methyl-D-aspartate-activated channels by zinc ions on cultured rat neurones. *J Physiol*, **429**, 429-449.

Levy, S., Beharier, O., Etzion, Y., Mor, M., Buzaglo, L., Shaltiel, L., Gheber, L.A., Kahn, J., Muslin, A.J., Katz, A., Gitler, D. & Moran, A. (2009) Molecular basis for zinc transporter 1 action as an endogenous inhibitor of L-type calcium channels. *J Biol Chem*, **284**, 32434-32443.

Li, Y., Hough, C.J., Suh, S.W., Sarvey, J.M. & Frederickson, C.J. (2001) Rapid translocation of Zn(2+) from presynaptic terminals into postsynaptic hippocampal neurons after physiological stimulation. *J Neurophysiol*, **86**, 2597-2604.

Lin, W., Mohandas, B., Fontaine, C.P. & Colvin, R.A. (2007) Release of intracellular Zn(2+) in cultured neurons after brief exposure to low concentrations of exogenous nitric oxide. *Biometals*, **20**, 891-901.

Liu, X.J., Gingrich, J.R., Vargas-Caballero, M., Dong, Y.N., Sengar, A., Beggs, S., Wang, S.H., Ding, H.K., Frankland, P.W. & Salter, M.W. (2008) Treatment of inflammatory and neuropathic pain by uncoupling Src from the NMDA receptor complex. *Nat Med*, **14**, 1325-1332.

Lorca, R.A., Rozas, C., Loyola, S., Moreira-Ramos, S., Zeise, M.L., Kirkwood, A., Huidobro-Toro, J.P. & Morales, B. (2011) Zinc enhances long-term potentiation through P2X receptor modulation in the hippocampal CA1 region. *Eur J Neurosci*, **33**, 1175-1185.

Low, C.M., Zheng, F., Lyuboslavsky, P. & Traynelis, S.F. (2000) Molecular determinants of coordinated proton and zinc inhibition of N-methyl-D-aspartate NR1/NR2A receptors. *Proc Natl Acad Sci U S A*, **97**, 11062-11067.

Luo, J., Bavencoffe, A., Yang, P., Feng, J., Yin, S., Qian, A., Yu, W., Liu, S., Gong, X., Cai, T., Walters, E.T., Dessauer, C.W. & Hu, H. (2018) Zinc Inhibits TRPV1 to Alleviate Chemotherapy-Induced Neuropathic Pain. *J Neurosci*, **38**, 474-483.

Malaiyandi, L.M., Vergun, O., Dineley, K.E. & Reynolds, I.J. (2005) Direct visualization of mitochondrial zinc accumulation reveals uniporter-dependent and -independent transport mechanisms. *J Neurochem*, **93**, 1242-1250.

Manev, H., Kharlamov, E., Uz, T., Mason, R.P. & Cagnoli, C.M. (1997) Characterization of zinc-induced neuronal death in primary cultures of rat cerebellar granule cells. *Exp Neurol*, **146**, 171-178.

Manzerra, P., Behrens, M.M., Canzoniero, L.M., Wang, X.Q., Heidinger, V., Ichinose, T., Yu, S.P. & Choi, D.W. (2001) Zinc induces a Src family kinase-mediated up-regulation of NMDA receptor activity and excitotoxicity. *Proc Natl Acad Sci U S A*, **98**, 11055-11061.

Marek, G.J., Behl, B., Bespalov, A.Y., Gross, G., Lee, Y. & Schoemaker, H. (2010) Glutamatergic (N-methyl-D-aspartate receptor) hypofrontality in schizophrenia: too little juice or a miswired brain? *Mol Pharmacol*, **77**, 317-326.

Maret, W. (1994) Oxidative metal release from metallothionein via zinc-thiol/disulfide interchange. *Proc Natl Acad Sci U S A*, **91**, 237-241.

Maret, W. (1995) Metallothionein/disulfide interactions, oxidative stress, and the mobilization of cellular zinc. *Neurochem Int*, **27**, 111-117.

Maret, W. & Krezel, A. (2007) Cellular zinc and redox buffering capacity of metallothionein/thionein in health and disease. *Mol Med*, **13**, 371-375.

Marin, P., Israël, M., Glowinski, J. & Prémont, J. (2000) Routes of zinc entry in mouse cortical neurons: role in zinc-induced neurotoxicity. *Eur J Neurosci*, **12**, 8-18.

Matsuzaki, M., Honkura, N., Ellis-Davies, G.C. & Kasai, H. (2004) Structural basis of long-term potentiation in single dendritic spines. *Nature*, **429**, 761-766.

McAllister, B.B. & Dyck, R.H. (2017) Zinc transporter 3 (ZnT3) and vesicular zinc in central nervous system function. *Neurosci Biobehav Rev*, **80**, 329-350.

McLaughlin, B., Pal, S., Tran, M.P., Parsons, A.A., Barone, F.C., Erhardt, J.A. & Aizenman, E. (2001) p38 activation is required upstream of potassium current enhancement and caspase cleavage in thiol oxidant-induced neuronal apoptosis. *J Neurosci*, **21**, 3303-3311.

Medvedeva, Y.V., Ji, S.G., Yin, H.Z. & Weiss, J.H. (2017) Differential Vulnerability of CA1 versus CA3 Pyramidal Neurons After Ischemia: Possible Relationship to Sources of Zn2+ Accumulation and Its Entry into and Prolonged Effects on Mitochondria. *J Neurosci*, **37**, 726-737.

Medvedeva, Y.V. & Weiss, J.H. (2014) Intramitochondrial Zn2+ accumulation via the Ca2+ uniporter contributes to acute ischemic neurodegeneration. *Neurobiol Dis*, **68**, 137-144.

Mellone, M., Pelucchi, S., Alberti, L., Genazzani, A.A., Di Luca, M. & Gardoni, F. (2015) Zinc transporter-1: a novel NMDA receptor-binding protein at the postsynaptic density. *J Neurochem*, **132**, 159-168.

Minckley, T.F., Zhang, C., Fudge, D.H., Dischler, A.M., LeJeune, K.D., Xu, H. & Qin, Y. (2019) Sub-nanomolar sensitive GZnP3 reveals TRPML1-mediated neuronal Zn(2+) signals. *Nat Commun*, **10**, 4806.

Mor, M., Beharier, O., Levy, S., Kahn, J., Dror, S., Blumenthal, D., Gheber, L.A., Peretz, A., Katz, A., Moran, A. & Etzion, Y. (2012) ZnT-1 enhances the activity and surface expression of T-type calcium channels through activation of Ras-ERK signaling. *Am J Physiol Cell Physiol*, **303**, C192-203.

Mott, D.D., Benveniste, M. & Dingledine, R.J. (2008) pH-dependent inhibition of kainate receptors by zinc. *J Neurosci*, **28**, 1659-1671.

Murakami, K., Whiteley, M.K. & Routtenberg, A. (1987) Regulation of protein kinase C activity by cooperative interaction of Zn2+ and Ca2+. *J Biol Chem*, **262**, 13902-13906.

Nakashima, A.S. & Dyck, R.H. (2010) Dynamic, experience-dependent modulation of synaptic zinc within the excitatory synapses of the mouse barrel cortex. *Neuroscience*, **170**, 1015-1019.

Nakazawa, K., Liu, M., Inoue, K. & Ohno, Y. (1997) pH dependence of facilitation by neurotransmitters and divalent cations of P2X2 purinoceptor/channels. *Eur J Pharmacol*, **337**, 309-314.

Nimmanon, T., Ziliotto, S., Morris, S., Flanagan, L. & Taylor, K.M. (2017) Phosphorylation of zinc channel ZIP7 drives MAPK, PI3K and mTOR growth and proliferation signalling. *Metallomics*, **9**, 471-481.

Nishito, Y. & Kambe, T. (2019) Zinc transporter 1 (ZNT1) expression on the cell surface is elaborately controlled by cellular zinc levels. *J Biol Chem*, **294**, 15686-15697.

Noh, K.M. & Koh, J.Y. (2000) Induction and activation by zinc of NADPH oxidase in cultured cortical neurons and astrocytes. *J Neurosci*, **20**, Rc111.

Nozaki, C., Vergnano, A.M., Filliol, D., Ouagazzal, A.M., Le Goff, A., Carvalho, S., Reiss, D., Gaveriaux-Ruff, C., Neyton, J., Paoletti, P. & Kieffer, B.L. (2011) Zinc alleviates pain through high-affinity binding to the NMDA receptor NR2A subunit. *Nat Neurosci*, **14**, 1017-1022.

Ohana, E., Hoch, E., Keasar, C., Kambe, T., Yifrach, O., Hershfinkel, M. & Sekler, I. (2009) Identification of the Zn2+ binding site and mode of operation of a mammalian Zn2+ transporter. *J Biol Chem*, **284**, 17677-17686.

Palmiter, R.D. (2004) Protection against zinc toxicity by metallothionein and zinc transporter 1. *Proc Natl Acad Sci U S A*, **101**, 4918-4923.

Palmiter, R.D., Cole, T.B., Quaife, C.J. & Findley, S.D. (1996) ZnT-3, a putative transporter of zinc into synaptic vesicles. *Proc Natl Acad Sci U S A*, **93**, 14934-14939.

Palmiter, R.D. & Findley, S.D. (1995) Cloning and functional characterization of a mammalian zinc transporter that confers resistance to zinc. *Embo j*, **14**, 639-649.

Pan, E., Zhang, X.A., Huang, Z., Krezel, A., Zhao, M., Tinberg, C.E., Lippard, S.J. & McNamara, J.O. (2011) Vesicular zinc promotes presynaptic and inhibits postsynaptic long-term potentiation of mossy fiber-CA3 synapse. *Neuron*, **71**, 1116-1126.

Paoletti, P., Ascher, P. & Neyton, J. (1997) High-affinity zinc inhibition of NMDA NR1-NR2A receptors. *J Neurosci*, **17**, 5711-5725.

Paoletti, P., Bellone, C. & Zhou, Q. (2013) NMDA receptor subunit diversity: impact on receptor properties, synaptic plasticity and disease. *Nat Rev Neurosci*, **14**, 383-400.

Paoletti, P., Perin-Dureau, F., Fayyazuddin, A., Le Goff, A., Callebaut, I. & Neyton, J. (2000) Molecular organization of a zinc binding n-terminal modulatory domain in a NMDA receptor subunit. *Neuron*, **28**, 911-925.

Paoletti, P., Vergnano, A.M., Barbour, B. & Casado, M. (2009) Zinc at glutamatergic synapses. *Neuroscience*, **158**, 126-136.

Park, J.A., Lee, J.Y., Sato, T.A. & Koh, J.Y. (2000) Co-induction of p75NTR and p75NTR-associated death executor in neurons after zinc exposure in cortical culture or transient ischemia in the rat. *J Neurosci*, **20**, 9096-9103.

Park, S.J., Min, S.H., Kang, H.W. & Lee, J.H. (2015) Differential zinc permeation and blockade of L-type Ca2+ channel isoforms Cav1.2 and Cav1.3. *Biochim Biophys Acta*, **1848**, 2092-2100.

Parsons, M.P. & Raymond, L.A. (2014) Extrasynaptic NMDA receptor involvement in central nervous system disorders. *Neuron*, **82**, 279-293.

Patrick Wu, H.P. & Dyck, R.H. (2018) Signaling by Synaptic Zinc is Required for Whisker-Mediated, Fine Texture Discrimination. *Neuroscience*, **369**, 242-247.

Pérez-Clausell, J. & Danscher, G. (1985) Intravesicular localization of zinc in rat telencephalic boutons. A histochemical study. *Brain Res*, **337**, 91-98.

Pérez-Clausell, J. & Danscher, G. (1986) Release of zinc sulphide accumulations into synaptic clefts after in vivo injection of sodium sulphide. *Brain Res*, **362**, 358-361.

Perez-Rosello, T., Anderson, C.T., Ling, C., Lippard, S.J. & Tzounopoulos, T. (2015) Tonic zinc inhibits spontaneous firing in dorsal cochlear nucleus principal neurons by enhancing glycinergic neurotransmission. *Neurobiol Dis*, **81**, 14-19.

Perez-Rosello, T., Anderson, C.T., Schopfer, F.J., Zhao, Y., Gilad, D., Salvatore, S.R., Freeman, B.A., Hershfinkel, M., Aizenman, E. & Tzounopoulos, T. (2013) Synaptic Zn2+ inhibits neurotransmitter release by promoting endocannabinoid synthesis. *J Neurosci*, **33**, 9259-9272.

Peters, S., Koh, J. & Choi, D.W. (1987) Zinc selectively blocks the action of N-methyl-D-aspartate on cortical neurons. *Science*, **236**, 589-593.

Petrenko, A.B., Yamakura, T., Baba, H. & Shimoji, K. (2003) The role of N-methyl-D-aspartate (NMDA) receptors in pain: a review. *Anesth Analg*, **97**, 1108-1116.

Pfaender, S., Sauer, A.K., Hagmeyer, S., Mangus, K., Linta, L., Liebau, S., Bockmann, J., Huguet, G., Bourgeron, T., Boeckers, T.M. & Grabrucker, A.M. (2017) Zinc deficiency and low enterocyte zinc transporter expression in human patients with autism related mutations in SHANK3. *Sci Rep*, **7**, 45190.

Prasad, A.S. (2003) Zinc deficiency. *Bmj*, **326**, 409-410.

Qian, J., Xu, K., Yoo, J., Chen, T.T., Andrews, G. & Noebels, J.L. (2011) Knockout of Zn transporters Zip-1 and Zip-3 attenuates seizure-induced CA1 neurodegeneration. *J Neurosci*, **31**, 97-104.

Qin, Y., Dittmer, P.J., Park, J.G., Jansen, K.B. & Palmer, A.E. (2011) Measuring steady-state and dynamic endoplasmic reticulum and Golgi Zn2+ with genetically encoded sensors. *Proc Natl Acad Sci U S A*, **108**, 7351-7356.

Quinta-Ferreira, M.E. & Matias, C.M. (2005) Tetanically released zinc inhibits hippocampal mossy fiber calcium, zinc and synaptic responses. *Brain Res*, **1047**, 1-9.

Rachline, J., Perin-Dureau, F., Le Goff, A., Neyton, J. & Paoletti, P. (2005) The micromolar zinc-binding domain on the NMDA receptor subunit NR2B. *J Neurosci*, **25**, 308-317.

Rassendren, F.A., Lory, P., Pin, J.P. & Nargeot, J. (1990) Zinc has opposite effects on NMDA and non-NMDA receptors expressed in Xenopus oocytes. *Neuron*, **4**, 733-740.

Redman, P.T., Hartnett, K.A., Aras, M.A., Levitan, E.S. & Aizenman, E. (2009) Regulation of apoptotic potassium currents by coordinated zinc-dependent signalling. *J Physiol*, **587**, 4393-4404.

Redman, P.T., He, K., Hartnett, K.A., Jefferson, B.S., Hu, L., Rosenberg, P.A., Levitan, E.S. & Aizenman, E. (2007) Apoptotic surge of potassium currents is mediated by p38 phosphorylation of Kv2.1. *Proc Natl Acad Sci U S A*, **104**, 3568-3573.

Reynolds, I.J. & Hastings, T.G. (1995) Glutamate induces the production of reactive oxygen species in cultured forebrain neurons following NMDA receptor activation. *J Neurosci*, **15**, 3318-3327.

Ruiz, A., Walker, M.C., Fabian-Fine, R. & Kullmann, D.M. (2004) Endogenous zinc inhibits GABA(A) receptors in a hippocampal pathway. *J Neurophysiol*, **91**, 1091-1096.

Sala, C. & Segal, M. (2014) Dendritic spines: the locus of structural and functional plasticity. *Physiol Rev*, **94**, 141-188.

Sanchez, V.B., Ali, S., Escobar, A. & Cuajungco, M.P. (2019) Transmembrane 163 (TMEM163) protein effluxes zinc. *Arch Biochem Biophys*, **677**, 108166.

Sanford, L., Carpenter, M.C. & Palmer, A.E. (2019) Intracellular Zn(2+) transients modulate global gene expression in dissociated rat hippocampal neurons. *Sci Rep*, **9**, 9411.

Sanford, L. & Palmer, A.E. (2020) Dissociated Hippocampal Neurons Exhibit Distinct Zn(2+) Dynamics in a Stimulation-Method-Dependent Manner. *ACS Chem Neurosci*, **11**, 508-514.

Scarr, E., Udawela, M., Greenough, M.A., Neo, J., Suk Seo, M., Money, T.T., Upadhyay, A., Bush, A.I., Everall, I.P., Thomas, E.A. & Dean, B. (2016) Increased cortical expression of the zinc transporter SLC39A12 suggests a breakdown in zinc cellular homeostasis as part of the pathophysiology of schizophrenia. *NPJ Schizophr*, **2**, 16002.

Schulien, A.J., Justice, J.A., Di Maio, R., Wills, Z.P., Shah, N.H. & Aizenman, E. (2016) Zn(2+) -induced Ca(2+) release via ryanodine receptors triggers calcineurin-dependent redistribution of cortical neuronal Kv2.1 K(+) channels. *J Physiol*, **594**, 2647-2659.

Searle, P.F., Stuart, G.W. & Palmiter, R.D. (1985) Building a metal-responsive promoter with synthetic regulatory elements. *Mol Cell Biol*, **5**, 1480-1489.

Segal, M. (2005) Dendritic spines and long-term plasticity. *Nat Rev Neurosci*, **6**, 277-284.

Sekler, I., Moran, A., Hershfinkel, M., Dori, A., Margulis, A., Birenzweig, N., Nitzan, Y. & Silverman, W.F. (2002) Distribution of the zinc transporter ZnT-1 in comparison with chelatable zinc in the mouse brain. *J Comp Neurol*, **447**, 201-209.

Sensi, S.L., Canzoniero, L.M., Yu, S.P., Ying, H.S., Koh, J.Y., Kerchner, G.A. & Choi, D.W. (1997) Measurement of intracellular free zinc in living cortical neurons: routes of entry. *J Neurosci*, **17**, 9554-9564.

Sensi, S.L., Paoletti, P., Bush, A.I. & Sekler, I. (2009) Zinc in the physiology and pathology of the CNS. *Nat Rev Neurosci*, **10**, 780-791.

Sensi, S.L., Ton-That, D., Sullivan, P.G., Jonas, E.A., Gee, K.R., Kaczmarek, L.K. & Weiss, J.H. (2003) Modulation of mitochondrial function by endogenous Zn2+ pools. *Proc Natl Acad Sci U S A*, **100**, 6157-6162.

Seo, S.R., Chong, S.A., Lee, S.I., Sung, J.Y., Ahn, Y.S., Chung, K.C. & Seo, J.T. (2001) Zn2+-induced ERK activation mediated by reactive oxygen species causes cell death in differentiated PC12 cells. *J Neurochem*, **78**, 600-610.

Sheline, C.T., Behrens, M.M. & Choi, D.W. (2000) Zinc-induced cortical neuronal death: contribution of energy failure attributable to loss of NAD(+) and inhibition of glycolysis. *J Neurosci*, **20**, 3139-3146.

Sheline, C.T., Ying, H.S., Ling, C.S., Canzoniero, L.M. & Choi, D.W. (2002) Depolarization-induced 65zinc influx into cultured cortical neurons. *Neurobiol Dis*, **10**, 41-53.

Shusterman, E., Beharier, O., Levy, S., Zarivach, R., Etzion, Y., Campbell, C.R., Lee, I.H., Dinudom, A., Cook, D.I., Peretz, A., Katz, A., Gitler, D. & Moran, A. (2017) Zinc transport and the inhibition of the L-type calcium channel are two separable functions of ZnT-1. *Metallomics*, **9**, 228-238.

Shusterman, E., Beharier, O., Shiri, L., Zarivach, R., Etzion, Y., Campbell, C.R., Lee, I.H., Okabayashi, K., Dinudom, A., Cook, D.I., Katz, A. & Moran, A. (2014) ZnT-1 extrudes zinc from mammalian cells functioning as a Zn(2+)/H(+) exchanger. *Metallomics*, **6**, 1656-1663.

Sindreu, C., Bayes, A., Altafaj, X. & Perez-Clausell, J. (2014a) Zinc transporter-1 concentrates at the postsynaptic density of hippocampal synapses. *Mol Brain*, **7**, 16.

Sindreu, C., Bayés, Á., Altafaj, X. & Pérez-Clausell, J. (2014b) Zinc transporter-1 concentrates at the postsynaptic density of hippocampal synapses. *Mol Brain*, **7**, 16.

Sinor, J.D., Du, S., Venneti, S., Blitzblau, R.C., Leszkiewicz, D.N., Rosenberg, P.A. & Aizenman, E. (2000) NMDA and glutamate evoke excitotoxicity at distinct cellular locations in rat cortical neurons in vitro. *J Neurosci*, **20**, 8831-8837.

Smart, T.G. & Constanti, A. (1982) A novel effect of zinc on the lobster muscle GABA receptor. *Proc R Soc Lond B Biol Sci*, **215**, 327-341.

Smirnova, I.V., Bittel, D.C., Ravindra, R., Jiang, H. & Andrews, G.K. (2000) Zinc and cadmium can promote rapid nuclear translocation of metal response element-binding transcription factor-1. *J Biol Chem*, **275**, 9377-9384.

Stork, C.J. & Li, Y.V. (2010) Zinc release from thapsigargin/IP3-sensitive stores in cultured cortical neurons. *J Mol Signal*, **5**, 5.

Stuart, G.W., Searle, P.F., Chen, H.Y., Brinster, R.L. & Palmiter, R.D. (1984) A 12-base-pair DNA motif that is repeated several times in metallothionein gene promoters confers metal regulation to a heterologous gene. *Proc Natl Acad Sci U S A*, **81**, 7318-7322.

Suh, S.W., Chen, J.W., Motamedi, M., Bell, B., Listiak, K., Pons, N.F., Danscher, G. & Frederickson, C.J. (2000) Evidence that synaptically-released zinc contributes to neuronal injury after traumatic brain injury. *Brain Res*, **852**, 268-273.

Suter, B.A., O'Connor, T., Iyer, V., Petreanu, L.T., Hooks, B.M., Kiritani, T., Svoboda, K. & Shepherd, G.M. (2010) Ephus: multipurpose data acquisition software for neuroscience experiments. *Front Neural Circuits*, **4**, 100.

Takeda, A., Suzuki, M., Tempaku, M., Ohashi, K. & Tamano, H. (2015) Influx of extracellular Zn(2+) into the hippocampal CA1 neurons is required for cognitive performance via long-term potentiation. *Neuroscience*, **304**, 209-216.

Tamano, H., Nishio, R. & Takeda, A. (2017) Involvement of intracellular Zn(2+) signaling in LTP at perforant pathway-CA1 pyramidal cell synapse. *Hippocampus*, **27**, 777-783.

Tang, A.H., Chen, H., Li, T.P., Metzbower, S.R., MacGillavry, H.D. & Blanpied, T.A. (2016) A trans-synaptic nanocolumn aligns neurotransmitter release to receptors. *Nature*, **536**, 210-214.

Taylor, K.M., Hiscox, S., Nicholson, R.I., Hogstrand, C. & Kille, P. (2012) Protein kinase CK2 triggers cytosolic zinc signaling pathways by phosphorylation of zinc channel ZIP7. *Sci Signal*, **5**, ra11.

Thanos, C.D., Goodwill, K.E. & Bowie, J.U. (1999) Oligomeric structure of the human EphB2 receptor SAM domain. *Science*, **283**, 833-836.

Timm, F. (1958) [Histochemistry of heavy metals; the sulfide-silver procedure]. *Dtsch Z Gesamte Gerichtl Med*, **46**, 706-711.

Tzounopoulos, T., Kim, Y., Oertel, D. & Trussell, L.O. (2004) Cell-specific, spike timing-dependent plasticities in the dorsal cochlear nucleus. *Nat Neurosci*, **7**, 719-725.

Vander Jagt, T.A., Connor, J.A., Weiss, J.H. & Shuttleworth, C.W. (2009) Intracellular Zn2+ increases contribute to the progression of excitotoxic Ca2+ increases in apical dendrites of CA1 pyramidal neurons. *Neuroscience*, **159**, 104-114.

Vergnano, A.M., Rebola, N., Savtchenko, L.P., Pinheiro, P.S., Casado, M., Kieffer, B.L., Rusakov, D.A., Mulle, C. & Paoletti, P. (2014) Zinc dynamics and action at excitatory synapses. *Neuron*, **82**, 1101-1114.

Vogler, N.W., Betti, V.M., Goldberg, J.M. & Tzounopoulos, T. (2020) Mechanisms Underlying Long-Term Synaptic Zinc Plasticity at Mouse Dorsal Cochlear Nucleus Glutamatergic Synapses. *J Neurosci*.

Vogt, K., Mellor, J., Tong, G. & Nicoll, R. (2000) The actions of synaptically released zinc at hippocampal mossy fiber synapses. *Neuron*, **26**, 187-196.

Vyas, Y., Lee, K., Jung, Y. & Montgomery, J.M. (2020) Influence of maternal zinc supplementation on the development of autism-associated behavioural and synaptic deficits in offspring Shank3-knockout mice. *Mol Brain*, **13**, 110.

Wang, T., Zheng, W., Xu, H., Zhou, J.M. & Wang, Z.Y. (2010) Clioquinol inhibits zinc-triggered caspase activation in the hippocampal CA1 region of a global ischemic gerbil model. *PLoS One*, **5**, e11888.

Wei, G., Hough, C.J., Li, Y. & Sarvey, J.M. (2004) Characterization of extracellular accumulation of Zn2+ during ischemia and reperfusion of hippocampus slices in rat. *Neuroscience*, **125**, 867-877.

Weiss, J.H., Hartley, D.M., Koh, J.Y. & Choi, D.W. (1993) AMPA receptor activation potentiates zinc neurotoxicity. *Neuron*, **10**, 43-49.

Wenzel, H.J., Cole, T.B., Born, D.E., Schwartzkroin, P.A. & Palmiter, R.D. (1997) Ultrastructural localization of zinc transporter-3 (ZnT-3) to synaptic vesicle membranes within mossy fiber boutons in the hippocampus of mouse and monkey. *Proc Natl Acad Sci U S A*, **94**, 12676-12681.

Westbrook, G.L. & Mayer, M.L. (1987) Micromolar concentrations of Zn2+ antagonize NMDA and GABA responses of hippocampal neurons. *Nature*, **328**, 640-643.

Westin, G. & Schaffner, W. (1988) A zinc-responsive factor interacts with a metal-regulated enhancer element (MRE) of the mouse metallothionein-I gene. *Embo j*, **7**, 3763-3770.

Wildman, S.S., King, B.F. & Burnstock, G. (1998) Zn2+ modulation of ATP-responses at recombinant P2X2 receptors and its dependence on extracellular pH. *Br J Pharmacol*, **123**, 1214-1220.

Wildman, S.S., King, B.F. & Burnstock, G. (1999a) Modulation of ATP-responses at recombinant rP2X4 receptors by extracellular pH and zinc. *Br J Pharmacol*, **126**, 762-768.

Wildman, S.S., King, B.F. & Burnstock, G. (1999b) Modulatory activity of extracellular H+ and Zn2+ on ATP-responses at rP2X1 and rP2X3 receptors. *Br J Pharmacol*, **128**, 486-492.

Wu, Q.J. & Tymianski, M. (2018) Targeting NMDA receptors in stroke: new hope in neuroprotection. *Mol Brain*, **11**, 15.

Xie, X.M. & Smart, T.G. (1991) A physiological role for endogenous zinc in rat hippocampal synaptic neurotransmission. *Nature*, **349**, 521-524.

Xu, Y., Xiao, G., Liu, L. & Lang, M. (2019) Zinc transporters in Alzheimer's disease. *Mol Brain*, **12**, 106.

Xue, J., Xie, T., Zeng, W., Jiang, Y. & Bai, X.C. (2020) Cryo-EM structures of human ZnT8 in both outward- and inward-facing conformations. *Elife*, **9**.

Yashiro, K. & Philpot, B.D. (2008) Regulation of NMDA receptor subunit expression and its implications for LTD, LTP, and metaplasticity. *Neuropharmacology*, **55**, 1081-1094.

Yasuda, H., Yoshida, K., Yasuda, Y. & Tsutsui, T. (2011) Infantile zinc deficiency: association with autism spectrum disorders. *Sci Rep*, **1**, 129.

Yeh, C.Y., Bulas, A.M., Moutal, A., Saloman, J.L., Hartnett, K.A., Anderson, C.T., Tzounopoulos, T., Sun, D., Khanna, R. & Aizenman, E. (2017) Targeting a Potassium Channel/Syntaxin Interaction Ameliorates Cell Death in Ischemic Stroke. *J Neurosci*, **37**, 5648-5658.

Yin, H.Z., Ha, D.H., Carriedo, S.G. & Weiss, J.H. (1998) Kainate-stimulated Zn2+ uptake labels cortical neurons with Ca2+-permeable AMPA/kainate channels. *Brain Res*, **781**, 45-56.

Yin, H.Z. & Weiss, J.H. (1995) Zn(2+) permeates Ca(2+) permeable AMPA/kainate channels and triggers selective neural injury. *Neuroreport*, **6**, 2553-2556.

Yokoyama, M., Koh, J. & Choi, D.W. (1986) Brief exposure to zinc is toxic to cortical neurons. *Neurosci Lett*, **71**, 351-355.

Yoo, M.H., Kim, T.Y., Yoon, Y.H. & Koh, J.Y. (2016) Autism phenotypes in ZnT3 null mice: Involvement of zinc dyshomeostasis, MMP-9 activation and BDNF upregulation. *Sci Rep*, **6**, 28548.

Zhang, J.V., Ren, P.G., Avsian-Kretchmer, O., Luo, C.W., Rauch, R., Klein, C. & Hsueh, A.J. (2005) Obestatin, a peptide encoded by the ghrelin gene, opposes ghrelin's effects on food intake. *Science*, **310**, 996-999.

Zhang, T., Liu, J., Fellner, M., Zhang, C., Sui, D. & Hu, J. (2017) Crystal structures of a ZIP zinc transporter reveal a binuclear metal center in the transport pathway. *Sci Adv*, **3**, e1700344.

Zhang, Y., Wang, H., Li, J., Jimenez, D.A., Levitan, E.S., Aizenman, E. & Rosenberg, P.A. (2004) Peroxynitrite-induced neuronal apoptosis is mediated by intracellular zinc release and 12-lipoxygenase activation. *J Neurosci*, **24**, 10616-10627.

Zhao, H. & Eide, D. (1996a) The yeast ZRT1 gene encodes the zinc transporter protein of a high-affinity uptake system induced by zinc limitation. *Proc Natl Acad Sci U S A*, **93**, 2454-2458.

Zhao, H. & Eide, D. (1996b) The ZRT2 gene encodes the low affinity zinc transporter in Saccharomyces cerevisiae. *J Biol Chem*, **271**, 23203-23210.

Zhao, W.J., Song, Q., Wang, Y.H., Li, K.J., Mao, L., Hu, X., Lian, H.Z., Zheng, W.J. & Hua, Z.C. (2014) Zn-responsive proteome profiling and time-dependent expression of proteins regulated by MTF-1 in A549 cells. *PLoS One*, **9**, e105797.

Zhou, L., Li, F., Xu, H.B., Luo, C.X., Wu, H.Y., Zhu, M.M., Lu, W., Ji, X., Zhou, Q.G. & Zhu, D.Y. (2010) Treatment of cerebral ischemia by disrupting ischemia-induced interaction of nNOS with PSD-95. *Nat Med*, **16**, 1439-1443.

Zhu, X., Zelmer, A. & Wellmann, S. (2017) Visualization of Protein-protein Interaction in Nuclear and Cytoplasmic Fractions by Co-immunoprecipitation and In Situ Proximity Ligation Assay. *J Vis Exp*, 1-5.